Developing Models for Estimating Winter Road Weather and Surface Conditions – An Empirical Investigation

by

Lian Gu

A thesis submitted in partial fulfillment of the requirements for the degree of

Master of Science

in

TRANSPORTATION ENGINEERING

Department of Civil and Environmental Engineering
University of Alberta

ABSTRACT

Inclement weather poses a threat to road safety and mobility for motorists in cold regions during winter. To facilitate more efficient winter maintenance decision support and reduce weather-related collisions, many transportation agencies have adopted one of the most critical highway infrastructures; namely, road weather information systems (RWIS). While RWIS are effective in collecting real-time road surface conditions (RSC) information, they are costly to install and operate. Equally important, RWIS provide point measurements that are often unrepresentative of distant surrounding areas. Acknowledging the limitations in present knowledge and methods pertaining to improving its spatial coverage, this research proposes a new systematic framework that uses one of the most advanced geostatistical interpolation techniques, namely, regression kriging (RK), to estimate continuous RSC between different pairs of existing RWIS stations.

This research contains two phases: Phase I first evaluates the feasibility of applying RK to road surface temperature (RST) and road surface index (RSI) estimations. A comparison study using different spatial interpolation methods, including inverse distance weighting, global polynomial interpolation, local polynomial interpolation, and thin plate spline, is conducted to further verify the robustness of the RK method proposed herein. Phase II of the thesis extends the application of the previously developed model in Phase I to estimate RSC using stationary RWIS data only. A sensitivity analysis is also carried out to investigate the influence of RWIS stations density on model performance. Lastly, a recommendation to optimize the RWIS network is introduced by incorporating a renowned combinatorial particle swarm optimization method with the objective of minimizing the total kriging estimation errors.

The case study areas are Highways 2 and 16, which are major traffic corridors between Edmonton and Calgary (approximately 300 km) and between Edmonton and Edson (approximately 150 km), respectively. The datasets used in this study are from twelve surveys on four winter nights on Highway 16 and six surveys on two winter nights on Highway 2. Weather events are classified based on the wind speed and snow on ground information to investigate the generalization potential of the models developed herein.

The main findings of this thesis are summarized as follows.

The findings of Phase I indicate that the kriging models developed in this thesis have a strong predictive ability in estimating road weather and surface conditions, as indicated by low average root mean square errors (RMSE) of 0.254ºC and 0.046ºC for RST and RSI estimations, respectively. The results also suggest that the RSC estimations can be greatly enhanced with the help of additional covariates included in the models. Furthermore, there exists a strong dependency between the variability in data sets and weather event categories, which can be further used to generalize the findings of this study. The comparison analysis further confirms the robustness of the RK models, whereby improving the accuracy of estimation by up to 50% when compared to other methods.

The findings in Phase II of the thesis suggests that the use of stationary RWIS data alone can generate reliable results (i.e., RMSE less than 1ºC) when a known semivariogram model is available. The sensitivity analysis also reveals that the increase in the number of RWIS stations will improve the accuracy of estimation until it reaches a certain level, when the magnitude of benefits decreases and stabilizes. Lastly, a proposed RWIS location allocation optimizer is

recommended to minimize the total kriging estimation error, for transportation authorities to delineate new site locations for improved monitoring capabilities.

The proposed approaches provide a unique opportunity for continuous monitoring and visualization of road weather and surface conditions, to promote more efficient mobilization of winter maintenance resources. It is also anticipated that the findings of this research will, undoubtedly, contribute to improving the overall quality of winter road maintenance services and create a safer and more mobile environment for all travellers.

PREFACE

Work presented in this thesis is either accepted, published or is under-review for publication in various journals and conferences in the areas of transportation engineering.

Journal Papers Accepted (in Press)

1. **Gu, L.**, Kwon, T.J., and Qiu, T.Z. (2018). A Geostatistical Approach to Winter Road Surface Condition Estimation using Mobile RWIS Data. *Canadian Journal of Civil Engineering*. Accepted in Nov 2018.

2. Wang, X., **Gu, L.**, Kwon, T.J., and Qiu, Z. (2018). A Geostatistical Investigation into the Effective Spatiotemporal Coverage of Road Weather Information Systems in Alberta, Canada. *Journal of Advanced Transportation*. Accepted in Nov 2018.

Conference Papers Published

1. **Gu, L.**, Kwon, T.J. and Qiu T.Z. (2018). Estimating Winter Road Surface Conditions of Alberta's Highway Network using Kriging with External Drift. Accepted for presentation at the *2018 Transportation Research Board Annual Conference*, Washington, D.C., United States, Jan 2018.

2. **Gu, L.**, Kwon, T.J. and Qiu T.Z. (2017). Modeling of Winter Road Surface Temperature (RST) – A GIS-Based Approach. Conference Proceeding at the *4th International Conference on Transportation Information and Safety (ICTIS)*, Banff, Alberta, Canada, August 2017.

ACKNOWLEDGEMENTS

First of all, I would like to express my sincere gratitude to my advisor, Professor Tae J. Kwon. I'd like to thank him for supporting, leading and encouraging me throughout my study. It is my great fortune to meet such a supportive supervisor as his mentorship is invaluable to me. I am also grateful to Dr. Tony Z. Qiu for providing me with many suggestions and encouragement. Without guidance from Dr. Kwon and Dr. Qiu, it would have been impossible for me to finish my thesis. I also want to thank Dr. Leila Hashemian and Dr. Yasser Mohamed for spending their valuable time reviewing my work and being committee members at my final defence.

Secondly, I would like to acknowledge the financial and operational assistance from both Alberta Transportation and the Natural Sciences and Engineering Research Council of Canada (NSERC). In particular, I wish to thank Dave Gary and Beata Bielkiewicz at Alberta Transportation for providing RWIS data, which was essential to this study.

Thirdly, many thanks to my great colleagues and CST lab mates for their inspiring suggestions and assistance during my study. I would like to thank Simita Biswas, Mingjian Wu, Cindy Wang, Andy Wong, Shuoyan Xu, Jiangchen Li, Chen Qiu, Yang Li, Can Zhang, Mudasser Seraj, Chenhao Wang, Yuwei Bie, Ai Teng and other team members. Without them, my graduate study would not have been as gratifying and enjoyable.

Most of all, special thanks to Difei He and Peiyao Zhang for always staying by my side and accompanying me through difficulties. I am lucky to have met them in my life.

Last but not least, I want to express my deepest gratitude to my beloved parents, Guoping Gu and Meiqin Xu for their understanding, support, and company at all times. It is their love that makes me brave in the face of difficulties.

TABLE OF CONTENTS

LIST OF FIGURES

LIST OF TABLES

LIST OF ABBREVIATIONS

BLUE	Best Linear Unbiased Estimates
CFM	Continuous Friction Measurement
CFME	Continuous Friction Measurement Equipment
DEM	Digital Elevation Model
EC	Environment Canada
FFS	Free Flow Speed
GIS	Geographic Information System
GLS	Generalized Least Squares
GPI	Global Polynomial Interpolation
IDW	Inverse Distance Weighting
LPI	Local Polynomial Interpolation
MAE	Mean Absolute Error
MLR	Multiple Linear Regression
NDVI	Normalized Difference Vegetation Index
OK	Ordinary Kriging
OLS	Ordinary Least Squares
PSO	Particle Swarm Optimization
RK	Regression Kriging
RMSE	Root Mean Square Error

RPU	Remote Processing Units
RSC	Road Surface Condition
RSI	Road Surface Index
RST	Road Surface Temperature
RWIS	Road Weather Information System
TAC	Transportation Association of Canada
TM	Thermal Mapping
TPS	Thin Plate Spline
WRM	Winter Road Maintenance

CHAPTER 1. INTRODUCTION

1.1 Background

In winter months, people from cold regions, in countries like Canada, often suffer from the unique challenges related to heavy snowfall and freezing temperatures. Among all these challenges, the detrimental influence on road safety and mobility for motorists is inevitable and cannot be neglected. According to past studies conducted by the U.S. Department of Transportation, nearly 22% of all crashes are a result of adverse weather conditions due to poor visibility and degradation of pavement friction (Federal Highway Administration [FHWA], 2005-2014). The Ontario Road Safety Annual Reports (1993-2009) illustrated that the total number of vehicle collisions increased by approximately 17% over 16 years because of wet or snowy and icy road surface conditions. In terms of mobility issues, Agarwal et al. (2005) found that the capacity and average operating speed could be decreased by 4.29%-22.43% and 4.17-13.46% because of the various snow events. Kwon et al. (2013) conducted an empirical investigation on how inclement weather conditions would impact highway capacity and free flow speed (FFS) based on observations made during two seasons from 2010-2012. Their findings indicated that snow-covered road surface conditions could reduce capacity and FFS by 44.24% and 17.01%, respectively.

Therefore, to reduce the number of weather-related accidents, it is paramount for roadway administrations and transportation agencies to acquire real-time or near-future road surface condition (RSC) information to make more informed decisions on their various winter road maintenance (WRM) activities (e.g., salting and plowing) and prevent road users from getting involved in accidents during inclement weather events. WRM operations, however, demand substantial financial cost and resources - it is estimated that more than US $2.3 billion is spent

annually by North American transportation authorities on winter road maintenance and CA $1 billion by the Canadian government alone (Transportation Association of Canada, 2003; FHWA, 2018). For this reason, time and effort are put forth to seek cost-effective ways to minimize the costs of WRM and maintain a high level of service at the same time.

To reduce both WRM expense and damage to pavement surface caused by deicing chemical treatments, transportation agencies invest large amounts of money to improve winter maintenance decision support and traveler information provisions. Considering the kind of varied RSCs that could develop during adverse weather events, an in-depth understanding of spatial variation of RSC is a prerequisite for optimizing the degree and location of WRM. For this reason, road weather information systems (RWIS) have gained attention for their ability to provide real-time road condition information and have become widely used over the last decade amongst highway authorities.

RWIS use innovative sensors and cameras to provide detailed, tailored information about road weather and surface conditions. The data collected by RWIS provide the input required for stimulating more efficient and cost-effective WRM, thus creating faster and safer road conditions for travelers. Although RWIS are superior in providing valuable information, stations are expensive to install and manage, and therefore, can only be installed at a limited number of locations. Furthermore, RWIS provides point measurements that are often unrepresentative of distant surrounding areas. Considering the vast road network that needs to be monitored and the possible inclement winter weather, it is necessary to accurately interpolate the road weather and surface conditions of locations between existing RWIS stations to help maintain safe driving conditions and reduce the costs of WRM activities. To resolve this deficiency, focus must move away from just ‘measuring’ and toward ‘modelling’.

1.2 Problem Statement and Motivation

Estimating the road surface conditions (RSC) over any given segment has long been recognized as challenging work as it is affected by a variety of different factors. Those factors include, but are not limited to:

- atmospheric parameters (e.g., cloud cover, wind speed, and precipitation type and rate),
- climate patterns at both micro and macro levels,
- geographical features (e.g., vegetation cover and presence of buildings or obstructions),
- topographical settings (e.g., mountainous, flat, or rolling), and
- traffic.

These factors collated can cause considerable variation in RSC from one location to another, making RSC difficult to estimate, thus triggering a higher frequency of road weather related collisions.

Since information capturing the spatial variation of RSC is key to identifying hot spots in need of frequent monitoring (e.g., adverse weather-related accident-prone areas) and performing proper treatment, it is worthwhile to study the two most important RSC variables: road surface temperature (RST) and road surface index (RSI).

RST plays a key role in winter road maintenance as it provides information that is indispensable for implementing ice and snow removal operations and predicting black-ice potential. Shao et al., (1996) found that RST can vary by more than 10℃ across a road network at night during the winter. These variations in RST imply that some segments of road may fall below the freezing point while

others may still be above freezing. Therefore, nocturnal RST is considered one of the main factors contributing to the formation of black-ice, which can subsequently pose a threat to travellers as it is transparent and, thus hard to see on black asphalt pavement.

Acknowledging the need for an accurate estimation of roadway RST, several numerical models have previously been proposed in an attempt to understand the spatial variation of nocturnal temperature. Sass (1992) developed a prediction model based on the heat condition and the surface energy-balance models. Chapman (2001) proposed a multiple regression model to demonstrate that up to 75% of the residual RST variation can be affected by surrounding geographical features (Chapman et al., 2001a). Sokol et al. (2017) applied an ensemble technique for RST forecasting using an energy balance and heat conduction model whereas the results tend to be underestimates. Though these prior studies helped provide some insights about how temperature varies over space, they suffer from one major limitation: the models were developed to provide only site-specific condition information rather than an entire segment of road. Having continuous RST information over a road network is critical, not only to road users for improved safety but also to winter maintenance personnel responsible for maintaining a good level of service.

RSI is the other important parameter used to indicate WRM performance because it measures the experience road users have with various winter maintenance operations (i.e., level of service). RSI is a numerical value ranging between 0 and 1, and can be viewed as a surrogate measure for the friction level of a pavement surface, depending on the degree of snow and ice coverage. There are limited studies currently available since the factors related to road surface, such as contaminants and tires, which are hard to observe and measure, affect the friction measurement and cause more uncertainty (Feng and Fu, 2010). Perchanok (2002) used a discriminant analysis with three friction measures, namely peak resistance, slip speed at which the peak resistance occurs, and locked wheel

resistance, to classify RSC into visually different road surface classes (e.g., bare wet, bare dry, loose snow, packed snow, slush, etc.). However, the validation results showed that accuracy of the classification would be improved when incorporating external variables such as geographical parameters (Perchanok, 2002). Fu et al. (2008) applied probability density parameters of continuous friction measurements (CFM), specifically skewness and variance, with mean friction level to calibrate a series of logistic regression models to classify RSC. The findings indicated that adding probability density parameters can enhance the discrimination power of the logit classifiers (Fu et al., 2008). In general, there are few studies that have attempted to investigate the continuous RSI estimation.

1.3 Research Objectives

Despite the unique advantages associated with RWIS, there still exists shortcomings that cannot be ignored in the RSC monitoring techniques, such as high operation and maintenance costs. Moreover, there is no reliable method to capture the spatial variation of surface conditions in between RWIS stations. To tackle such challenges, this thesis proposes to develop a new methodological framework that estimates key road weather and surface condition variables - *road surface index (RSI)* and *road surface temperature (RST)* between different pairs of existing RWIS stations to create safer driving conditions for the traveling public. In particular, this thesis has five specific objectives as follows:

1) Synthesize knowledge on factors including weather, geographical, and topographical features that may affect road weather and surface condition variations;
2) Explore different types of information that can be extracted using state-of-the-art geomatics techniques (i.e., GIS and satellite remote sensing). This will include the use of innovative data sets including digital elevation model (DEM) and LANDSAT satellite images;

3) Develop a series of event-specific models that can estimate spatial variation of nocturnal RSCs;
4) Propose a systematic framework for estimating RSCs between stationary RWIS stations based on the spatial structure constructed using mobile RWIS; and
5) Make recommendation for new potential RWIS station locations considering the needs of WRM and the road users.

1.4 Thesis Organization

This thesis consists of five chapters. The remaining content is organized as follows:

Chapter 2 is a literature review covering current RSC monitoring methods and technologies, various factors that would affect the variations of the two variables under investigation - RSI and RST.

Chapter 3 describes the proposed methodology that incorporates an advanced geostatistical interpolation technique known as regression kriging (RK) and provides a brief introduction of other widely used interpolation methods.

Chapter 4 first presents real world case studies to describe the study area, data gathered and processed using GIS, application and development of RK models and discussions of results. A comparison analysis between RK and other interpolation methods is also included to demonstrate the superiority of the proposed method. The second part of this chapter connotes the application of RK to estimate conditions between stationary RWIS stations using a priori knowledge. Lastly, a recommendation of new potential RWIS station locations is made after evaluating the existing RWIS network.

Chapter 5 highlights the main findings and contributions of this research, and potential extensions for future research.

CHAPTER 2. LITERATURE REVIEW

This chapter provides a review of the current RSC monitoring techniques and factors possibly affecting RST and RSI respectively. The summary of this chapter is presented at the end with a discussion of limitations of previous research.

2.1 Current Practices on Road Surface Conditions Monitoring

Since timely and accurate information about road surface and weather conditions are a basic requirement for making efficient maintenance strategies and operation plans, many techniques are being developed and applied to collect such information. Some popular RSC monitoring instruments and systems are introduced below.

2.1.1 Thermal mapping

Thermal mapping (TM) is one of the techniques that aim at quantifying the spatial distribution of RST over a highway. It is equipped with a vehicle-mounted infrared thermometer to collect data under different weather conditions, which can then be graphically depicted by drawing thermal maps or fingerprints (Shao 1990; Chapman and Thornes 2005; Marchetti et al. 2011). Typically, thermal surveys are carried out by a fleet of vehicles along a road network over multiple nights with varying weather conditions to avoid the influence of the sun, thus a reliable amplitude of RST variations can be obtained (Chapman and Thornes, 2008). Areas that are likely freezing or snow covered can be visually identified using thermal maps such that specialized maintenance activities can be implemented without delay. Using this technique may allow maintenance personnel to identify the hotspots, but it requires more frequent monitoring and additional treatment (Marchetti et al., 2014; Zwahlen et al., 2003). Nevertheless, thermal mapping is limited to only providing pavement temperature, which is an incomplete representation of surface conditions. Besides that,

the process of generating thermal maps drawn by thermal fingerprints is laborious, time consuming, and expensive. This becomes more problematic for cities where a large-scale implementation is a necessity. Compounding the limitations, thermal mapping only provides a static forecast of minimum RST and thermal maps are merely a snapshot, which do not capture the temporal thermal behavior of road surface conditions.

2.1.2 Continuous friction measurement

The lack of sufficient friction between vehicle tires and pavement has been recognized as a contributing factor in crashes during wet weather conditions. Therefore, it is necessary for highway authorities to monitor pavement friction frequently and systemically to reduce accidents. Arousing concerns as a practical alternative to support RSC monitoring (Najafi et al., 2013), Continuous friction measurement (CFM) measures the coefficient of friction or the friction number. The friction coefficient is measured by specially designed tires attached to an on-board device (Linton, 2015) in a travelling vehicle, which means it is able to collect continuous friction measures over space. Furthermore, the measurement provided is a quantitative RSC measure other than a descriptive way, making it more intuitive for transportation engineers to investigate and identify hotspots. In practice, several Nordic countries and some states in the U.S., like Virginia, have used the continuous friction measuring equipment (CFME) to minimize friction-related vehicle crashes and improve WRM decision making (Najafi et al., 2013). However, this type of friction measuring is still quite a new concept for both transportation agencies and researchers, so a good understanding of the measuring systems and proper guidance are required to make the best use of it.

In spite of the benefits of CFM, the issues associated with this technique cannot be neglected. For instance, Najafi et al., (2013) found that CFM is sensitive to grade and vehicle testing speed. He suggests it is better to establish standard testing conditions to control measurement accuracy. Another common issue is its limited representation of the whole surface, since the contact area is very small and the data collected could be a misrepresentation of RSC on a multilane highway (Linton, 2015).

2.1.3 Road weather information systems

Recently, road weather information systems (RWIS) have gained more attention and become widely used in many places. Helping road maintenance agencies effectively plan anti-icing and snow removal, and reduce chemical material usage, RWIS consist of advanced sensors that collect, transmit and propagate current and near-future road weather and surface condition information. Furthermore, the disseminated information provides the inputs required for enabling WRM agencies to deliver more efficient and cost-effective maintenance services to the right place at the right time with the right treatment. RWIS are also valuable to the traveling public for making the travel related decisions such as whether or not to travel, when, where, and in what mode to travel, and what highway to choose. For these reasons, more than 3,000 RWIS stations are currently installed and used in North America and the number will continue growing to improve their existing WRM services and maximize the return on their investments (Foley et al., 2009; Kwon and Gu, 2017).

In general, there are two types of RWIS called stationary and mobile. The stationary RWIS, as depicted in Figure 1, is generally installed in situ within or along a roadway and provides detailed and tailored weather forecasts. The components of a typical RWIS station tower include cameras,

road surface sensors, remote processing units (RPU), and communication hardware. While a mobile RWIS (shown in Figure 2) is a patrol vehicle equipped with innovative sensors and collects data as it travels along the road. The data collected by mobile RWIS is sent through cellular communication to the maintenance center. Measurements collected from these two RWIS categories include, but are not limited to, air and road surface temperatures, dew point, wind speed and direction, surface status, etc. Additionally, mobile RWIS also provide direct measurements of chemical concentration and pavement friction, which help maintenance agencies adjust treatment to better match the actual conditions. However, due to different data collection mechanisms, the stationary RWIS provides high temporal but limited spatial coverage, while a mobile RWIS is able to provide spatially continuous but temporally discrete measurements.

While effective in conveying information, it is estimated to cost more than $50,000 to install an RWIS station with basic function, not to mention the cost of maintenance and additional sensors (Buchanan and Gwartz, 2005). Considering the high cost, the sitting of RWIS location has always been challenged by highway planning authorities since it is not economically feasible to have a high spatial density RWIS network. In addition, point measurements collected by stations are not reliable for places faraway, which can only draw an incomplete map of surface conditions. One possible solution may be to fuse information obtained from mobile RWIS to fill in the gap between stationary RWIS to improve and extend its spatial representativeness.

Figure 1. A typical RWIS station

Figure 2. A mobile RWIS data collection unit equipped with spectral road surface temperature sensor

2.2 Factors Affecting Road Surface Conditions

Estimations for RSC have been the topic of study for researchers, maintenance authorities, and policy makers for years. Obtaining accurate estimations are difficult due to the inherent variability of road weather and surface conditions, especially during the winter. In exploring possible

solutions, focus should be given to two essential components. One is road surface temperature (RST) and the other is road surface index (RSI), which represents the pavement's slipperiness.

2.2.1 Road surface temperature (RST)

Road surface temperature is affected by numerous interacting parameters, which include meteorological (i.e., solar radiation, wind speed, cloud cover), geographical (i.e., altitude, topography, land-use), and road construction (i.e., traffic, diffusivity). Thornes (1991b) tested the sensitivity of individual meteorological parameters with a control variable method to study their influence on RST. As expected, air temperature was found to be the most influential parameter controlling RST as air and surface temperature are closely related (Thornes and Shao, n.d.). Therefore, any variations in air temperature caused by geographical parameters across the mesoscale landscape will affect the road surface (Chapman et al., 2001b).

Some key factors that influence RST are summarized below:

Latitude

Latitude has the effect of controlling the theoretical maximum incoming short-wave radiation, which imposes a constraint on the climate and RST. However, the influence on the minimum night-time RST is small as the radiative cooling processes begins to dominate after sunset (Chapman et al., 2001a; Oke, 1987). For example, countries at higher latitudes always have more snow and ice problems than lower latitude countries.

Altitude

When altitude increases RST decreases, typically from 6.5 $^{\circ}$C and up to a maximum of 9.8°C per 1000 m (Tabony, n.d.). A study conducted by Shao (1997) in Nevada, U.S., outlines the impacts of altitude on RST, demonstrating that altitude has a non-linear relationship with RST (Shao et al.,

1997). Furthermore, the effects of altitude would be more noticeable when the atmospheric stability, which describes the tendency of air to rise or not, is low.

Topography

Topography is a main factor resulting in RST differences during extreme nights (Bogren Jorgen and Gustavsson, 1991; Yang et al., 2015). Slight differences in topography can cause large variations in road surface temperature. Several studies show that katabatic wind flow can generate pools of freezing air in hollows and valley bottoms (Gustavsson, 1990). Overall, temperature variations that rise from topography result in the lowest air temperatures on road networks, and any variation in air temperature is linearly related to RST (Chapman et al., 2001b). To study this influence, variables including slope and other descriptive features of the terrain are selected to represent topography. Jessica et al. (2007) studied slopes of the Sierra Nevada, in the vicinity of Yosemite National Park, California, to explore surface temperature variability. The results show that surface temperatures tend to be higher on the east slope compared with the west slope, which further proves the impact of terrain on temperature (Lundquist and Cayan, 2007). These variables can also be extracted by a digital elevation model (DEM).

Land-use

Land-use has a significant impact on RST, and can be observed through a comparison between urban and rural temperatures (Faghih Mirzaei et al., 2015). The phenomenon known as the "urban heat island effect" can account for increased temperatures in urban environments, where built up areas are commonly a little warmer than surrounding rural areas. In order to estimate the associated impacts, Normalized Difference Vegetation Index (NDVI), a variable used to describe the spatial heterogeneity of vegetation cover, can be adopted to represent the land-use (Garrigues et al., 2006). NDVI is calculated from the visible and near-infrared light reflected by vegetation, which

represents the density or the state of health of the vegetation since different kinds of vegetation absorb visible light and reflect near-infrared light to different extents (Kršmanc et al., 2013).

Wind Speed and Cloud Cover

The prevailing wind speed impacts the variation of air temperature. Strong winds prevent ground temperature inversions, but even a breeze can disturb developed cold air pools and drainage of cold air (Gustavsson, 1990). Previous researchers found that the eddy diffusivity is closely related to wind speed and increases rapidly with rising wind speed. The findings also show that the minimum temperature is normally higher on windy nights than on calm nights (Gustavsson, 1990). Shitara et al., (1973) proposed that the drop in temperature is most reduced during windy nights compared to that of calm ones. The variation of surface temperature is also affected by the atmospheric stability. Thornes (1991) used thermal mapping to quantify the spatial variation of nocturnal RST along a road network, finding that the amplitude of the thermal fingerprint is dependent on weather conditions during the survey and is greatest during times of high atmospheric stability. The variation of surface conditions usually decreases in line with atmospheric stability and is quantified by Pasquill-Gifford stability classes, which consider average wind speeds and cloud cover over the 12-hour period preceding the mapping survey. Therefore, estimating RST per stability class could generalize the findings. The classification method proposed by Thornes is shown in Table 1 (Thornes, 1991).

Table 1. Classification of weather events with respect to Pasquill Gifford Stability classes and Thornes (1991) classification

Surface Wind Speed (m/s)	Thinly overcast or ≥4/8 oktas of low cloud		<4/8 oktas cloud	
	Pasquill Gifford stability classes	Thornes classification	Pasquill Gifford stability classes	Thornes classification
<2	G	extreme	G	extreme
2-3	E	light	F	light
3-5	D	damped	E	moderate
5>	D	damped	D	damped

Pavement material

Pavement material is a key factor that contributes to the urban heat island phenomenon, as it can absorb and store great amounts of heat throughout the day. Hence, different surface materials influence the variation of RST. According to previous researches, new and darker surface materials absorb and store more solar and terrestrial infrared radiations, which will heat up during daytime and reradiate the heat over night (Ahmed Memon et al., 2008; Benrazavi et al., 2016). It is found that the surface temperature, heat storage and emission to the atmosphere of asphalt is greater than that of concrete or bare soil (Asaeda et al., 1996). Besides, a study conducted by Rosenfeld et al., (1995) indicated that pavement materials caused high urban surface temperatures in dry and hot area, as it will increase surface temperatures and turns air temperatures 2-3°C higher than the surroundings.

2.2.2 Road surface index (RSI)

To classify the surface state, transportation authorities around the world proposed and developed a wide variety of terminologies and classification schemes. Boselly (2000) synthesized different classification methods used by seven states in the US as described in Table 2 (Boselly, 2000).

In Canada, different provinces have their own winter road condition classification schemes and reporting systems. For instance, the Ministry of Transportation Ontario applies a condition description system including seven major categories and 486 subcategories for reporting possible road conditions in the winter season (Usman et al., 2012). Ministry of Transportation Alberta and Ministry of Transportation Quebec classify road surface conditions into three categories — bare (dry or wet), partly covered (snow or ice), and covered (snow or ice) (Fu et al., 2016). According to the Transportation Association of Canada (TAC), RSI is defined based on five major road surface state classes using friction measurements, as summarized in Table 3 (Feng and Fu, 2010; Transportation Association of Canada, 2009). Varying from 0.1 (poorest, e.g., ice covered) to 1.0 (best, e.g., bare and dry), RSI is often assumed to be similar to road surface friction values. Each category in the major classes is assigned a specific RSI value range.

Table 2. RSC classification systems used by some of the U.S. DOTs

North Dakota	Missouri	Iowa	Virginia	Ohio	Washington state	Montana
• Snow covered	•Covered	• Normal winter driving	• Minor	• Wet	• Dry	• Snow packed and icy
• Scattered snow or drift	• Partly covered	• Partly-mostly snow or ice covered	• Moderate	• Snow/ice	• Wet	• Intermittent snow pack with possible ice
• Frost	• Wet	• Snow or ice covered	• Severe	•Severe/snow/ice /drifting	• Ice/snow	• Icy or frost
•Compacted snow	• Dry					• Black ice
• Ice						
• Wet or slush						
• Dry						

Table 3. RSI for road surface condition classification

Road surface condition major classes	RSI range
Bare and dry	0.9-1.0
Bare and wet	0.8-0.89
Partly snow covered	0.5-0.79
Snow covered	0.25-0.49
Snow packed	0.2-0.24
Slushy	0.16-0.19
Icy	0.1-0.15

Likewise, the factors affecting RST would also influence RSI to a certain extent. For example, if the surface temperature is below the dew point temperature and then falls below freezing, the water will freeze, potentially forming black ice, which is quite dangerous for motorists. Some of the other factors are listed below.

Surface contaminant

Surface contaminant mainly represents the water, snow, and ice cover on the pavement. The thickness of the snow, ice, and water layer is highly correlated with the pavement friction coefficient (Juga et al., 2013). In this case, some researchers use camera images obtained by probe vehicles to determine the type of road surface contaminants along the survey route where friction and other condition variables were sampled and served as the basis for further supervised classifier calibration (Feng and Fu, 2010).

Precipitation

Precipitation can determine the thickness of the surface contaminant over a short term. Kangas (2015) found that precipitation intensity and phase impact the mobility of traffic in winter due to the decrease of surface friction (Kangas et al., 2015).

Pavement Texture

Previous studies suggest that pavement friction can be affected by texture. Different materials provide different surface conditions. Surface friction is improved when both fine and coarse angular aggregates are used in the asphalt mixtures.

There are also many factors affecting RST and RSI that are difficult to measure such as solar radiation and heat flux. Factors involving traffic, such as volume, speed, and even the types of tires used, can also affect road surface conditions. However, these features vary a lot and the effect caused by these factors is minimal when compared with the other factors mentioned above. Hence, researchers tend to focus on exploring the relationship that these geographical and topographical features have with RST and RSI.

2.3 Summary

In this chapter, the current major RSC monitoring technologies have been reviewed, the limitations and possible problems of these methods are discussed. In addition, factors affecting RST, RSI, and the relationship between these variables are discussed.

Previous studies have highlighted of the importance of RSC monitoring and RWIS turns out to be the most widely accepted method for collecting real-time road surface and weather information. Nevertheless, the issue of stationary RWIS stations being unable to capture the full variation of RSC needs to be dealt with. To explore the situation between RWIS stations, the spatial structure of RSC variables should be extracted from mobile RWIS data sources to improve the RSC estimation. Parameters that impact the change of RSC also need to be focused to improve the reliability of the model.

In the next chapter, details of the proposed methodological framework are introduced to estimate RSC between RWIS stations based on a geographic information system (GIS) and other well-known spatial interpolation methods.

CHAPTER 3. PROPOSED METHOD

Recognizing the limitations in spatial coverage of RWIS stations measurements, transportation authorities are seeking a way to obtain reliable and accurate RSC information at a lower expense. To remedy this challenge, this chapter provides an overview of the proposed method for RSC estimation and the underlying theory of the algorithm implemented. Detailed descriptions of each processing procedure including data processing and model calibration are also included. Furthermore, other spatial interpolation methods selected for a comparative analysis are briefly described.

3.1 Proposed Methodological Framework

The research is mainly aimed at solving two problems: one is to evaluate the feasibility of one of the most advanced variants of kriging methods; namely, regression kriging (RK) on RSC estimation and compare it with other interpolation methods; and the other is to explore the applicability of RK and make recommendations for RWIS location selections.

According to the literature review, acquiring proper RSC information has been a concern for many years, but most of the models developed suffer from one major limitation – they can only provide site-specific estimation rather than for an entire segment of road.

To address this challenge, a new geostatistical method that has seldom been explored in the transportation field, is proposed to show the feasibility of better capturing the spatial variations of the variable of interest. Regression kriging (RK) is a hybrid geostatistical interpolation method that provides best linear unbiased estimates (BLUE) for variables that tend to vary over space (and time). Due to its unique feature that combines both deterministic and stochastic components of random variables under investigation, not only does it provide estimates but also estimation

uncertainty at unknown locations based on a set of known observations (details to be further discussed in Section 3.3.2). In particular, advanced geomatics applications, such as remote sensing and GIS, are implemented in this study to further improve the predictability of the proposed model. Figure 3 shows the overview of the steps involved in data collection, integration and aggregation on a GIS platform, and the methodology used in this study.

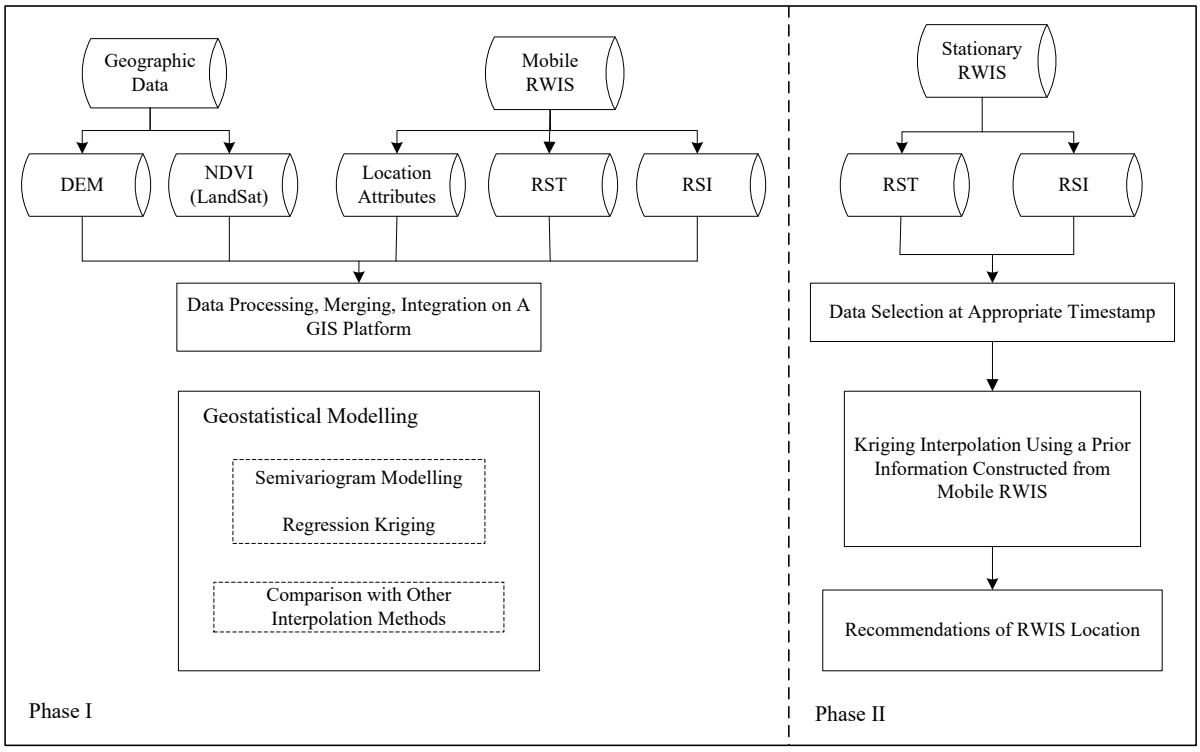

Figure 3. An overview of proposed methodology framework

As can be seen from the above figure, a RK model is developed to estimate RSC with geographical parameters extracted from remote sensing images in Phase I, in which the model calibration and validation are also conducted in this feasibility study. Other interpolation methods including inverse distance weighting (IDW), global polynomial interpolation, etc., are compared with RK to verify the superiority of the proposed method. Phase II is built on the first one, using ordinary kriging (OK) to interpolate stationary RWIS data with the spatial structure quantified by mobile

RWIS data from Phase I. After RSC estimations, a recommendation of new RWIS locations will be investigated to help maintenance agencies make a more informed-decision on where additional RWIS stations should be deployed to maximize its network monitoring capability. The details of the data processing, and how the models are developed will be explained in the following Sections 3.2 and 3.3.

3.2 Data Collection and Processing

The main data collection technique used in this study is via a mobile RWIS unit. It is a newer method for collecting road weather and surface information using patrol vehicles equipped with innovative technologies such as non-intrusive spectral sensors that provide accurate road surface temperature and grip levels that represent road surface slipperiness. Furthermore, the mobile RWIS can also provide observations of various parameters that could possibly further contribute to explaining the variations in the RST and RSI, including geographical parameters (e.g., latitude, longitude, altitude), meteorological parameters (e.g., air temperature, dew-point temperature) and road surface condition (e.g., snow cover situation).

In order to apply the proposed method to estimate RSC variables, auxiliary information such as location attributes, geographical and topographical features are required for a thorough analysis. Therefore, variables like slope and aspect derived from Digital Elevation Model (DEM) and Normalized Difference Vegetation Index (NDVI) calculated by LANDSAT satellite images can be used to better explain the spatial variation. Considering the large data sets, a GIS is utilized to process and extract the required data in an efficient manner. GIS are computer software packages that integrate user-friendly interfaces for storing, retrieving, analyzing, and visualizing all types of geographically referable data (Gu et al., 2017). Not only is GIS capable of dealing with vector and raster data, but it can also effectively process substantial amounts of geospatial datasets.

For stationary RWIS, it collects road surface and weather conditions constantly (every 10-20 min) at a fixed location. In this study, the data selected should be near the time when mobile RWIS passes by for the sake of comparisons between estimation results and mobile RWIS data.

Additional geographical and meteorological features are explored to determine the influence they have on RSC variations. Factors such as average wind speed and snow on the ground will be used to analyze the effects associated with different weather events.

3.3 Geostatistical Model Development

3.3.1 Steps for RK model development

As mentioned earlier, the objective of this study is to develop a methodological framework to estimate RSC on a given stretch of roadways as well as between existing RWIS stations. To achieve this goal, an advanced geostatistical interpolation method, RK, is developed and implemented for a continuous estimation of RST or RSI with help of covariates (i.e., external factors). In general, RK can be decomposed into five steps as summarized below:

i. *Perform stepwise multiple linear regression (MLR):* This step involves fitting a first-order polynomial to each set of target variables, using multiple covariates to better explain variations in RST or RSI data;

ii. *Model the covariance structure of the residuals:* In this step, collected data is used to develop a semivariogram model for each set of RWIS data (see Section 3.3.3 for details);

iii. *Determine kriging estimation map using residuals obtained in Step 1:* This step uses RK to interpolate the residuals at unknown locations by using semivariograms calibrated in the previous step;

iv. *Perform crossvalidation to ensure the accuracy of the models developed:* This step ensures that the models developed are accurate using various statistical measures such as RSME or MAE.

v. *Generate final RSC estimation maps:* This step adds the resulting map obtained in Step 3 to the regressed map generated in Step 1. The outcome of this step is the final RST and RSI estimation maps.

For Phase II, the semivariogram models that have been previously constructed using mobile RWIS data are adopted as prior information to estimate conditions between RWIS stations. The main difference between the two phases is that the inputs of the kriging model in Phase II are the stationary RWIS data, indicating that the whole RSC map is generated by only a few data points.

The following Sections 3.2.2 and 3.3.3 introduce the theoretical background of kriging and how semivariogram models can be calibrated to represent the underlying spatial structure, respectively.

3.3.2 Theory of Kriging

Kriging is a geostatistical interpolation method proposed by the mining engineer D.G. Krige for the estimation of mineral content (Goovaerts, 1997). It provides interpolated values at locations with no observations or measurements, based on a set of available observations by characterizing and quantifying spatial variability of the area of interest.

Let x and x_k be location vectors for the estimation point and a set of observations at known locations, respectively, with $k = 1, \ldots, m$, and Z be a random variable of interest (e.g. RST/RSI). The expression of a general kriging model is as follows (Goovaerts, 1997):

$$\hat{Z}(x) = m(x) + \sum_{k=1}^{m} \lambda_k [Z(x_k) - m(x_k)] \quad (1)$$

where $\hat{Z}(x)$ is the estimated value of the target variable at a location of interest. The terms *m(x)*and *m(x_k)* are expected values (means) of the random variables *Z*(*x*) and *Z*(x_k), and λ_k is a kriging weight assigned to datum *Z*(x_k) for estimation location *x*.

The results of kriging would vary by the model adopted for the random function *Z(x*) itself but all kriging methods share the same goal that the weights λ_k are chosen when estimation error variance is minimized:

$$\sigma_E^2(x) = Var\{\hat{Z}(x) - Z(x)\} \tag{2}$$

under the following constraint,

$$E\{\hat{Z}(x) - Z(x)\} = 0 \tag{3}$$

The random field, *Z*(*x*) can be divided into two components, namely, residual component *R*(*x*) and a trend component *m*(*x*), and presented as $Z(x) = R(x) + m(x)$ with *R*(*x*) is the constant stationary function with covariance $C_R(h)$:

$$E\{R(x)\} = 0, \quad Cov\{R(x), R(x+h)\} = E\{R(x) \cdot R(x+h)\} = C_R(h) \tag{4}$$

where *h* is a lag or separation distance between the observed points, and $C_R(h)$ is the residual covariance function, which is typically obtained from a semivariogram model, $\gamma(h)$. Under a second order stationarity assumption (i.e., constant mean, and covariance is dependent solely on distance vector *h* between any pairs of points), the following expression is satisfied (Goovaerts, 1997):

$$C_R(h) = C_R(0) - \gamma(h) = Sill - \gamma(h) \tag{5}$$

where *Sill* denotes the semivariance value for large lag distances wherever spatial autocorrelation between the data appears to be very small thus negligible. Therefore, the semivariogram that is used in the kriging system represents the residual component of the variable of interest. All different variants of kriging can be distinguished according to the model considered for the trend component, $m(x)$.

Ordinary Kriging (OK) is one of the most popular kriging methods. It assumes the mean, $m(x)$, is unknown but constant over each local neighboring area as depicted in Figure 4.

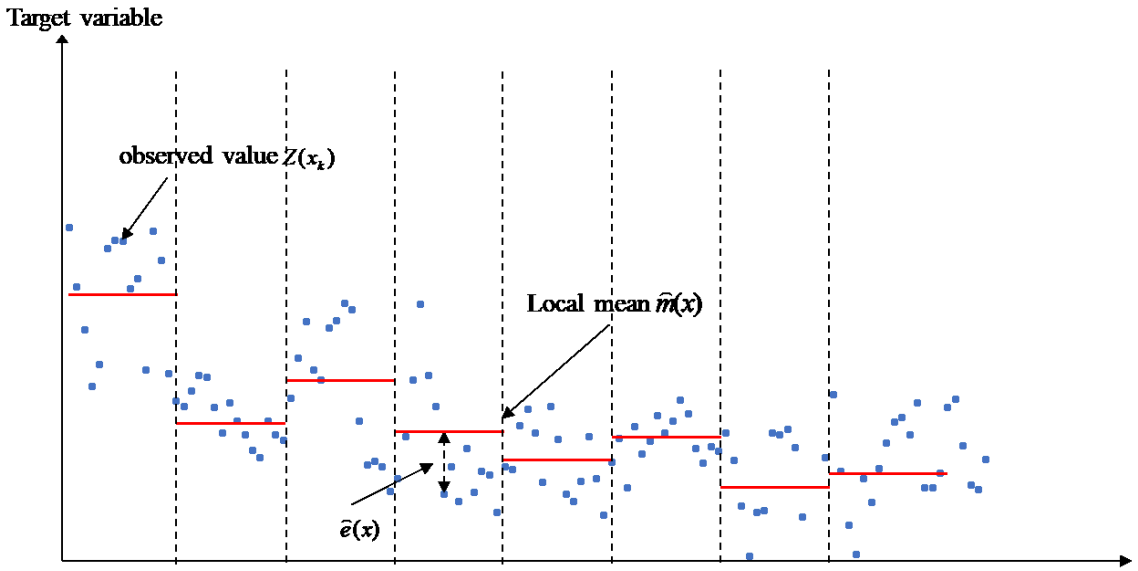

Figure 4. An example of ordinary kriging

This implies that OK takes the local fluctuation in to consideration by limiting the domain of stationarity of the mean to the local neighbourhood (Olea, 2003), which is of great value for the study of environmental or meteorological variables that typically show numerical fluctuations over space (Goovaerts, 1997).

In this case, the kriging estimator can be written as (Olea, 2003):

$$\hat{Z}(x) = \sum_{k=1}^{m} \lambda_k(x)\, Z(x_k) + [1 - \sum_{k=1}^{m} \lambda_k(x)]m(x) \qquad (6)$$

The unknown local mean is filtered from the linear estimator by forcing the sum of the OK weights to 1.

While in recent years, to strengthen the explanation of the target variable, hybrid interpolation techniques, which combine two conceptually different methods to model and map spatial variability, have received attention among geostatisticians. These techniques generate interpolations not only based on point observations of the target variable, but also use regression analysis on auxiliary variables (e.g., parameters derived from digital elevation models, satellite imagery, etc.). One of the most renowned hybrid interpolation methods is RK, which involves various combinations of regressions on auxiliary environmental information and kriging (Hengl et al., 2007; Ligas and Kulczycki, 2010). The estimations are made separately for the drift (by multiple linear regression) and residuals (by OK) and then added back together as shown in Equation (7):

$$\hat{Z}(x) = \hat{m}(x) + \hat{e}(x) = \sum_{i=0}^{p} \hat{\beta}_k \cdot q_k(x) + \sum_{k=1}^{m} \lambda_k \cdot e(x_k) \quad (7)$$

where $\hat{m}(x)$ is the fitted drift, $\hat{e}(x)$ is the interpolated residual, $\hat{\beta}_k$ are coefficients of the estimated drift model and $\hat{\beta}_0$ is the estimated intercept, p is the number of auxiliary variables, λ_k are kriging weights and $e(x_k)$ is the regression residual. Figure 5 provides a visual representation of the general concepts of RK that combines both deterministic and stochastic components of spatial variations of the variable under investigation (i.e., RSC). In this figure, a linear regression model is used first to remove the trend of the target variable, followed by kriging interpolation on the residuals by characterizing and quantifying the underlying spatial structure of the observed measurements (to be further discussed in Section 3.3.3). The estimated residuals are then added back to the regression results and generate the final estimations.

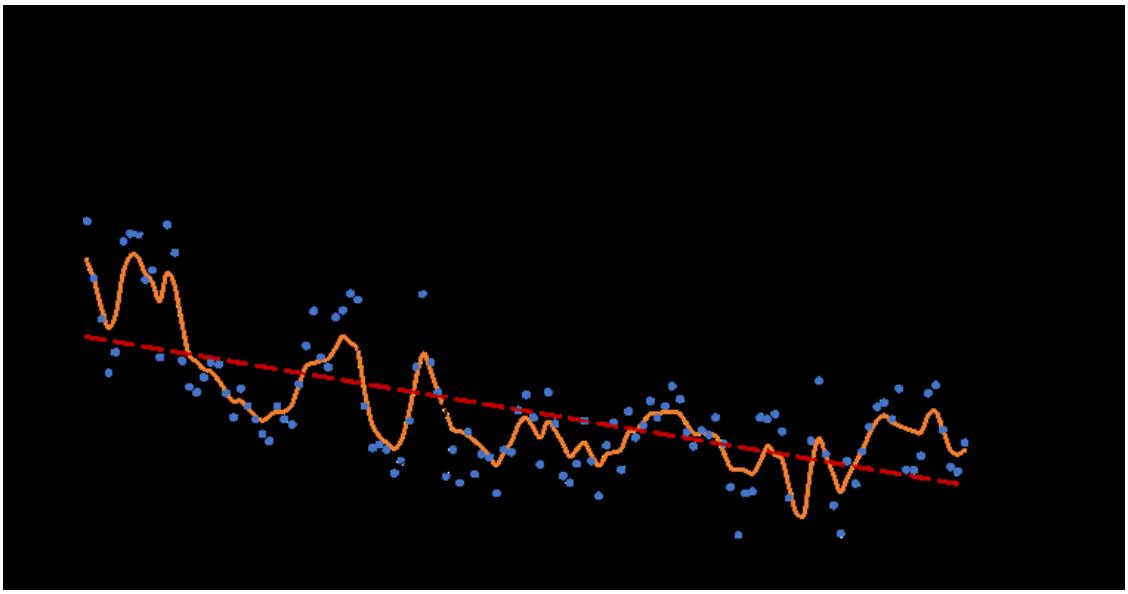

Figure 5. The general idea of regression kriging

Specifically, the coefficients $\hat{\beta}_k$ of the regression model are estimated using ordinary least squares (OLS) or, optimally, generalized least squares (GLS). The advantage of GLS is that it accounts for the spatial correlation of the residuals obtained from the regression model. The equation of GLS is described as follows:

$$\hat{\beta}_{GLS} = (q^T \cdot C^T \cdot q)^{-1} \cdot q^T \cdot C^{-1} \cdot z \tag{8}$$

Where $\hat{\beta}_{GLS}$ is the vector of estimated coefficients, C is the covariance matrix of residuals described below, and q is a matrix of estimates at measured locations.

$$\mathrm{C} = \begin{bmatrix} C(x_1, x_1) & \cdots & C(x_1, x_n) \\ \vdots & \ddots & \vdots \\ C(x_n, x_n) & \dots & C(x_n, x_n) \end{bmatrix} \tag{9}$$

After the trend has been estimated, the residual can be interpolated using kriging and added back to the estimated trend. The regression kriging can be conveniently expressed in matrix notation:

$$\hat{Z}(x) = q_0^T \cdot \hat{\beta}_{GLS} + \lambda_0^T \cdot (Z - q \cdot \hat{\beta}_{GLS}) \tag{10}$$

where q_0 is the vector of $p+1$ estimates and λ_0 is the vector of n kriging weights used to interpolate the residuals at unknown locations.

Previous research indicated that these hybrid techniques tend to outperform the plain geostatistical methods such as simple kriging or OK. They can yield more detailed and accurate estimations by incorporating various covariates in modeling the trend component (Hengl et al., 2004). Since RST is known to be influenced by many external factors, including geographical characteristics and meteorological elements, RK is a better option to be considered and thus used in this study. The grip information provided by the mobile RWIS are a combination of measurements that take into account the road contaminant influence, therefore OK is capable of estimating RSI.

3.3.3 Semivariogram for building a spatial structure

Quantifying the spatial autocorrelation structure of the variable of interest is a prerequisite when developing any kriging model. The spatial variability can be measured by modeling a semivariogram that depicts how the data is correlated with its spatial distance based on the observations and location information (Journel and Heuvelink, 1978). Due to scarce data points in reality, the points are typically grouped per distance vector h and the resulting semivariogram is expressed as follows:

$$\hat{\gamma}(h) = \frac{1}{2m(h)} \sum_{k=1}^{m(h)} [Z(x_k) - Z(x_k + h)]^2 \quad (11)$$

where $\hat{\gamma}(h)$ is the sample semivariogram, $Z(x_k)$ is a measurement taken at location x_k, and $m(h)$ is the number of pairs of observations separated by the lag |h| in the direction of the vector. The number of pairs to be estimated in this model should at least be equal to 30. Also, the lag distance for an experimental semivariogram should be constrained to half of the diameter in the sampling

domain for all direction analysis (Journel and Heuvelink, 1978). Note that there should be no trend of systematic variation, thus the estimated result is independent from the individual site x_k..

Generally, three key parameters are used to describe a semivariogram model, including nugget effect, sill, and range, as graphically illustrated in Figure 6.

The nugget effect represents micro scale variations and measurement errors, or any spatial variability that exists at a distance smaller than the shortest distance of two measurements. The value of *h* means the lag distance, and the range indicates lag separation distance at which a plateau is reached (i.e., values separated by distances greater than this are considered uncorrelated). Sill represents the variance of the random field and magnitude of the plateau beyond the range.

Typically, an experimental semivariogram is smoothed by a mathematical model due to the fact that the estimated model is commonly irregular and the real spatial structure of the region is unlikely known (Oliver and Webster, 1990). There are many negative definite functions that can be fitted to describe the semivariances of the sample data such that, negative values of variances can be avoided. The most commonly adopted models are exponential, Gaussian and spherical models, and the detailed descriptions of these models can be found in (Olea, 2006). The most commonly adopted models are described in Table 4.

Since it is critical to ensure that the model selected best captures the shape of the spatial variability of the observations, assessing the goodness of fit for each model is imperative. Cross-validation is one possible approach that can be adopted to quantitatively analyze the performance of a predictive model using various statistical measures. It is a verification process in which every single observation would be “removed with replacement” to generate an estimate at the same site of the removal (Olea, 2006). The difference between the “observed value” and the “estimated value” is

regarded as error. The root mean square error (RMSE) value indicates the performance of the model.

Table 4. Most commonly used semivariogram models (adopted from Olea, 2006)

Exponential	$Ex(h) = C\left(1 - e^{-\frac{3h}{a}}\right)$
Gaussian	$G(h) = C\left(1 - e^{-3(\frac{h}{a})^2}\right)$
Spherical	$Sp(h) = \begin{cases} C\left(\frac{3h}{2a} - \frac{1}{2}\cdot\left(\frac{h}{a}\right)^3\right), & 0 \le \lvert h\rvert < \lvert a\rvert \\ C, & \lvert a\rvert \le \lvert h\rvert \end{cases}$

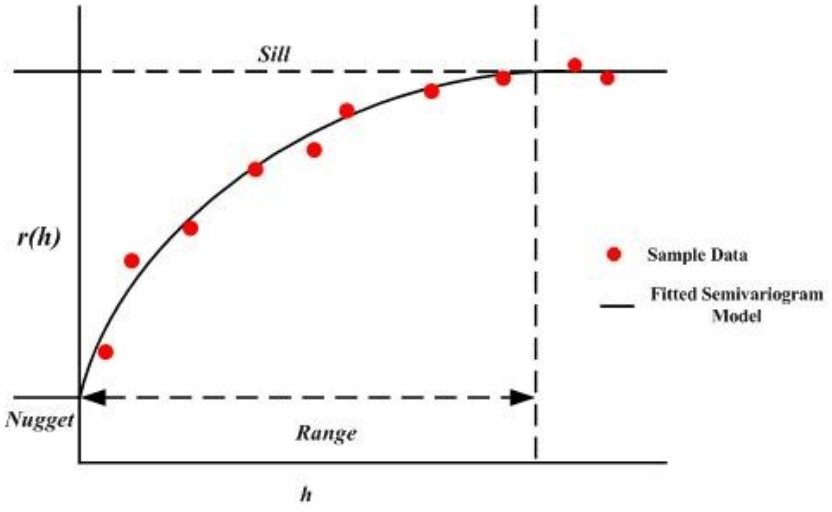

Figure 6. An example of generic semivariogram with key parameters

3.4 Other Spatial Interpolation Methods

Spatial interpolation approaches have been used to estimate unknown surface and analyze the spatial distribution of variables of interest in different disciplines (Li and Heap, 2008; Zarco-Perello and Simões, 2017). The core of a spatial interpolation method is the understanding of the geographical features of the sampling data (i.e., observations) to generate the estimation map.

According to different mathematical principles, spatial interpolation methods can be generally classified into two categories: deterministic and indeterminate (geostatistical) (Yang et al., 2016). In terms of deterministic method, the distance or closeness of sample points to neighbours is taken into consideration in mathematical functions (e.g., inverse distance weighting, thin plate spline). For indeterminate method, it deals with both stochastics and deterministic elements as statistics is further used to estimate unknown points (e.g., kriging) (Ziary and Safari, 2007). In this study, four widely used interpolation methods are introduced as a benchmark to verify the performance of RK.

Inverse Distance Weighting (IDW)

Inverse distance weighting (IDW) is an exact method that assumes the estimated value of an unknown point, and it is influenced more by nearby known points than those far away (Chang, 2012). The weights assigned to the interpolated locations are the inverse of the distance between the samples and the estimated points. The general equation of IDW method is (Robinson and Metternicht, 2006; Sankar et al., 2018):

$$\hat{Z}(x) = \frac{\sum_{i=1}^{n} \frac{x_i}{h_{ij}^{\beta}}}{\sum_{i=1}^{n} \frac{1}{h_{ij}^{\beta}}} \tag{12}$$

Where $\hat{Z}(x)$ is the estimated value, n represents the total number of sampling, x_i is the ith data, $h_{ij}$is the distance between interpolated value and point i, β is the weighting power.

Global Polynomial Interpolation (GPI)

Global polynomial interpolation (GPI) method fits a smooth surface that is defined by a mathematical function (a polynomial) to the observed points. The GPI changes gradually and captures coarse-scale pattern in the sampling data (Apaydin et al., 2004). A slightly varying surface is created by low-order polynomials that might capture physical features. Nevertheless, it is more

difficult to describe the physical meaning when the polynomial model becomes more complex. Not to mention that a single polynomial method may not fit well if the surface has various terrain.

Local Polynomial Interpolation (LPI)

Local Polynomial Interpolation (LPI) fits the local polynomial using points only within specified overlapping neighborhoods, while GPI fits the entire surface. The estimated value is estimated at the center of the neighborhood. LPI is capable of surfaces that captures more local variation (Apaydin et al., 2004; Sankar et al., 2018).

Thin Plate Splines (TPS)

Thin Plate Splines (TPS) generate the estimated surface that passes through the sample points and has the least possible change in slope at all points. In other words, TPS fits the known points with a minimum curvature surface. The approximation of TPS is described below:

$$\hat{z}(x,y) = \sum A_i d_i^2 \, log \, d_i + a + bx + cy \tag{13}$$

Where x and y are the coordinates of the interpolated point, $d_i = (x - x_i)^2 + (y - y_i)^2$, and x_i, y_i are the coordinates of point i, TPS includes two components, one is the local trend function represented by $a + bx + cy$, and another is the basis function represented by $d_i^2 \, log \, d_i$, which is aimed to obtain minimum curvature surfaces (Franke, 1982; Kang tsung Chang, 2012).

3.5 Summary

This chapter provides an overview of the proposed methodological framework, detailed explanation of data collection, processing, model development and other well-known spatial interpolation methods.

This study first explores the predictability of RSC variations using the geostatistical approach by investigating how covariates (i.e., location attributes, topographical parameters) would affect the

variation in RSC, followed by the comparative analysis with other spatial interpolation methods. According to the semivariogram models developed in Phase I that quantify the spatial structure of mobile RWIS data, Phase II of this study uses the calibrated model variables (i.e., sill, nugget, and range) in conjunction with stationary RWIS data to infer the conditions between the different pairs of existing RWIS stations. Given the complexity of problems being tackled in this thesis, the proposed kriging method, which is indeterminate in nature, is anticipated to be a promising method that can provide a complete image by capturing the local variation of RSC along any given stretch of roads – truly a unique feature that will make up for the limitations of previous research.

CHAPTER 4. CASE STUDY

The proposed methodology is applied via case study covering selected stretches of Highways 2 and 16 (approx. 300 km and 180 km in length) in the province of Alberta, as shown in Figure 7. The figure also shows the location of existing RWIS stations currently in operation. There is a total of eleven stationary RWIS stations (red triangle) sited along the survey route: four on Highway 16 and seven on Highway 2. These two highways are chosen due to their available data for nocturnal weather events, varied topographical terrain, and environmental conditions, such as residential areas, prairie expanses, and woodland habitats. For the feasibility study of RK, these two routes were segmented into three sections (i.e., A, B, and C) to minimize the potential effects associated with temporal variations of the RSC variables under investigation, with each of the routes being approximately 60km (for Highway 16) and 100km (for Highway 2) long.

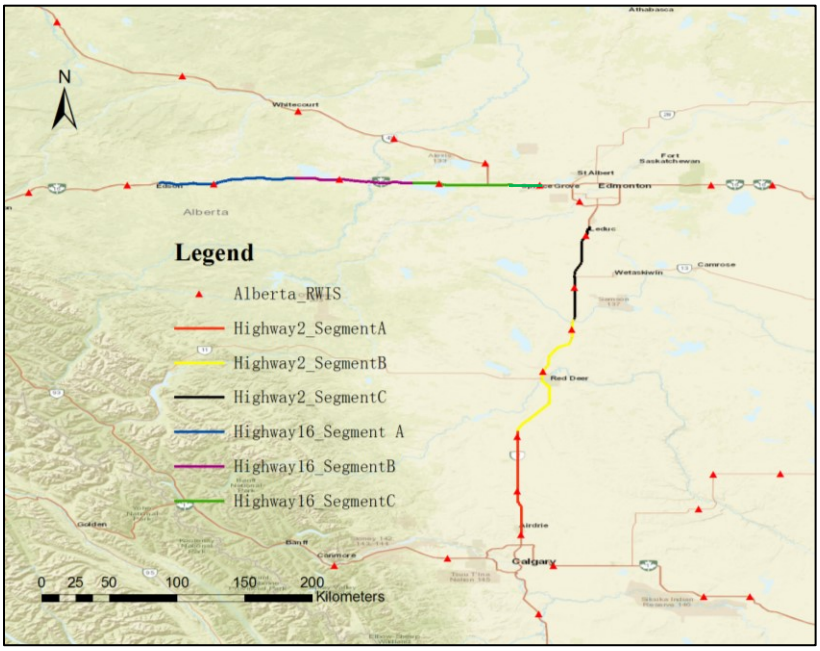

Figure 7. Study area of this research

4.1 Data Description and Processing

The mobile RWIS data points collected in this study are constantly logged every 3 seconds as the vehicle travels along the road, and it can provide spatially continuous measurements, providing the unique opportunity to calibrate robust statistical models. Although mobile RWIS cannot measure the surface friction directly, it can provide a grip value varying from 0 to 1, which represents road slipperiness. Thus, the grip value is assumed to be identical to RSI to represent road surface condition. Additionally, the location attributes (e.g., latitude, longitude, altitude) collected via mobile RWIS are also used to analyze the RSC variation.

Data sets collected by mobile RWIS are from twelve surveys carried out over four winter nights on Highway 16, and six surveys carried out on two winter nights on Highway 2. The descriptive statistics of the RST and RSI data for Highways 16 and 2 are summarized in Tables 5 and 6, respectively.

Road surface temperature, road surface status, wind speed, etc. are recorded every 20 minutes by stationary RWISs located in the study area. The temporally continuous RST information is used as a model input to estimate RST conditions between RWIS stations. Besides wind speed, snow on ground condition obtained from Environment Canada's (EC) weather stations near the road of interest, are used to classify weather conditions to further generalize the findings.

In this study, Esri's ArcGIS 10.3 is used for data processing. The RST and RSI datasets with the same spatial reference from mobile RWIS were converted into shapefiles and imported with other geographical parameters. The data points were joined to generate vector road data; in this case, each point would have road attribute data appended to it. Furthermore, to reduce the mathematical complexity of the proposed method and obtain representative geographical data, a uniform buffer

zone of 500m was created as a minimum spatial grid to aggregate the observations. Measurements of variables that fell within each equal-length cell were averaged and assigned to the centroid by a geoprocessing tool available in ArcGIS.

Table 5. Descriptive analysis of RST and RSI data on Highway 16

Highway 16 Segment	Date	RST(°C)				RSI				
		Min	Max	Mean	STD	Min	Max	Mean	STD	No. of Records
A	20150203	-16.1	-9.4	-13.67	0.73	0.11	0.82	0.70	0.22	679
	20150209	-11.1	-8.2	-9.22	0.44	0.13	0.82	0.78	0.11	658
	20141218	-11.5	-2.4	-8.82	0.90	0.6	0.82	0.82	0.02	669
	20161201	-21.8	-17.5	-19.62	0.77	0.12	0.82	0.73	0.14	654
B	20150203	-15.8	-11.7	-13.68	0.82	0.1	0.82	0.71	0.22	674
	20150209	-11.4	-7.9	-9.07	0.55	0.17	0.82	0.79	0.08	651
	20141218	-12.5	-7.4	-9.94	1.17	0.36	0.82	0.81	0.03	647
	20161201	-3.1	-0.4	-1.54	0.63	0.55	0.82	0.81	0.02	671
C	20150203	-14.6	-10.6	-12.47	0.58	0	0.82	0.79	0.11	657
	20150209	-11.5	-7.8	-9.07	0.45	0.35	0.82	0.80	0.07	649
	20141218	-10.7	-5.1	-7.42	1.12	0.59	0.82	0.82	0.02	639
	20161201	-2.5	0.1	-0.73	0.06	0.55	0.82	0.81	0.01	663

Table 6. Descriptive analysis of RST and RST data on Highway 2

Highway 2 Segment	Date	RST				RSI				
		Min	Max	Mean	STD	Min	Max	Mean	STD	No. of Records
A	20150209	-11.3	-6.3	-9.12	0.96	0.12	0.82	0.81	0.04	1306
	20150113	-4.2	-0.8	-2.63	0.61	0.26	0.82	0.80	0.07	883
B	20150209	-12.9	-9.6	-11.02	0.72	0.21	0.82	0.71	0.15	1269
	20150113	-7.4	-0.3	-2.52	0.88	0.24	0.82	0.85	0.06	984
C	20150209	-12.5	-8.3	-10.57	0.83	0.42	0.82	0.77	0.08	775
	20150113	-3.2	1	-0.76	1.03	0.78	0.82	0.81	0.01	811

The variable slope was derived from DEM using standard surface analysis functions embedded in ArcGIS. For studying the influence of spatial vegetation cover, Landsat satellite images were used to calculate NDVI as shown in Figure 8.

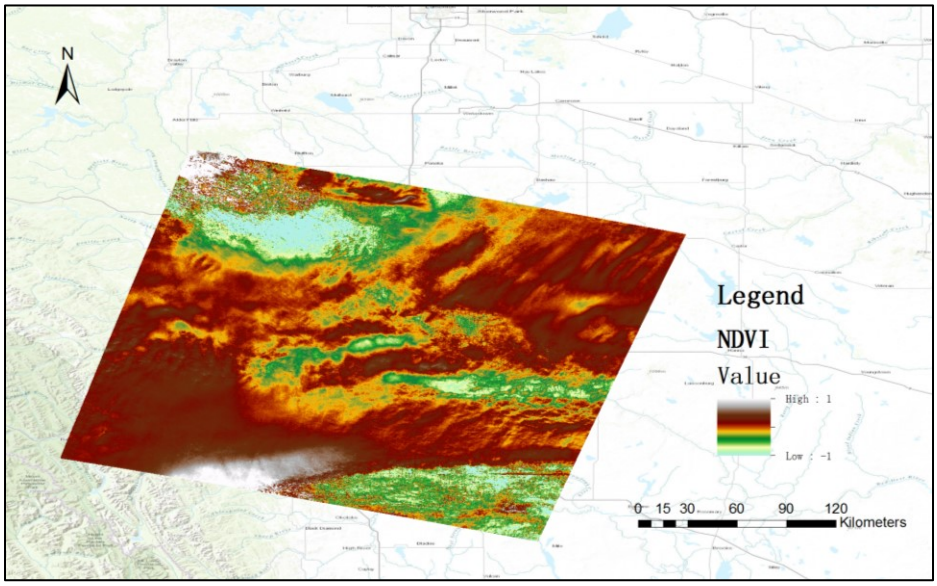

Figure 8**.** Landsat satellite images used for DEM calculations

The collected images contain reflected light bands in the spectrum of blue, green, red, near-infrared, etc. Since the data comes in a raster format, it can be conveniently integrated and calculated from RED and NIR reflectance on a GIS platform with the following equation:

$$NDVI = \frac{NIR - RED}{NIR + RED} \tag{14}$$

The result of NDVI varies from -1 to +1; a value close to zero refers to barren areas of rock, or sand, and a value closer to +1 indicates a high density of green vegetation. Consequently, five geographical factors, namely, latitude, longitude, altitude, slope, and NDVI are considered for RST estimation in this study. For RSI, OK is employed since the regression analysis can hardly explain the variation of RSI.

4.2 Classification of Weather Events

4.2.1 Classification For RST

According to Thornes' (1991) study, RSC variations usually decrease in line with atmospheric stability (Chapman et al., 2001a; Thornes, 1991). The general temperature trends remain constant under similar weather conditions. To better generalize the findings of the developed models and further improve their transferability, the weather conditions can be categorized into four categories based on the Thornes Classification method. Since wind speed takes the key role in this method, and considering the lack of cloud cover data, only the wind speed index will be used to classify the weather events. The four categories and the criteria are shown in Table 7, and the classification results (i.e., category) are illustrated in Table 8.

4.2.2 Classification For RSI

RSI is more complex when compared to RST. When the road surface condition is completely dry or snow covered, the grip collected by mobile RWIS is consistent and the semivariogram model might not be able to quantify the data structure, since the data feature is not significant. Equally important, estimating homogeneous road surface conditions whose surface index would likely be uniform, thus easily predictable, has less practical value in. Therefore, the weather event classification method will only be applied when the road surface friction undergoes a considerable amount of fluctuation. According to literature review, road contaminants (e.g., water, snow, ice) were found to be one of the key factors affecting RSI and is negatively correlated with RSI. With the snow on ground data from Environment Canada, the weather events were classified into three categories, shown in Table 9 and the resulting categories for all study segments are shown in Table 10.

Table 7. Classification of weather events for RST estimation

Surface Wind Speed (m/s)	Category
<2	extreme
2-3	light
3-5	moderate
<5	damped

Table 8. Weather events of different segments for RST estimation

Highway	Segment	Date	Avg. wind speed (km/h)	Category
Highway 16	A	20150209	2.70	extreme
	A	20141218	3.06	extreme
	A	20150203	8.64	light
	A	20161201	6.60	extreme
	B	20150209	3.24	extreme
	B	20141218	5.28	extreme
	B	20150203	10.2	light
	B	20161201	15.25	moderate
	C	20150209	8.52	light
	C	20141218	4.68	extreme
	C	20150203	14.40	moderate
	C	20161201	10.20	light
Highway 2	A	20150209	11.34	moderate
	A	20150113	21.60	damped
	B	20150209	8.46	light
	B	20150113	12.20	moderate
	C	20150209	8.64	light
	C	20150113	12.69	moderate

Table 9. Classification of weather events for RSI estimation

Snow on Ground (cm)	Category
<15	low
15-30	light
20-45	moderate
46>	heavy

Table 10. Weather events of different segments for RSI estimation

Highway	Segment	Date	Snow on Ground (cm)	Category
Highway 16	A	20150209	42	moderate
	A	20141218	19	light
	A	20150203	47	heavy
	A	20161201	14	low
	B	20150209	32	moderate
	B	20141218	22	light
	B	20150203	44	moderate
	B	20161201	10	low
	C	20150209	22	light
	C	20141218	25	light
	C	20150203	17	light
	C	20161201	5.0	low
Highway 2	A	20150209	25	light
	A	20150113	21	light
	B	20150209	25	light
	B	20150113	22	light
	C	20150209	25	light
	C	20150113	20	light

4.3 Phase I –Feasibility Evaluation of RK for Estimating RSC

4.3.1 Model development for RST

As previously described, the RK model can be developed using a few key steps. Firstly, a multiple linear regression (MLR) analysis is performed to see how much the variance in RST could be explained by select geographical parameters, including latitude, longitude, altitude, slope and NDVI. Secondly, a semivariogram model is applied to quantify the data structure and then the kriging interpolation approach is used to modify the estimated RST obtained from MLR. The last part of the process is the validation of the calibrated models.

The stepwise MLR analysis was performed using the SPSS software by fitting a first-order polynomial to each set of the target variables and ensuring the variable is free of trend. Note that a 95% confidence interval was adopted to test the significance of each parameter and the p-value was used to confirm if the independent variable was statistically significant at a significance level of 5%. Tables 11 and 12 show the MLR results for Highways 16 and 2, respectively.

By inspecting the sign of coefficients, all regression coefficients of geographical parameters make intuitive sense. For instance, the surface temperature increases when the NDVI value increases due to higher density of green vegetation. Furthermore, the studied Highway 16 is placed in west-east directions, which implies a greater variation along longitude axis. In this case, the RST decreases with the increase of longitude. For Highway 2, longitude also has a negative effect on RST. The trends continue for latitude and altitude as the RST drops as it moves north and to a higher elevation. Slope, the measure of the steepness or the degree of inclination of the horizontal plane, also has a negative relationship with RST, as expected.

Table 11. Summary of MLR results for RST estimation on Highway 16

Segment	Date	Category	Significant Variables	Sign of Coefficients	R^2
A1	20141218	Extreme	longitude / slope	(−) / (−)	42%
A2	20150203	Light	longitude / NDVI	(−) / (+)	28%
A3	20150209	Extreme	longitude / slope	(−) / (−)	68%
A4	20161201	Extreme	altitude / NDVI	(−) / (+)	72%
B1	20141218	Extreme	latitude / NDVI	(−) / (+)	65%
B2	20150203	Light	latitude / NDVI	(−) / (+)	51%
B3	20150209	Extreme	longitude / altitude	(−) / (−)	36%
B4	20161201	Moderate	longitude	(−)	83%
C1	20141218	Extreme	longitude / NDVI	(−) / (+)	49%
C2	20150203	Moderate	slope	(−)	1%
C3	20150209	Light	slope	(−)	9%
C4	20161201	Light	latitude	(−)	40%

Table 12. Summary of MLR results for RST estimation on Highway 2

Segment	Date	Category	Significant Variables	Sign of Coefficients	R^2
A1	20150209	Moderate	longitude / latitude	(−) / (−)	84%
A2	20150113	Damped	latitude	(−)	26%
B1	20150209	Light	latitude / slope	(−) / (−)	73%
B2	20150113	Moderate	latitude	(−)	10%
C1	20150209	Light	altitude	(−)	49%
C2	20150113	Moderate	altitude / longitude NDVI	(−) / (−) (+)	87%

The predictive ability of the regression models varies a lot for both highways. One possible cause of these results could be different weather conditions. In general, the predictive ability of the model is lower in damped conditions than in extreme conditions. The major reason for this is that when the atmospheric stability is low, the model cannot accurately incorporate the impacts of topography due to the more complex surface conditions, which could potentially impede the accuracy of the model. Overall, the shortfalls in RST estimations suggest that using MLR alone may not achieve desirable results and that the proposed kriging method be incorporated to further refine the model and improve the accuracy.

Following the previous analysis, the next two steps are to quantify and model the spatial autocorrelation structure of the residuals of the target variable and generate an estimation map accordingly. In this case, 70% of observed data for each event were chosen randomly as the training datasets, and the remaining 30% were used as the testing datasets. To fulfill these tasks, extensive amount of effort has been put forth to develop a robust semivariogram for all the analysis days under investigation. The mathematical semivariogram used to smooth the experimental model here is stable model, which is more flexible than exponential and Gaussian models. The equation of stable semivariogram is shown below:

$$\gamma(h) = \sigma(0)\left[1 - \exp(-\frac{3h^{\omega}}{r^{\omega}})\right] \quad (15)$$

where $\sigma(0)$ is sill, r is the effective range parameter; distance at which 95% of sill reached. As described previously, nugget, sill, range and the power value ω are summarized in Table 13.

Using the semivariogram models developed for each event date, RK technique is employed to interpolate the values at unobserved locations and generate residual estimation maps. The residual maps are then added back to the generated maps using MLR in the previous step. The following

figures show two examples of the estimation results for Highways 16 and 2. To ensure the models selected provide the best fit, crossvalidation is used to quantitatively assess the "goodness of fit" using various statistical measures such as root-mean-square-error (RMSE). It is a verification process in which each observation is "removed with replacement" to estimate a new value at the same site of the removal. After that, 30% testing datasets are used to validate the kriging estimation. Validation is a necessary step to further test the goodness of fit of the calibrated model using RMSE or other measures. The crossvalidation results of model performance are depicted in Figure 9 (b, d) and the detailed statistics are summarized in Table 14.

Table 13. Semivariogram models for RST

Highway	Segment	Date	RST			
			Nugget	Sill	Range (km)	Power value
Highway 16	A	20141218	0	0.3233	17.92	0.57
		20150203	0	0.3269	5.24	0.88
		20150209	0.0317	0.3906	13.95	0.87
		20161201	0.0177	0.1188	2.55	2.00
	B	20141218	0.0386	0.3991	5.14	1.22
		20150203	0.0742	0.2657	2.51	1.77
		20150209	0.0284	0.2014	14.13	1.07
		20161201	0	0.0793	19.04	0.78
	C	20141218	0.1306	0.6967	24.51	1.03
		20150203	0.0663	0.203	19.71	1.21
		20150209	0.0267	0.1993	26.04	1.84
		20161201	0.0105	0.3626	10.29	1.83
Highway 2	A	20150209	0.0153	0.0546	5.133	1.54
		20150113	0.0001	0.1158	0.935	2.00
	B	20150209	0	0.119	32.344	0.61
		20150113	0.021	0.47	5.774	1.53
	C	20150209	0.017	0.2052	12.787	1.16
		20150113	0.019	0.1026	6.479	1.46

Figure 10 and 11 vividly show the comparison between the estimation results and the observations for Segment A. A visual inspection confirms that the estimated RST models well capture the general variation pattern seen in the observed dataset. The largest difference between the estimated and observed values is less than 0.5°C, attesting the strong predictability of the RK models developed in this study.

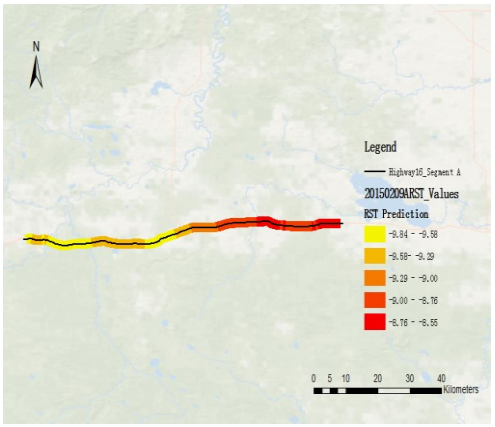

(a) RST map for highway 16

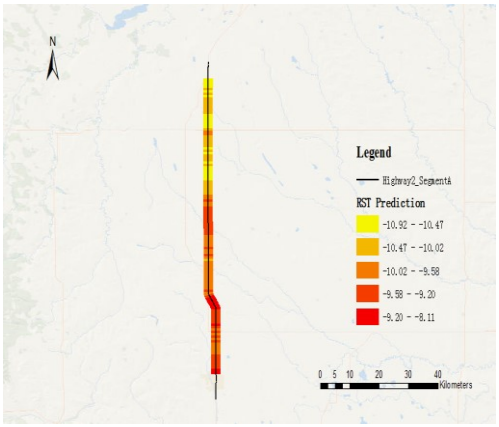

(b) RST map for highway 2

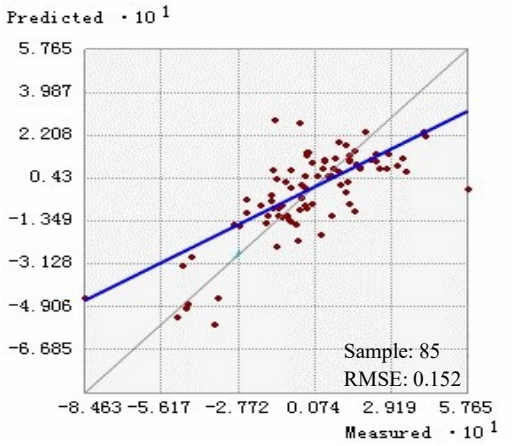

(c) Crossvalidation for highway 16

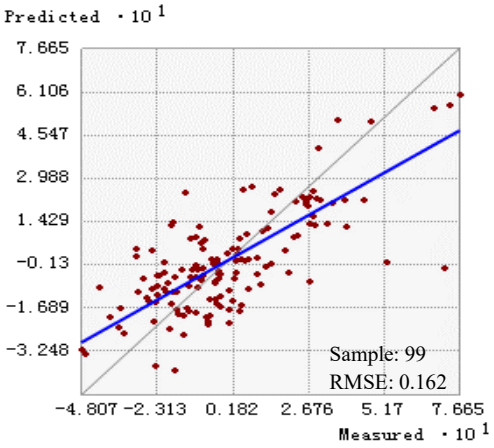

(d) Crossvalidation for highway 2

Figure 9. Final RST estimation results for two highways on same date: February 9th, 2015

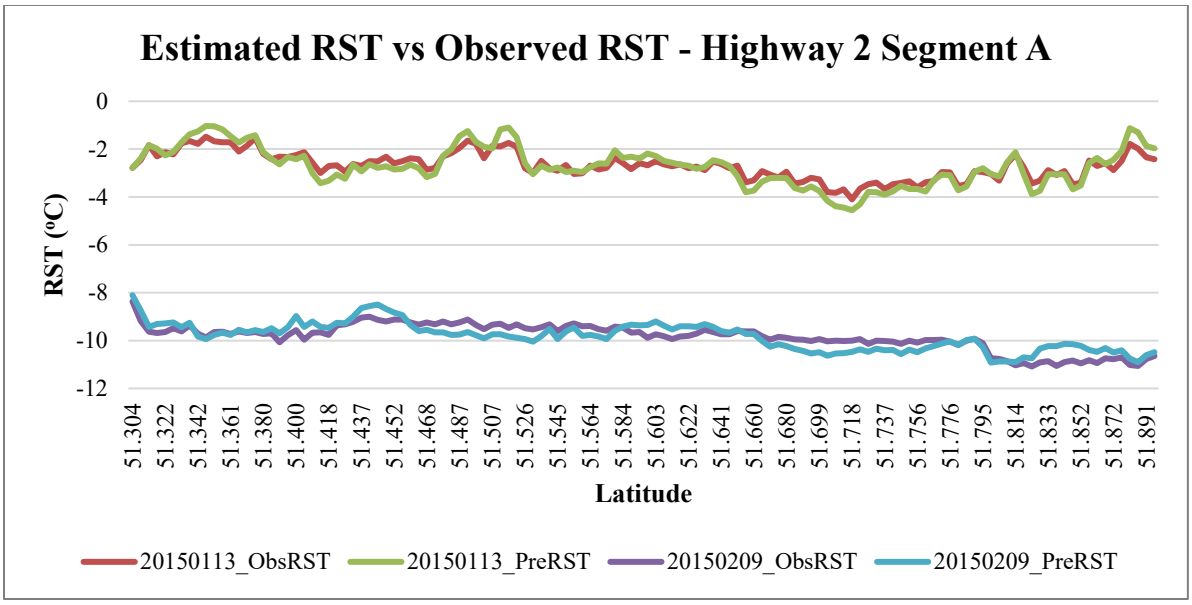

Figure 10. Estimated RST vs observed RST for Highway 2 segment A

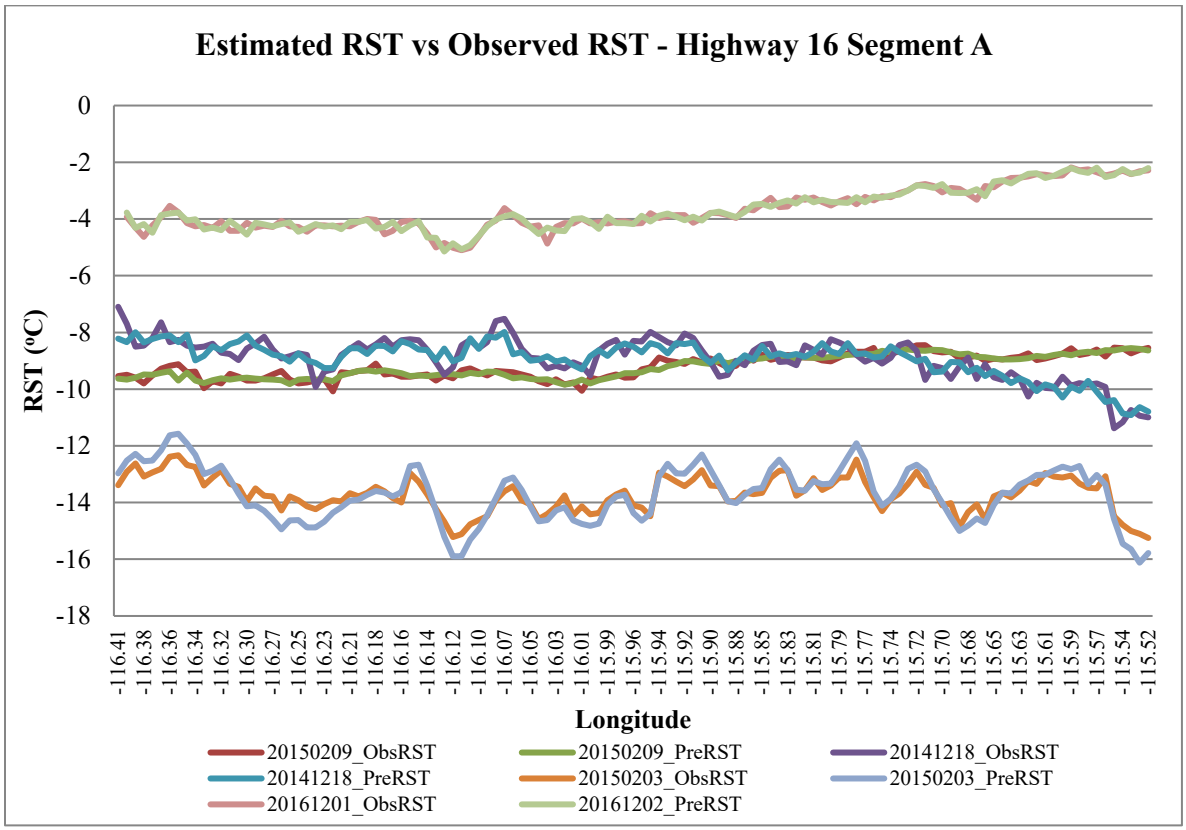

Figure 11. Estimated RST vs observed RST for Highway 16 segment A

As for the crossvalidation of training data sets, the RMSE values of all study segments were found to be relatively small, indicating a good estimation capability of the developed models.

Additionally, the average RMSE value from validation of the testing datasets is 0.275ºC, representing a good performance of the estimation models and further supporting the significant forecasting ability of the developed models. To see how close the data are to the fitted kriging models, the mean standardize error was calculated and the value is -0.001, which is almost equal to zero. This shows that it greatly enhances the predictive power of the MLR models. All the results of this study indicate that RK has the potential to be adopted to improve the accuracy of model outputs by taking into account the geographical parameters and quantifying the autocorrelation structure of the variable under investigation.

Table 14. Summary of model results for RST estimation

Highway	Segment	Date	Category	RMSE of Calibration	RMSE of Validation
Highway 16	A	20141218	light	0.382	0.455
		20150203	heavy	0.364	0.318
		20150209	moderate	0.152	0.162
		20161201	low	0.221	0.469
	B	20141218	light	0.365	0.369
		20150203	moderate	0.39	0.407
		20150209	moderate	0.23	0.239
		20161201	low	0.11	0.285
	C	20141218	light	0.373	0.442
		20150203	light	0.271	0.33
		20150209	light	0.154	0.231
		20161201	low	0.122	0.136
Highway 2	A	20150209	light	0.175	0.159
		20150113	light	0.275	0.376
	B	20150209	light	0.157	0.153
		20150113	light	0.258	0.214
	C	20150209	light	0.179	0.21
		20150113	light	0.001	0.001

4.3.2 Model development for RSI

As mentioned above, the mobile RWIS provides grip information to represent road surface slipperiness. The grip value varies from 0 to 1, indicating a perfectly icy condition to a perfectly dry condition, respectively. Since the characteristic of grip is quite close to RSI, the grip value is used to represent RSI in this study.

The grip value is not a direct measurement as road surface friction is; however it is calculated by a certain algorithm that takes into consideration the road surface contaminants, such as snow and ice. Since road surface slipperiness may well be associated with physical randomness, and the factors attributing to such are difficult to define, OK approach is implemented to model RSI values. Since the previous analysis has proven the good performance of the kriging model and crossvalidation is a strong statistical method to evaluate the model goodness of fit, all the RSI datasets are used in model calibration this time.

The procedure required to develop OK models is the same as the three steps described previously. It is worthwhile reiterating that the semivariogram and kriging models no longer need to deal with residuals obtained from the MLR analysis and that the end results of OK are the interpolated RSI maps (refer to Section 3.3.2 for details). Table 15 shows the developed semivariogram models and Figure 12 shows two examples of RSI estimation maps for different highways.

Table 15. Semivariogram models for RSI estimation

Highway	Segment	Date	RSI			
			Nugget	Sill	Range (km)	Power value
Highway 16	A	20141218	1.48E-03	4.71E-03	2.35	1.99
		20150203	0.00E+00	5.12E-02	5.18	1.13
		20150209	3.15E-03	9.10E-04	1.79	2.00
		20161201	0.00E+00	1.15E-03	19.92	0.32
	B	20141218	1.17E-04	1.63E-05	3.84	2.00
		20150203	0.00E+00	4.78E-02	22.11	0.36
		20150209	1.02E-03	3.73E-03	6.81	1.32
		20161201	6.99E-06	8.70E-05	4.98	1.12
	C	20141218	2.31E-04	1.41E-04	7.57	0.89
		20150203	4.19E-03	3.40E-03	4.44	1.73
		20150209	9.97E-04	2.21E-03	4.38	1.93
		20161201	0.00E+00	6.10E-05	33.93	0.36
Highway 2	A	20150209	2.46E-04	1.19E-04	34.733	1.97
		20150113	2.38E-04	5.30E-05	1.427	1.35
	B	20150209	0.00E+00	7.25E-03	2.169	0.85
		20150113	0.00E+00	9.49E-04	11.804	0.41
	C	20150209	0.00E+00	2.45E-03	2.627	0.92
		20150113	7.00E-06	2.06E-05	6.016	0.89

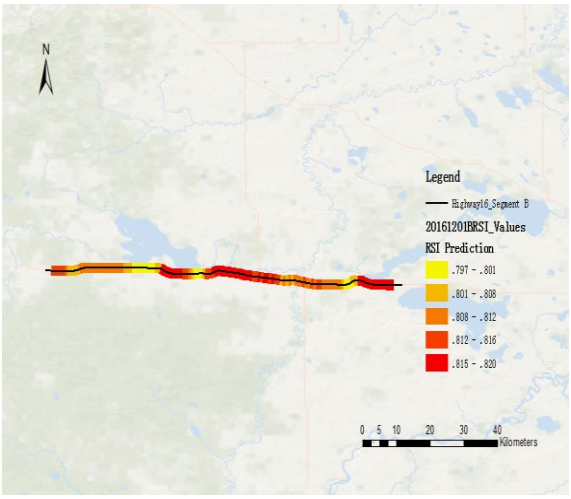

(a) RSI map for highway 16

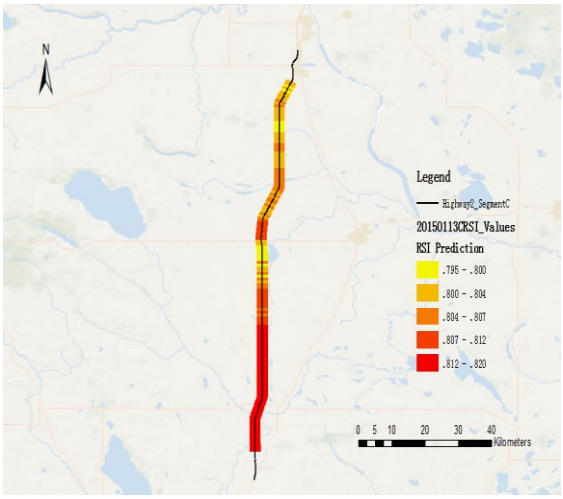

(b) RSI map for highway 2

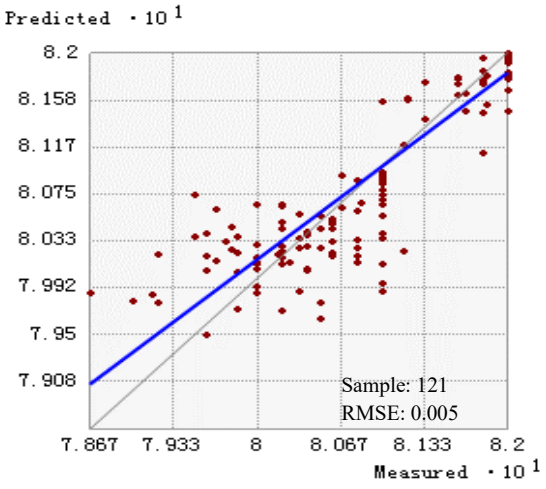

(c) Crossvalidation for highway 16

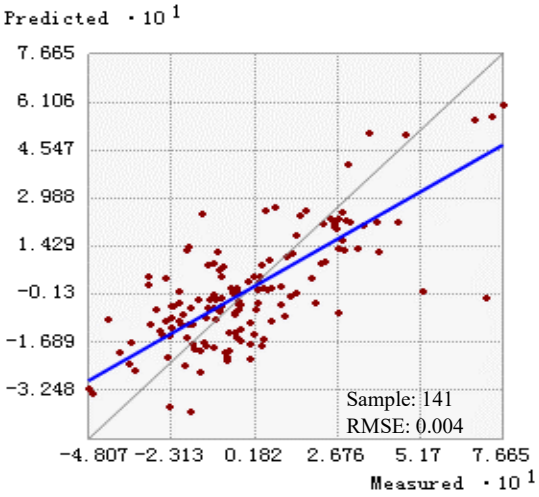

(d) Crossvalidation for highway 2

Figure 12. Final RSI estimation results for two highways on two dates

After kriging interpolation, crossvalidation is used to measure model performance. The results are shown in Table 16. The RMSE values are quite close to zero with its average value for all events being 0.046ºC and it is even smaller than the RST estimation results. This may be caused by the small magnitude of RSI data sets. These results also represent the strong predictive power of kriging models. Figure 13 and 14 indicate that the estimation error is less than 0.1, which also supports the satisfactory performance of this model. Additionally, if other auxiliary information

like traffic information and meteorological parameters are available, RK can also be applied to improve the model performance.

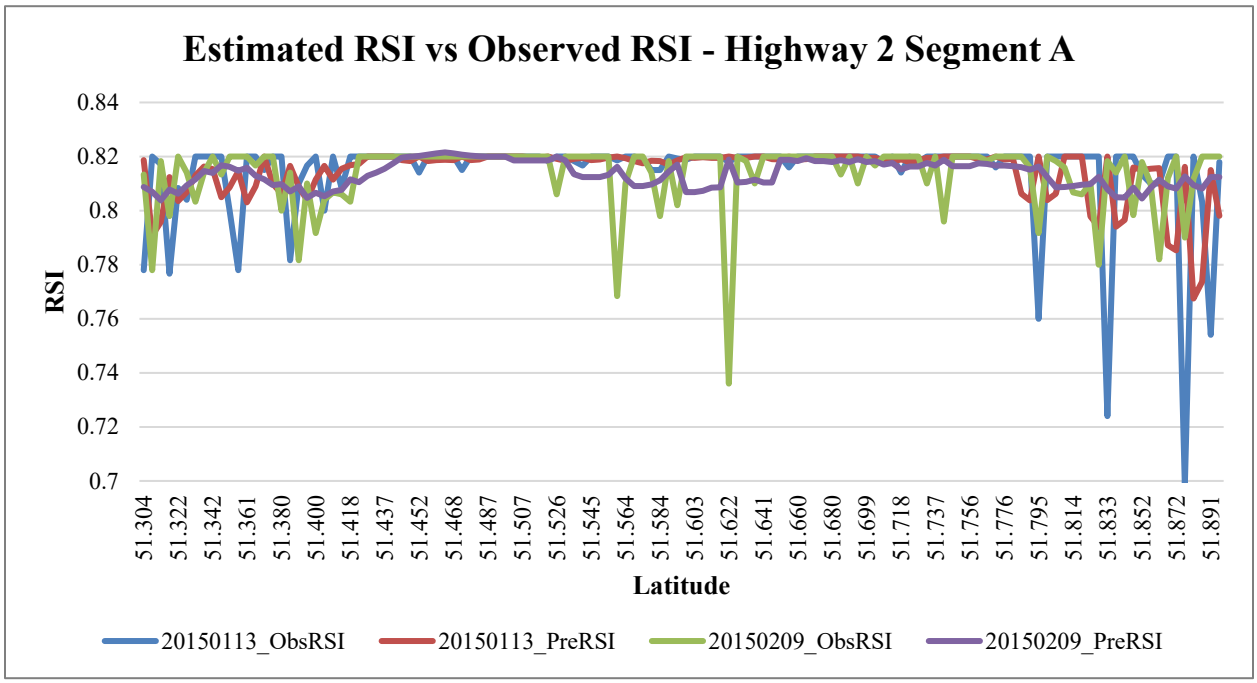

Figure 13. Estimated RSI vs observed RSI for Highway 2 Segment A

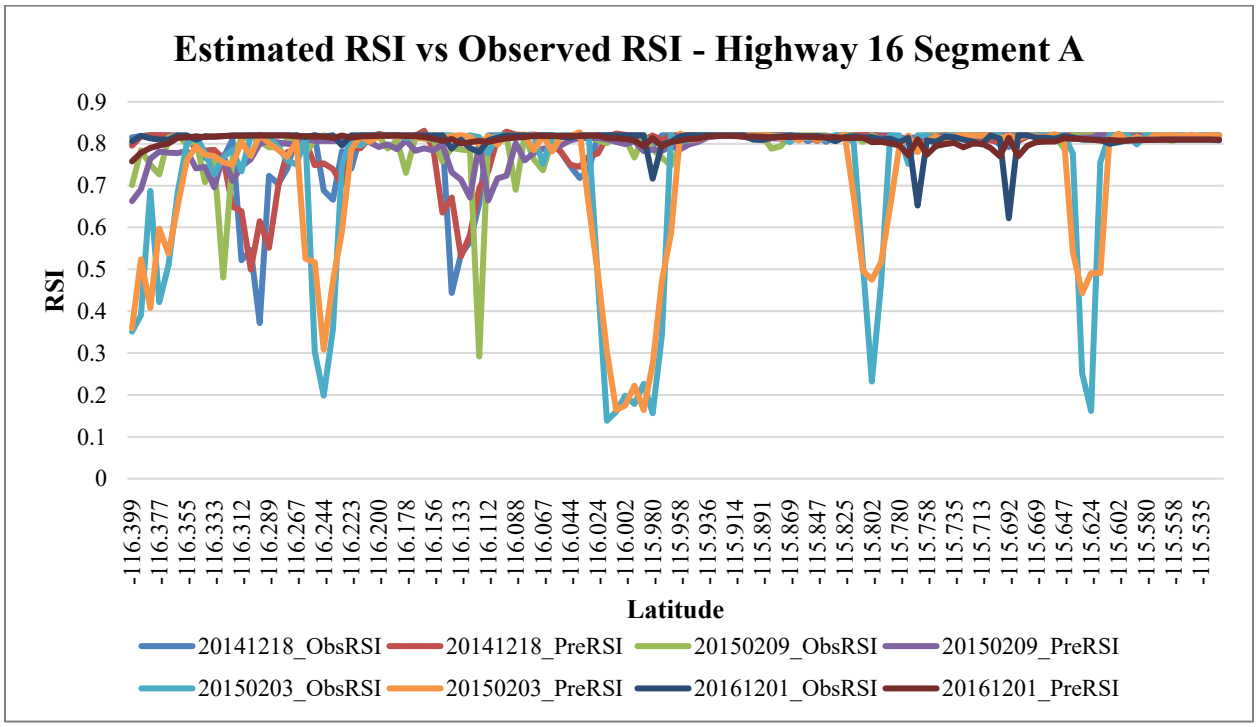

Figure 14. Estimated RSI vs observed RSI for Highway16 segment A

Table 16. Summary of model results for RSI estimation

Highway	Segment	Date	Category	RMSE of Crossvalidation
Highway 16	A	20141218	light	0.047
		20150203	heavy	0.085
		20150209	moderate	0.169
		20161201	low	0.036
	B	20141218	light	0.011
		20150203	moderate	0.157
		20150209	moderate	0.041
		20161201	low	0.005
	C	20141218	light	0.018
		20150203	light	0.075
		20150209	light	0.036
		20161201	low	0.006
Highway 2	A	20150209	light	0.018
		20150113	light	0.020
	B	20150209	light	0.068
		20150113	light	0.029
	C	20150209	light	0.040
		20150113	light	0.004

4.3.3 Weather Events Influence on RSC Variations

By examining one of the critical semivariogram model parameters, the sill, which represents the variance in data based on the spatial structure, varies a lot. For example, the values vary from 0.05 to 0.7 of RST data, and from 1.6E-5 to 0.05 of RSI data. Similarly, the range of each data set also varies to a greater extent. One possible cause for different semivariogram values could be

attributed to the differences in weather conditions. To verify this possibility, the exponential semivariogram model, rather than the optimally fitted model, was used to re-calculate the range of detrended RST and non-detrended RSI data. The relationship between the sill values and the event category can be seen in Figure 15 and 16.

In terms of RST semivariogram, the sill values are found to be negatively correlated with weather events, which means when the wind speed increases, surface temperature tends to be more consistent and the variability is low. For RSI, it shows a different pattern, in that the sill values increase with heavier snow amounts. If the surface is perfectly dry or snow covered, the RSI value will be fairly consistent along the whole road segment, which is easy to distinguish. This finding can be particularly useful when making an inference about estimating road surface temperatures, via different weather groups, since the parameters for both the semivariogram and kriging models should be similar for each.

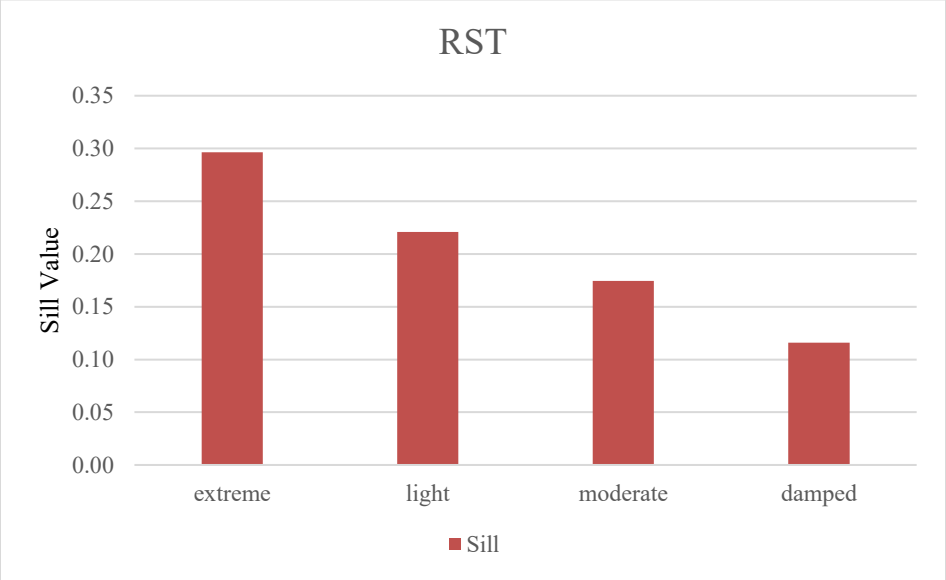

Figure 15. The relationship between semivariogram sill and RST weather category

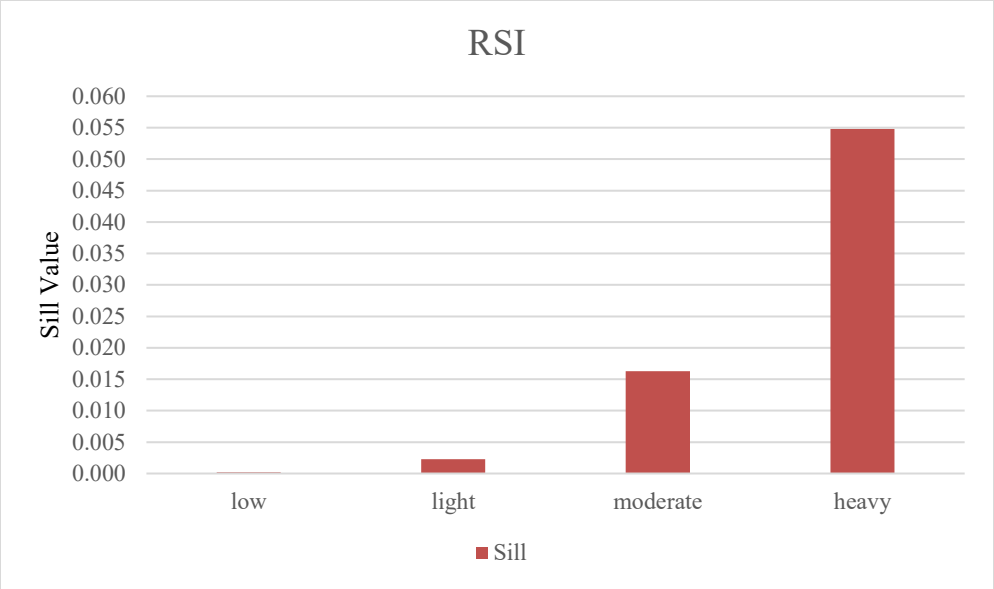

Figure 16. The relationship between semivariogram sill and RSI weather category

4.3.4 Comparison with Other Spatial Interpolation Methods

For a long time, spatial interpolation methods have been investigated to estimate the spatial distribution of the variable of interest. The accuracy of the interpolation results is influenced by many aspects, like data density, measurement error, and topography or other climate factors (Jain and Flannigan, 2017). However, these methods have been seldom applied to estimate the road surface conditions. In order to explore whether, the proposed method RK performs better than other methods, four widely applied interpolation methods including inverse distance weighting (IDW), global polynomial interpolation (GPI), local polynomial interpolation (IPL), thin plate spline (TPS) are compared with RK to estimate RST using mobile RWIS data.

The details about how these interpolation methods work are introduced in section 3.4. For evaluating and comparing the model performance, the crossvalidation technique is adopted. The sample data was arbitrarily divided into two datasets, with one used to train a model and the other used to validate the model (Sankar et al., 2018). The root mean square error (RMSE) for error

measurement is used to assess the accuracy of interpolation results. Table 17 shows the crossvalidation results of different methods. In terms of segment analysis, RK outperforms the other methods for all segments except Highway 16, segment B. For that case, the difference between RMSE values of RK and LPI is quite small; almost negligible. It is more obvious that RK has the smallest average RMSE with regards to overall model evaluation. To quantify the relative performance, the percentage improvement of RK over other interpolation methods is also calculated. It is clearly indicated that RK is able to increase the performance over each model by at least 9%. The accuracy of interpolation results will increase by approximately 50% when RK is chosen to replace GPI.

One possible reason to explain this result is that RK not only deals with the deterministic element, it also deals with stochastic part compared with other methods. It incorporates data spatial autocorrelation and statistically optimizes the weights to estimated unknown locations. This comparison analysis shows the importance of the proposed method for RSC estimation improvement.

Table 17. Crossvalidation results of all the interpolation methods

Highway	Segment	RK	IDW	GPI	LPI	TPS
16	A	0.281	0.302	0.472	0.323	0.348
	B	0.266	0.278	0.502	0.266	0.284
	C	0.230	0.237	0.489	0.246	0.265
2	A	0.225	0.231	0.346	0.253	0.242
	B	0.208	0.239	0.499	0.218	0.218
	C	0.090	0.177	0.420	0.177	0.140
Average RMSE		0.231	0.253	0.466	0.257	0.266
Performance increased by		N/A	8.92%	50.44%	10.05%	13.13%

4.4 Phase II – Applicability of RK for Inferring RSC via Stationary RWIS

Since what is commonly available to highway maintenance personnel is stationary RWIS data, further investigation would be required to infer the RSC using stationary RWIS data, based on the findings generated from mobile RWIS data. As the semivariogram models developed in Phase I are used to quantify the spatial structure of our mobile RWIS data, it is worthwhile to scrutinize how the model variables (i.e., sill, nugget, and range) could be used in conjunction with stationary RWIS data to conjecture the conditions between the RWIS stations. Therefore, the following study aims at applying the RK method to integrate the stationary and mobile RWIS data to draw a compete map of RSC.

As no related RSI or grip information is provided by stationary RWIS, RST data sets are chosen to show the idea of the proposed method. In addition, the preliminary comparison of stationary and mobile RWIS data reveals that there is about 2^{o}C difference between the two data collection methods. This difference may be due to different senor types as well as testing locations. For example, stationary RWIS sensors are more likely to be affected by the accumulation of surface contaminants (i.e., snow, ice). Since the primary goal of Phase II is to propose a methodological framework that estimates conditions between each pair of existing RWIS stations using known semivariogram models, RST collected by a stationary RWIS is assumed to be the same as that collected by a mobile RWIS unit, at a similar time and location.

The study area of Phase II is extended to include more RWIS stations and includes total length of approximlately150 km of Highway 16, starting from Edson, and a main section of Highway 2, between Edmonton and Calgary (approx. 180 km and 300 km in length). This analysis will focus on the whole stretch of highways instead of segment analysis. There are four RWIS stations on Highway 16 and seven stations on Highway 2, while one station on Highway 2 does not work

(marked in grey), as shown in Figure 17. Thus, data from six stations are considered in this analysis. In addition, the stationary RWIS measurement used for interpolation is at or close to the time when a mobile RWIS unit passes by such that the estimated RSC can be compared with mobile RWIS measurements to validate the model performance. Table 18 summarizes the locations of and surrounding information for these stations.

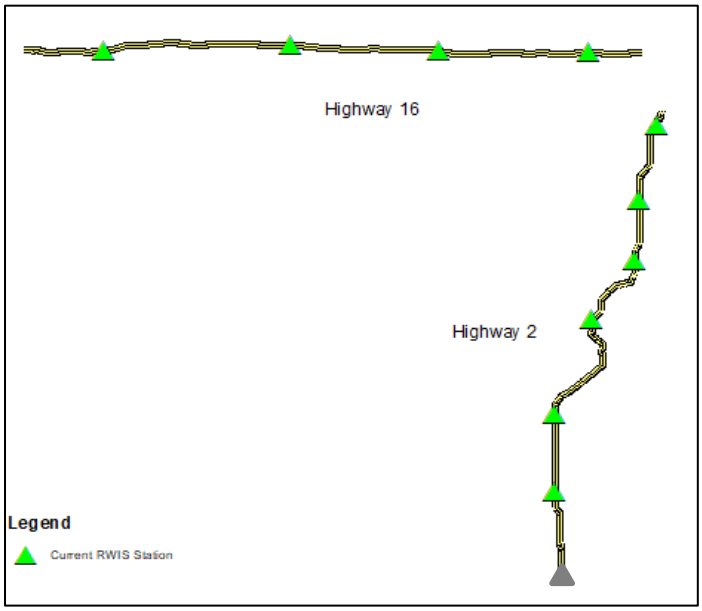

Figure 17. Current RWIS stations on Highway 16 and Highway 2

Table 18. Geographical information of RWIS stations

Highways 16 & 2 RWIS Station Information				
ID	Lat	Long	Altitude	Slope
MX0500	53.578	-116.046	884.900	1.772
MX0501	53.609	-115.207	800.000	0.569
MX0502	53.582	-114.546	794.000	0.841
MX0503	53.571	-113.875	670.000	0.472
MX0473	-114.025	51.534	1037.890	1.989
MX0474	-114.026	51.898	992.100	1.260
MX0475	-113.664	52.608	839.670	2.037
MX0476	-113.856	52.331	892.185	0.593
MX0477	-113.643	52.890	796.790	2.050
MX0478	-113.568	53.236	736.290	1.062

4.4.1 Application of RK for RSC Estimations using Stationary RWIS Data

Understanding the spatial structure that indicates how data varies over the space of RSC is essential before interpolating stationary RWIS data. Hence, the semivariogram models developed from the residuals of MLR using mobile RWIS in Phase I of this thesis become the foundation of Phase II. The MLR model generated previously using mobile RWIS data is applied to stationary data to remove the possible influence from the geographical features. After this, OK is implemented to interpolate the stationary RST residuals with the semivariogram model variables (i.e., sill, nugget, and range) constructed in Phase I. Lastly, the interpolated results are added back to the MLR estimations to generate final OK estimates, which are then validated using mobile RWIS observations. All the analyses have been conducted in R statistical computing environments with a "gstat" package (Pebesma, 2004).

As mentioned previously, the stepwise MLR analysis was first applied to mobile RWIS data to remove the possible influence of external features (i.e., geography and topography) on RST variations. Note that the significance of each parameter was tested on the bases of the 95% confidence interval and a 5% level of significance. Table 19 shows the MLR results for whole stretch of Highways 16 and 2, respectively.

From Table 19, it can be clearly seen that all regression coefficients pertaining to geographic characteristics make intuitive sense. However, none of the variables are significant for Highway 16, on 29th February, 2015, indicating the geographical factors have little influence on the variation on RST. Since the purpose of the regression analysis is to detrend the data, if there is no trend caused by related covariates, the residuals will be calculated by subtracting the local mean

of the data sets. The same MLR model is also applied on stationary RWIS measurement to calculate the residuals for further analysis.

Table 19. MLR results for Highway 16 and Highway 2 analysis

Highway	Date	Significant Variables	Sign of Coefficients	R^2
Highway 16	20141218	latitude	(-)	61%
	20150203	latitude	(-)	37%
	20150209	-	-	-
	20161201	altitude	(-)	83%
Highway 2	20150113	altitude	(-)	37%
	20150209	longitude / slope	(-) / (-)	15%

Next step is to use semivariogram to quantify the spatial autocorrelation structure of the mobile RWIS residuals, which is a prerequisite for the interpolation of stationary data. The three key parameters of semivariogram model are summarized in Table 20. The semivariogram model developed herein will replace the one that should be generated by stationary RWIS data during kriging interpolation, as it is able to provide a clearer insight of RST variation than that developed only by several stationary observations. To compare with observed mobile RWIS data, the estimation results will be added back to the MRL results of both stationary and mobile RWIS data.

Table 20. Semivariogram models for residuals of RST from mobile RWIS

Highway	Date	Nugget	Sill	Range (km)
Highway 16	20141218	0	1.4	25.84
	20150203	1.2	1.8	20.53
	20150209	0.01	0.29	34.32
	20161201	0	0.33	14.41
Highway 2	20150113	0	1	17.28
	20150209	0.04	0.62	46.13

The following Figures 18 and 19 show two examples of the estimation results for Highways 16 and 2, respectively. The grey bars indicate the location of the RWIS stations. As can be seen from these figures, the general trend of how RST variance is well captured by the estimation results, especially on days that the fluctuation of RST is not dramatic.

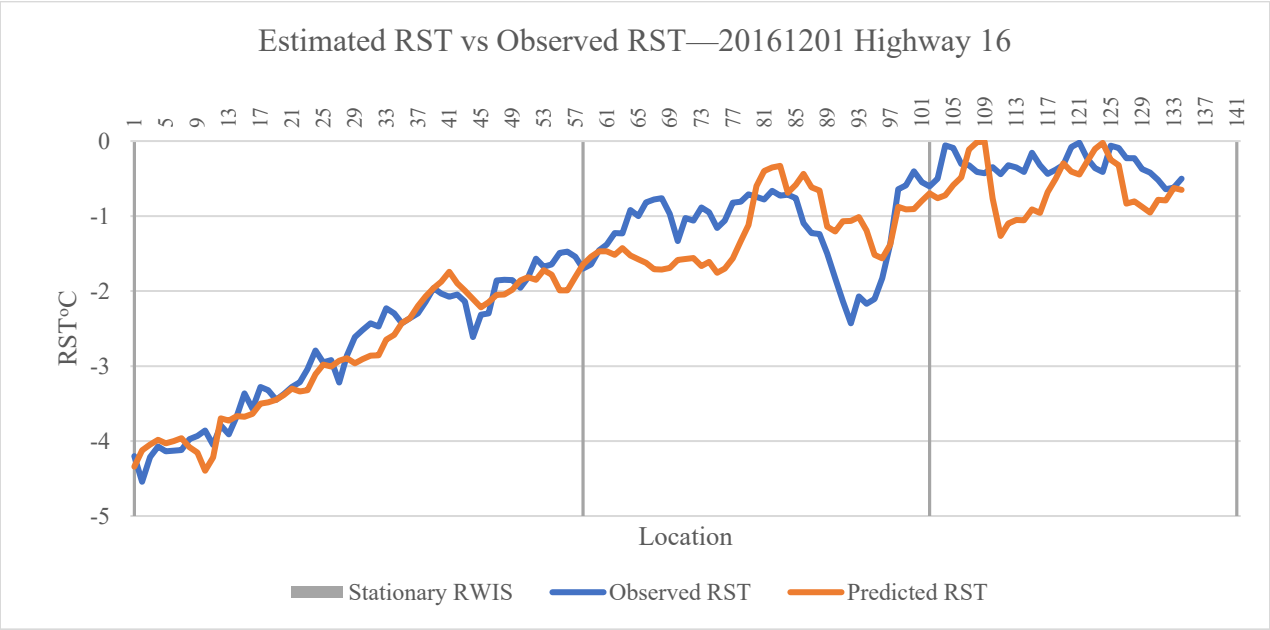

Figure 18. Estimated RST vs observed RST on 20161201 for Highway 16

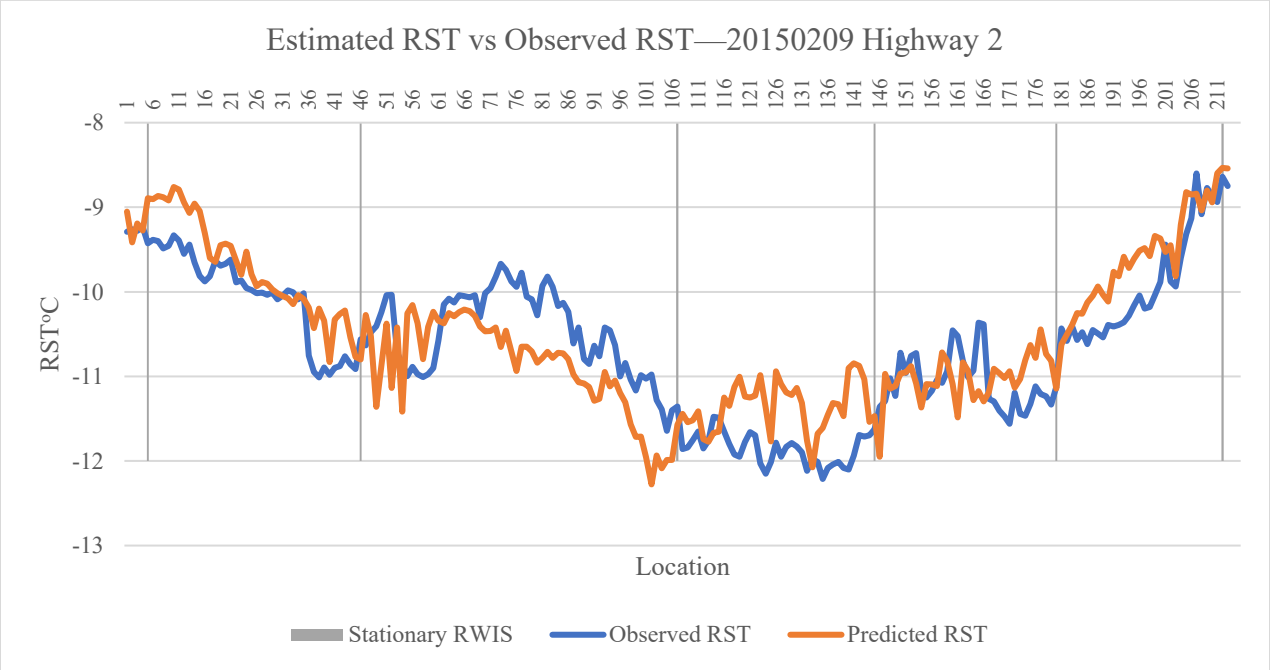

Figure 19. Estimated RST vs observed RST on 20150209 for Highway 2

To better evaluate the model performance, statistical measurements, including mean absolute error (MAE), root mean square error (RMSE), and standardize root mean square error, are adopted to quantitatively assess the goodness of fit. MAE measures the average magnitude of the errors in estimation and RMSE indicates how closely the model estimates the measured values. For standardized RMSE, the value should be close to one if the estimation standard errors are valid. The evaluation of model performance is depicted in Table 21.

According to Table 21, it is noticeable that all the MAE and RMSE values are smaller than 1°C, indicating a good estimation capability. In terms of Standardized RMSE, all the values are close to one that demonstrates the estimated results have similar variability with the observed data. The model validation results show the feasibility to apply RK to integrate stationary and mobile RWIS data together to improve the accuracy of RST estimation.

Table 21. Summary of model performance

Highway	Date	MAE	RMSE	Standardized RMSE
Highway 16	20141218	0.87	0.88	1.09
	20150203	0.52	0.66	1.04
	20150209	0.31	0.41	1.01
	20161201	0.34	0.43	1.04
Highway 2	20150113	0.63	0.79	1.07
	20150209	0.44	0.52	1.02

4.4.2 Sensitivity Analysis

Sensitivity analysis is a common technique to perform quantitative assessments that evaluate how different model inputs will impact the uncertainty of the outputs under a given set of assumptions.

In this case, the sensitivity analysis is conducted to verify whether the changes in data density (i.e., number of RWIS stations) will affect the model performance. As there are only a few stations on the area of interest, the mobile RWIS measurements have been randomly selected and assumed to represent additional "new stationary RWIS" to scrutinize the performance of the developed models. Table 22 describes the evaluation of the sensitivity analysis.

Table 22. Sensitivity analysis results

Highway	Date	# of stns + added stns	MAE	RMSE	Standardized RMSE
Highway 16	20141218	4	0.87	0.88	1.09
		4+5	0.73	0.897	1.00
		4+10	0.67	0.84	1.00
		4+15	0.64	0.81	1.00
	20150203	4	0.52	0.66	1.04
		4+5	0.49	0.63	1.00
		4+10	0.47	0.615	1.00
		4+15	0.45	0.607	1.00
	20150209	4	0.31	0.41	1.01
		4+5	0.3	0.39	1.00
		4+10	0.27	0.36	1.00
		4+15	0.25	0.35	1.00
	20161201	4	0.34	0.43	1.04
		4+5	0.32	0.41	1.02
		4+10	0.27	0.35	1.00
		4+15	0.26	0.34	1.01
Highway 2	20150113	6	0.63	0.79	1.07
		6+5	0.63	0.83	1.06
		6+10	0.47	0.62	1.01
		6+15	0.42	0.57	1.01
	20150209	6	0.44	0.52	1.02
		6+5	0.34	0.43	1.00
		6+10	0.31	0.4	1.00
		6+15	0.3	0.39	1.00

It can be seen from the table that the density of RWIS stations is changed by five more, ten more, and fifteen more. Overall, the performance increases with the increase of RWIS stations. It is interesting to find that the increase between fifteen more stations and ten more stations is smaller compared with the other two situations. The findings attest that the marginal benefits gained by adding additional RWIS stations decrease as the number of stations increases. There are two days that show a different story, which is 20141218 for Highway 16 and 20150113 for Highway 2. When there are five more stations, the RMSE value increases instead of decreases. One possible cause for this phenomenon could be the selection of the new stations' location. If the selected value happens to be the peak value or the valley value, it will enlarge the difference between the estimated value and the observed value. The circled part in Figure 20 vividly illustrates this problem.

From the sensitivity analysis, even though the model performance improves when there are more RWIS stations, it is slight and does not make a huge difference to the results, which further supports the applicability of the proposed method.

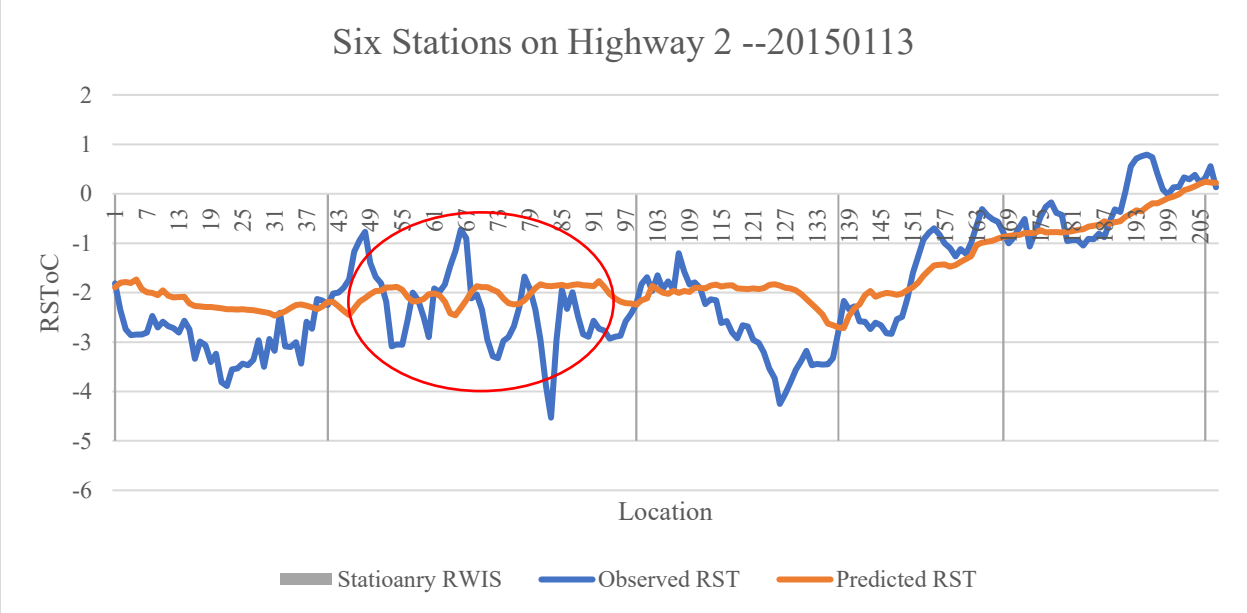

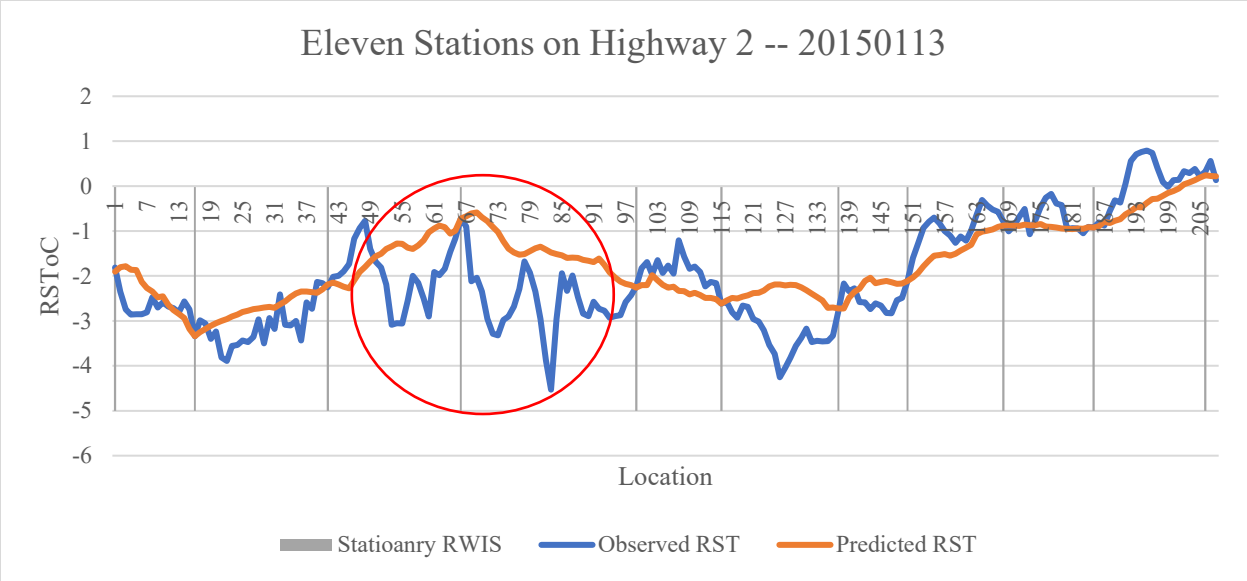

Figure 20. The difference of inputs density influence

4.4.3 Recommendation for New RWIS Locations

As can be seen from the sensitivity analysis, the selected of RWIS location is also a factor that influences the estimation accuracy. Besides, the installation of RWIS stations is expensive and the spatial coverage is limited. Therefore, it is important to choose an appropriate site to locate RWIS stations to help transportation agencies make more informed decisions on a strategic RWIS extension planning process. To address such challenging issues, an RWIS station location allocation optimization is proposed with an objective of minimizing the total kriging estimation errors (i.e., OK variance). The objective function formulated, and its related computation process are shown below.

$$G = \begin{bmatrix} \gamma(x_1,x_2)\ \gamma(x_2,x_1) \dots \gamma(x_k,x_1)\ 1 \\ \gamma(x_1,x_2)\ \gamma(x_2,x_2) \dots \gamma(x_k,x_2)\ 1 \\ \dots \\ \gamma(x_1,x_k)\ \gamma(x_2,x_k) \dots \gamma(x_k,x_k)\ 1 \\ 1 \quad 1 \quad \dots \quad 1 \quad 0 \end{bmatrix} \tag{16}$$

Where, x_i (i=1, 2, …, k) is the sampling site of a sample subset of size k, and in this case, k is equal to the number of RWIS stations. $\gamma(x_i, x_j)$is the semivariance between sampling site i and j.

$$\mathrm{g} = [\gamma(x_0, x_1)\ \gamma(x_0, x_2) \ldots\ \gamma(x_0, x_k)\ 1]' \tag{17}$$

Where, x_0 is the estimation location and x_i (i=1, 2, …, k) is the sampling site of a sample subset of size k. Then the minimum mean square error for OK for the estimation location x_0 is:

$$\sigma_{OK}^2(x_0) = g' G^{-1} g \tag{18}$$

Based on above three equations, the objective function of this work can be formulated as below:

Subject to: $$f(w) = \frac{\sum_{i=1}^{n-k} \sigma_{OK}^2(x_0)}{n} \tag{19}$$

$n =$ Total number of candidate RWIS station locations in the road

To find the optimal solution to this large-size optimization problem, a heuristic algorithm is usually used. Particle Swarm Optimization (PSO) is a random search algorithm that simulates a natural evolutionary process and performs good characteristics for solving these optimization problems (Xu et al., 2010). First proposed by Kennedy and Eberhart (Kennedy and Eberhart, 1995), PSO has the characteristics of being of easily implemented and computationally inexpensive, since its memory and CPU speed requirements are low. All of these make PSO widely used in scientific computation.

PSO is a population-based optimization method, and it is initialized with a population of random particles and the algorithm searches for optima by updating generations. Each particle is treated as a point in an *n*-dimensional space. The i^{th} particle is represented as $\boldsymbol{x}_i=(x_{i1},x_{i2},\ldots,x_{in})$. The best previous position p_{best} of the i^{th} particle is recorded and represented as $\boldsymbol{p}_i=(p_{i1}, p_{i2},\ldots,p_{in})$. The index of the best particle among all the particles in the population (global model) is represented by the subscript *g*. The rate of the position change (velocity) for particle *i* is represented by $\boldsymbol{v}_i=(v_{i1},v_{i2},\ldots,v_{in})$. The particles are manipulated according to the following equations:

$$v_{id} = \omega v_{id} + c_1\zeta(p_{id} - x_{id}) + c_2\eta(p_{gd} - x_{id}) \tag{20}$$

$$x_{id} = x_{id} + v_{id} \tag{21}$$

where d is the dimension ($1 \leqslant d \leqslant n$), c_1 and c_2 are positive constants, ζ and η are two random functions in the range [0,1] and ω is the inertia weight. The performance of each particle is measured according to a predefined fitness function, which is related to the problem to be solved. The workflow of PSO to look for locations for additional two RWIS stations is shown in Figure 21.

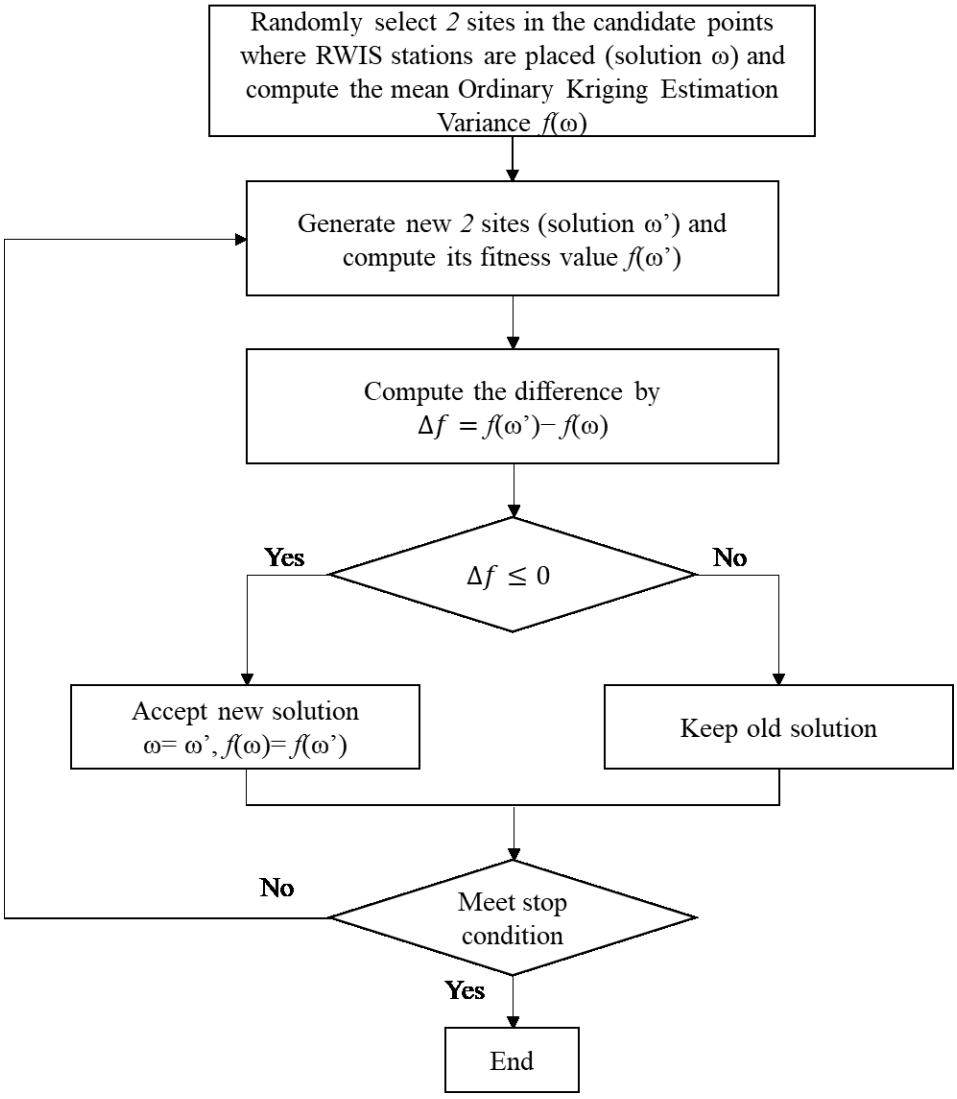

Figure 21. Workflow of PSO in this optimization problem

As can be seen from Figure 21, this optimization is an iterative process with an objective function to minimize the mean OK variance (or maximize coverage of RWIS) based on existing RWIS stations and additional RWIS stations to be deployed. For an illustration purpose, two RWIS stations are added to the two highway networks under investigation – Highways 2 and 16. It is worthwhile noting that the framework proposed in this thesis can be used for any number of RWIS stations to be installed on any given highway network.

Here, observations made on 18th December, 2014, along Highway 16, and 13rd January, 2015, along Highway 2, are selected as examples to show the applicability of the optimization method developed herein. Each highway is divided into over 200 candidate points with the interval of 1 km between each, using ArcGIS 10.3.0 for the placement of new RWIS stations. The semivariogram models developed from section 4.4.1 are applied to provide the autocorrelation range of RST observations. Number of iterations was set to 200, after which the search process for the two locations was set to stop. The example of the optimization results for finding the best locations of additional two RWIS stations on Highway 2 and Highway 16 are shown in Figure 22.

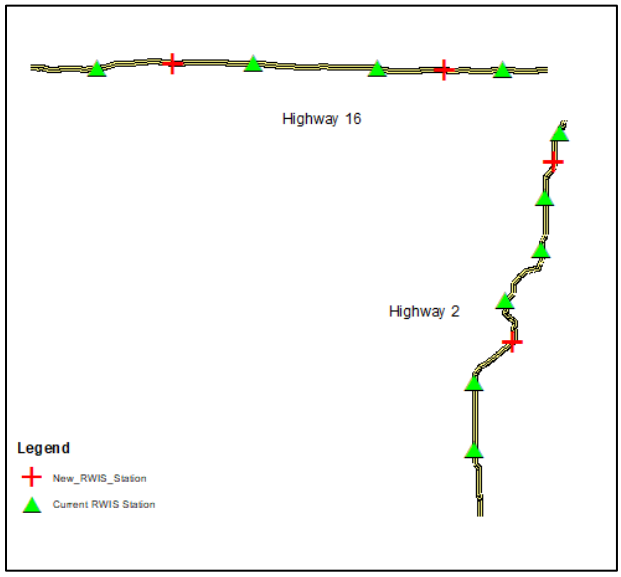

Figure 22. Optimal locations for additional two RWIS stations after optimization

4.5 Summary

In this chapter, two phase studies, including the evaluation on the feasibility of using RK to estimate RSC and the application of RK with stationary RWIS data, are illustrated via case studies on two highways in Alberta.

The first phase proposes a methodological framework, in which RK is developed and implemented to estimate RST and RSI using mobile RWIS data. Geographical parameters, including locational attributes (lat/long), altitude, slope and NDVI, which could potentially impact the variation of nocturnal RSTs, are analyzed by removing the trend in the target variable. All the model calibration and validation results show the proposed method herein is able to provide a good estimation when compared with actual RSC measurements. The comparison analysis with other spatial interpolation methods also indicate the superiority of RK in terms of estimation accuracy.

For Phase II, the semivariogram model variables developed from mobile RWIS data in Phase I is used in conjunction with stationary RWIS measurements to estimate the RSC between RWIS stations. The low MAE and RMSE values obtained indicates the robust performance and applicability of the proposed method. In addition, to maximize the benefits of the RWIS network, the spatial autocorrelation range of RWIS measurements is applied to optimize the selection of new RWIS locations. This recommendation could in turn benefit road users in general (i.e., improved safety and mobility) and RWIS planning authorities in particular (i.e., maximizing the return on RWIS investments).

CHAPTER 5. CONCLUSIONS AND FUTURE WORK

This chapter provides a summary of the thesis, and highlights the major findings and the contributions of the work presented herein. The limitations of this thesis are also discussed in this chapter along with the recommendation for future study.

5.1 Research Overview

Inclement weather poses a threat to the safety and mobility of travelers during winter seasons, thus it is essential for transportation authorities to understand the spatial variation of RSC, such that hot spots (e.g., black-ice) can be identified more effectively to improve the efficiency of WRM. For this reason, the RWIS has gained attention and become widely used among highway agencies for its ability to provide real-time road weather and surface information. However, RWIS stations are not only expensive to install and operate but also only able to provide point measurement that is unrepresentative of distant area and. Considering the vast road network that require frequent monitoring in cold countries or regions, the varied road conditions, road weather and surface conditions between RWIS stations must be accurately estimated to instruct and guide successful WRM operations.

This thesis has been motivated by this challenging topic, and has attempted to tackle the problem of RSC estimation. This research contains two phases: Phase I is to evaluate the feasibility study of RK to estimate RSC; Phase II focuses on the application of RK using stationary RWIS data. Specifically, in Phase I, one of the renowned geostatistical methods called RK was proposed to show its feasibility for developing a systematic framework for estimating road surface condition. The variables of interest, RST and RSI were used separately, and spatial structures of these two data sets were quantified and modeled using semivariograms. Geographical parameters are prepared for removing their influence on RSC variation. Moreover, a comparison between

different spatial interpolation methods is conducted to see the applicability of RK. For Phase II, the RK method is applied with stationary RWIS data based on the prior information that quantifies the autocorrelation range of RSC. Lastly, a recommendation of new RWIS locations is provided based on the PSO method. Highway segments in Alberta, Canada, were used as a case study to implement the methods proposed in this research. The following section summarizes the main findings.

5.2 Research Findings

5.2.1 Phase I – Feasibility of a Geostatistical Method for RSC estimation

- The hybrid technique named RK has been developed for RSC estimation. As the geographical parameters, including locational attributes (lat/long), altitude, and slope, could potentially contribute to the variation of nocturnal RSTs, those parameters were prepared and analysed on a GIS platform for efficient data handling. Furthermore, LANDSAT satellite images were used to calculate the NDVI to examine the effect of landuse on RST. Using these external parameters as input, MLR models were first calibrated, followed by ordinary kriging to generate highly accurate RST estimation maps
- In terms of RST estimation, according to the MLR analysis using various geographical parameters, the key factors affecting the variation of RST were found to be longitude, altitude, slope, and NDVI. The sign of their coefficients makes intuitive sense – a negative sign for longitude (continentality), altitude (elevation), and slope (varied topography); and a positive sign for NDVI. The low R^2 values of the MLR models posed a strong need for furthering improving the model quality using the proposed kriging method. Then ordinary

kriging was used to interpolate the residuals of the MLR outputs and generate the final estimation maps with high R^2 values (higher than 80%).

- For RSI estimation, ordinary kriging was employed to generate a series of highly accurate RSI estimation maps directly since the detrend operation is not very significant. Both RSI and RST maps can potentially be used by the respective highway authorities to make more informed decisions on their various winter maintenance activities, and prevent road users from getting involved in, for instance, black-ice related collisions during winter seasons.
- To examine the applicability of the model developed herein, additional analyses were conducted to further explore if there was any relationship between the sill of the semivariogam models and weather events. The findings indicated that there was a strong dependency between these two variables. For RST, the sill values decrease as the wind speeds increase. For RSI, it is a positive correlation. Although the relationship relies on small samples, it evidently demonstrates the potential to be used for estimating the condition as per different weather groups.
- A comparison between RK, IDW, GPI, IPL, TPS was conducted to show that RK has a better predictability than other spatial interpolation methods in terms of RSC estimation. The RK method is able to increase the estimation accuracy by up to 50% over other methods.

5.2.2 Phase II – RSC Estimations using stationary RWIS data

- To show the feasibility and applicability of RK applications on stationary RWIS data, the prior semivariogram model variables (i.e., sill, nugget, and range) that capture the spatial variation of RSC was used in conjunction with stationary RWIS measurements to infer the RSC between stations. The MAE and RMSE values are found all smaller than 1°C, which

indicates that RK is capable of integrating stationary and mobile RWIS data together to improve the accuracy of RST estimation.

- The sensitivity analysis was performed to see how different densities of RWIS stations would influence the model performance. It is found that the performance improves when the number of stations increases, but reaches a stable level when there are enough RWIS stations. Besides, the location of RWIS stations was also found to impact the model accuracy.

5.3 Research Contributions

- This research provided a detail literature review including current practices on RSC monitoring and factors affecting RSC, which helps transportation authorities better understand the spatial variation of RSC and offer new insights in RSC estimation.
- A renowned geostatistical method known as RK, which has seldom been explored in the transportation field, is proposed in this research to show the feasibility of better capturing the spatial variations of the variable of interest and improve the reliability of estimation results.
- The proposed RK methodology framework that integrates stationary and mobile RWIS data makes it possible for highway maintenance agencies to estimate RSC between RWIS stations and conduct effective and timely WRM operations.
- It is recommended that the PSO method is used for locating new RWIS stations with the geostatistical semivariogram analysis of RWIS data in an effort to determine the RWIS monitoring coverage of RSC. The proposed optimization framework could make contributions to RWIS network planning.

- Using the models proposed and developed herein, it is anticipated that the winter road maintenance contractors continuous monitoring and visualization of road weather and surface conditions could be possible, improving the overall quality of their maintenance services while reducing the cost of road patrolling. Long term, it is also expected to generate a significant body of new knowledge in the application of geostatistics to advance the transportation research in general and road weather and surface conditions estimations in particular.

5.4 Limitations and Recommendations for Future Work

Limitations and further research are summarized in the following specific directions:

- For RST estimation, other external parameters that may affect the RST variation, such as the distance from mountains and roadside features, should be considered to improve the accuracy of the models developed. Additionally, Lidar data can be used to represent the vegetation cover since the NDVI cannot distinguish the heights of vegetation which could affect the RST.
- For RSI estimation, variables, such as precipitation and snow cover on the ground, currently used to evaluate the surface condition might be applied to classify the weather events, like Thrones classification scheme, and in turn generalize the findings.
- More RSC variables including pavement materials, snow cover condition should be investigated to further improve the identification of RSC and accelerate the implementation of WRM.
- The methodology should be extended to account both spatial and temporal attributes of road weather and surface condition variables as they can be markedly affected by those two domains.

- More case studies should be carried out to examine the generality and sensitivity of the model results using other factors, such as different weather events and types, as well as data collected during the daytime.
- How to overcome the difference between measurements from mobile and stationary RWIS needs to be further investigated to better integra and fusion these two data sources for application in real-time RSC estimation and connected vehicle communication.

BIBLIOGRAPHY

Agarwal, M., Maze, T.H., Souleyrette, R.R., 2005. Impacts of Weather on Urban Freeway Traffic Flow Characteristics and Facility Capacity. Proc. 2005 Mid-Continent Transp. Res. Symp. 14p.

Ahmed Memon, R., Leung, D.Y., Chunho, L., 2008. A review on the generation, determination and mitigation of Urban Heat Island. J. Environ. Sci. 20, 120–128. https://doi.org/10.1016/S1001-0742(08)60019-4

Apaydin, H., Kemal Sonmez, F., Yildirim, Y.E., 2004. Spatial interpolation techniques for climate data in the GAP region in Turkey. Clim. Res. 28, 31–40. https://doi.org/10.3354/cr028031

Asaeda, T., Ca, V.T., Wake, A., 1996. Heat storage of pavement and its effect on the lower atmosphere. Atmos. Environ. 30, 413–427. https://doi.org/10.1016/1352-2310(94)00140-5

Benrazavi, R.S., Binti Dola, K., Ujang, N., Sadat Benrazavi, N., 2016. Effect of pavement materials on surface temperatures in tropical environment. Sustain. Cities Soc. 22, 94–103. https://doi.org/10.1016/j.scs.2016.01.011

Bogren Jorgen, Gustavsson, T., 1991. Nocturnal Air and Road Surface Temperature Variations in Complex Terrain. Int. J. Climatol. 11, 443–445.

Boselly, S.E., 2000. IDENTIFICATION AND DOCUMENTATION OF WEATHER AND ROAD CONDITION DISSEMINATION DEVICES AND DATA FORMATS Mn / DOT Agreement No . 79575 Submitted by.

Buchanan, F., Gwartz, S., 2005. Road Weather Information Systems at the Ministry of Transportation, Ontario, in: Annual Conference of the Transportation Association of Canada.

Chapman, L., Thornes, J.E., 2008. Small-scale road surface temperature and condition variations across a road profile . ID : 01. Sirwec 2008 14–16.

Chapman, L., Thornes, J.E., 2005. The influence of traffic on road surface temperatures: Implications for thermal mapping studies. Meteorol. Appl. 12, 371–380. https://doi.org/10.1017/S1350482705001957

Chapman, L., Thornes, J.E., Bradley, A. V, 2001a. Modelling of road surface temperature from a geographical parameter database. Part I: Statistical. Meteorol. Appl. 8, 421–436. https://doi.org/10.1017/S1350482701004042

Chapman, L., Thornes, J.E., Bradley, A. V, 2001b. Modelling of road surface temperature from a geographical parameter database. Part 2: Numerical. Meteorol. Appl. 8, 421–436. https://doi.org/10.1017/S1350482701004042

Faghih Mirzaei, N., Fairuz Syed Fadzil, S., Binti Taib, N., Abdullah, A., 2015. Micro-scale Evaluation of the Relationship between Road Surface and Air Temperature with Respect to Various Surrounding Greenery Covers. Res. J. Appl. Sci. Eng. Technol. 11, 454–459. https://doi.org/10.19026/rjaset.11.1802

Feng, F., Fu, L., 2010. Comparison of Alternative Models for Road Surface Condition Classification, in: Transportation Research Board 2010 Meeting. pp. 1–18.

Foley, J., Thompson, W., and Warren, R., 2009. The use of the 85 percentile speed data as a measure of winter maintenance performance, in: National Rural Intelligent Transportation Society Conf. Seaside, OR, USA.

Franke, R., 1982. Smooth Interpolation of Scattered Data by Local Thin Plate Splines. Comput. Math. with Appl. 8, 273–281.

Fu, L., Feng, F., Perchanok, M.S., 2008. Probabilistic Models for Discriminating Road Surface Conditions Based on Friction Measurements. Transp. Res. Board 87th Annu. Meet. 18p.

Fu, L., Thakali, L., Kwon, T.J., Usman, T., 2016. A risk-based approach to winter road surface condition classification. Can. J. Civ. Eng. Civ. Eng. 10, 1–10. https://doi.org/10.1139/cjce-2016-0215

Garrigues, S., Allard, D., Baret, F., Weiss, M., 2006. Quantifying spatial heterogeneity at the landscape scale using variogram models. Remote Sens. Environ. 103, 81–96. https://doi.org/10.1016/j.rse.2006.03.013

Goovaerts, P., 1997. Geostatistics for Natural Resources Evaluation. Oxford University, New York.

Gustavsson, T., 1990. Variation in road surface temperature due to topography and wind. Theor. Appl. Climatol. 41, 227–236. https://doi.org/10.1007/BF00866454

Hengl, T., Heuvelink, G.B.M., Rossiter, D.G., 2007. About regression-kriging: From equations to case studies. Comput. Geosci. 33, 1301–1315. https://doi.org/10.1016/j.cageo.2007.05.001

Hengl, T., Heuvelink, G.B.M., Stein, A., 2004. A generic framework for spatial prediction of soil variables based on regression-kriging. Geoderma 120, 75–93. https://doi.org/10.1016/j.geoderma.2003.08.018

Jain, P., Flannigan, M.D., 2017. Comparison of methods for spatial interpolation of fire weather in Alberta , Canada 1658, 1646–1658.

Journel, A.G., Heuvelink, G.B.M., 1978. Mining Geostatistics. Academic Press, New York.

Juga, I., Nurmi, P., Hippi, M., 2013. Statistical modelling of wintertime road surface friction. Meteorol. Appl. 20, 318–329. https://doi.org/10.1002/met.1285

Kangas, M., Heikinheimo, M., Hippi, M., 2015. RoadSurf: a modelling system for predicting road weather and road surface conditions. Meteorol. Appl. 22, 544–553. https://doi.org/10.1002/met.1486

Kang tsung Chang, 2012. Introduction to Geographic Information Systems, sixth. ed.

Kennedy, J., Eberhart, R., 1995. Particle Swarm Optimization, in: 1995 IEEE International Conference on Neural Networks. pp. 1942–1948. https://doi.org/10.1109/ICNN.1995.488968

Kršmanc, R., Slak, A.Š., Demšar, J., 2013. Statistical approach for forecasting road surface temperature. Meteorol. Appl. 20, 439–446. https://doi.org/10.1002/met.1305

Kwon, T., Fu, L., Jiang, C., 2013. Effect of Winter Weather and Road Surface Conditions on Macroscopic Traffic Parameters. Transp. Res. Rec. J. Transp. Res. Board 2329, 54–62. https://doi.org/10.3141/2329-07

Kwon, T.J., Gu, L., 2017. Modelling of winter road surface temperature (RST) - A GIS-based approach. 2017 4th Int. Conf. Transp. Inf. Safety, ICTIS 2017 - Proc. 551–556. https://doi.org/10.1109/ICTIS.2017.8047820

Li, J., Heap, A., 2008. A review of spatial interpolation methods for environmental scientists. Geoscience Australia, Record 2008/23.

Ligas, M., Kulczycki, M., 2010. Simple spatial prediction - least squares prediction, simple kriging, and conditional expectation of normal vector. Geod. Cartogr. 59, 69–81. https://doi.org/10.2478/v10277-012-0002-0

Linton, M.A., 2015. A Smartphone-based Connected Vehicle Solution for Winter Road Surface Condition Monitoring.

Lundquist, J.D., Cayan, D.R., 2007. Surface temperature patterns in complex terrain: Daily variations and long-term change in the central Sierra Nevada, California. J. Geophys. Res. Atmos. 112, 1–15. https://doi.org/10.1029/2006JD007561

Lysyk, B., Chagani, G., Stavropoulos, B., Amerski, S., Shah, A., Truong, K., Randoja, T., Green, M., 2015. Winter Highway Maintenance, Special Report.

Marchetti, M., Chapman, L., Khalifa, A., Buès, M., 2014. New Role of Thermal Mapping in Winter Maintenance with Principal Components Analysis. Adv. Meteorol. 2014. https://doi.org/10.1155/2014/254795

Marchetti, M., Moutton, M., Ludwig, S., Ibos, L., Feuillet, V., Dumoulin, J., 2011. Road networks winter risk estimation using on-board uncooled infrared camera for surface temperature measurements over two lanes. Int. J. Geophys. 2011. https://doi.org/10.1155/2011/514970

Ministry of Transportation Ontario, MOT, 2009. Ontario Road Safety Annual Reports.

Najafi, S., Flintsch, G.W., McGhee, K.K., 2013. Assessment of operational characteristics of continuous friction measuring equipment (CFME). Int. J. Pavement Eng. 14, 706–714. https://doi.org/10.1080/10298436.2012.667097

Oke, T.R., 1987. Canyon geometry and the nocturnal urban heat island: Comparison of some model and field observations. J. Climatol. 1, 237–254.

Olea, R.A., 2006. A six-step practical approach to semivariogram modeling. Stoch. Environ. Res. Risk Assess. 20, 307–318. https://doi.org/10.1007/s00477-005-0026-1

Olea, R.A., 2003. GEOSTATISTICS FOR ENGINEERS AND EARTH SCI ENTISTS.

Oliver, M.A., Webster, R., 1990. Kriging: A method of interpolation for geographical information

systems. Int. J. Geogr. Inf. Syst. 4, 313–332. https://doi.org/10.1080/02693799008941549

Pebesma, E. j., 2004. Multivariable geostatistics in S: the gstat package. Comput. Geosci. 30(7), 683–691.

Perchanok, M.S., 2002. Patchiness of Snow Cover and Its Relation to Quality Assurance in Winter Operations: World Road Association - PIARC. New Challenges Winter Road Serv. XIth Int. Winter Road Congr. 10.

Robinson, T.P., Metternicht, G., 2006. Testing the performance of spatial interpolation techniques for mapping soil properties. Comput. Electron. Agric. 50, 97–108. https://doi.org/10.1016/j.compag.2005.07.003

Rosenfeld, A.H., Akbari, H., Bretz, S., Fishman, B.L., Kurn, D.M., Sailor, D., Taha, H., 1995. Mitigation of urban heat islands: materials, utility programs, updates. Energy Build. 22, 255–265. https://doi.org/10.1016/0378-7788(95)00927-P

Sankar, G., Kumar, P., Maiti, R., 2018. Comparison of GIS-based interpolation methods for spatial distribution of soil organic carbon (SOC). J. Saudi Soc. Agric. Sci. 17, 114–126. https://doi.org/10.1016/j.jssas.2016.02.001

Sass, B.H., 1992. A Numerical Model for Prediction of Road Temperature and Ice. J. Appl. Meteorol. https://doi.org/10.1175/1520-0450(1992)031<1499:ANMFPO>2.0.CO;2

Shao, J., 1990. A winter road surface temperature prediction model with comparison to others. University of Birmingham.

Shao, J., Lister, P.J., Hart, G.D., Pearson, H.B., 1996. Thermal mapping: Reliability and repeatability. Meteorol. Appl. https://doi.org/10.1002/met.5060030405

Shao, J., Swanson, J.C., Patterson, R., Lister, P.J., McDonald, A.N., 1997. Variation of winter road surface temperature due to topography and application of Thermal Mapping. Meteorol. Appl. 4, 131–137. https://doi.org/10.1017/S135048279700042X

Shitara, H., Hosokawa, K., Ishikawa, Y., Kikuchi, R., Makita, H., Sasaki, Y., 1973. On the micro-scale distribution of the nocturnal cooling in a small basin.

Sokol, Z., Bližňák, V., Sedlák, P., Zacharov, P., Pešice, P., Škuthan, M., 2017. Ensemble forecasts of road surface temperatures. Atmos. Res. 187, 33–41. https://doi.org/10.1016/j.atmosres.2016.12.010

Tabony, R.C., n.d. The variation of surface temperature with altitude. Meteorol. Appl. 114, 37–48.

Thornes, J.E., 1991. Thermal mapping and road-weather information systems for highway engineers. Highw. Meteorol. 39–67.

Thornes, J.E., Shao, J., n.d. Spectral analysis and sensitivity tests for a numerical road surface temperature prediction model. Meteorol. Appl. 120, 117–123.

Transportation Association of Canada, 2009. Winter maintenance performance measurement

using friction testing.

Transportation Association of Canada, 2003. Salt smart train, the trainer program. Salt smart learning guide.

U.S. DOT Federal Highway Administration (FHWA), 2018. How Do Weather Events Impact Roads? - FHWA Road Weather Management. URL https://ops.fhwa.dot.gov/weather/q1_roadimpact.htm (accessed 7.31.18).

U.S. DOT Federal Highway Administration (FHWA), n.d. Snow & Ice - FHWA Road Weather Management. URL https://ops.fhwa.dot.gov/weather/weather_events/snow_ice.htm (accessed 6.8.18).

Usman, T., Fu, L., Miranda-Moreno, L.F., 2012. A disaggregate model for quantifying the safety effects of winter road maintenance activities at an operational level. Accid. Anal. Prev. 48, 368–378. https://doi.org/10.1016/j.aap.2012.02.005

Xu, M., Yang, J., Gao, Z., 2010. Particle swarm optimization algorithm in transport continuous network design problems. 3rd Int. Jt. Conf. Comput. Sci. Optim. CSO 2010 Theor. Dev. Eng. Pract. 2, 513–517. https://doi.org/10.1109/CSO.2010.53

Yang, J., Wong, M.S., Menenti, M., Nichol, J., 2015. Study of the geometry effect on land surface temperature retrieval in urban environment. ISPRS J. Photogramm. Remote Sens. 109, 77–87. https://doi.org/10.1016/j.isprsjprs.2015.09.001

Yang, Q., Zheng, J., Liu, Z., 2016. WHICH ONE IS THE BEST : THE INTERPOLATION METHODS COMPARISON ON AVERAGE ANNUAL TEMPERATURE IN XINJIANG FROM 1951 TO 2013 School of Resources & Environment Science , Xinjiang University , Urumqi 830046 , China Xinjiang Key Lab of Smart city and Environment 4466–4469.

Zarco-Perello, S., Simões, N., 2017. Ordinary kriging vs inverse distance weighting: spatial interpolation of the sessile community of Madagascar reef, Gulf of Mexico. PeerJ 5, e4078. https://doi.org/10.7717/peerj.4078

Ziary, Y., Safari, H., 2007. To Compare Two Interpolation Methods : IDW , KRIGING for Providing Properties (Area) Surface Interpolation Map Land Price . District 5 , Municipality of Tehran area 1 . Integr. Vlsi J. 13–17.

Zwahlen, H.T., Russ, A., Vatan, S., 2003. Evaluation of ODOT Roadway/Weather Sensor Systems for Snow and Ice Removal Operations- Part I: RWIS. Ohio Res. Inst. Transp. Environ. FHWA/OH-20.

APPENDIX

Table 23. Final estimation RST maps for Highway 16

	(1) 2014/12/18	(2) 2015/02/09
A	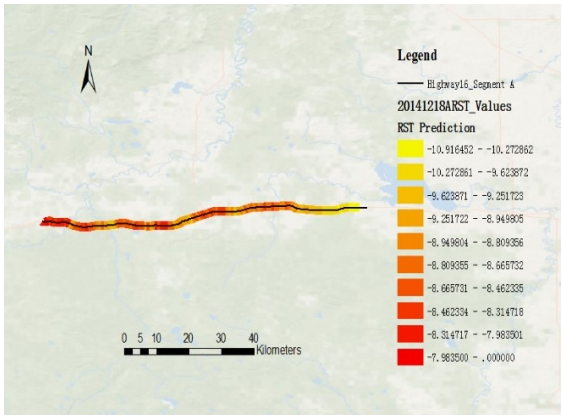	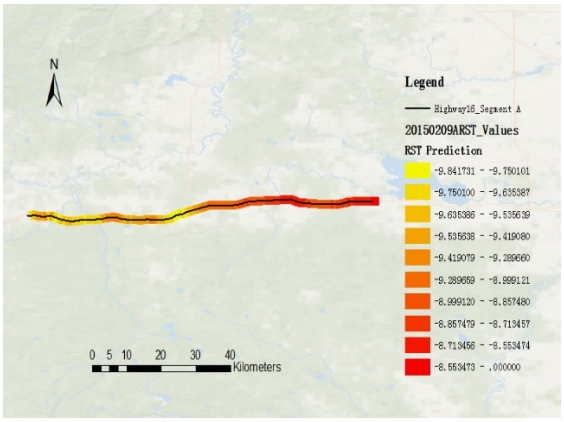
	RMSE: 0.382, Range: 17.92 km	**RMSE: 0.152, Range: 13.95 km**
B	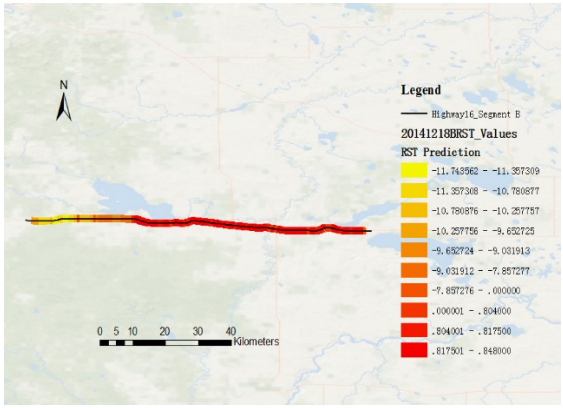	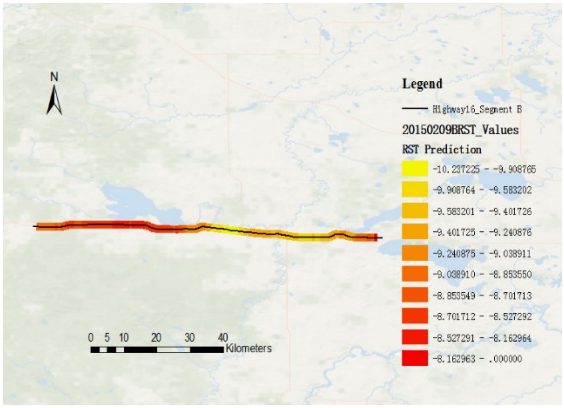
	RMSE: 0.381, Range: 5.14 km	**RMSE: 0.230, Range: 14.13 km**
C	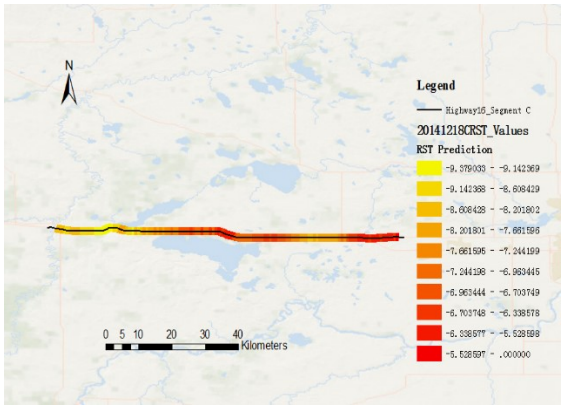	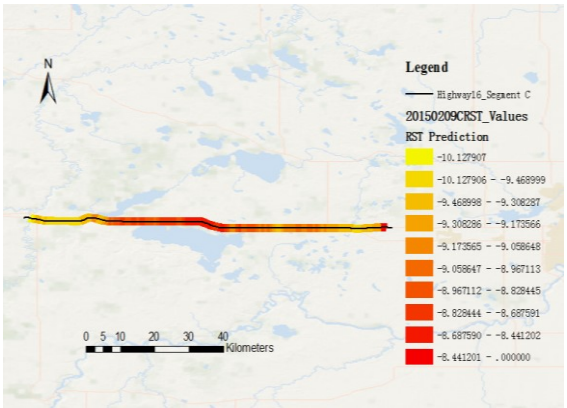
	RMSE: 0.407, Range: 24.51 km	**RMSE: 0.163, Range: 26.04 km**

	(3) 2015/02/03	(4) 2016/12/01
A	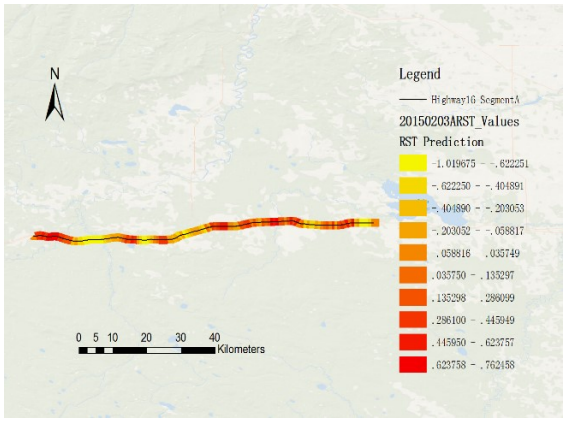	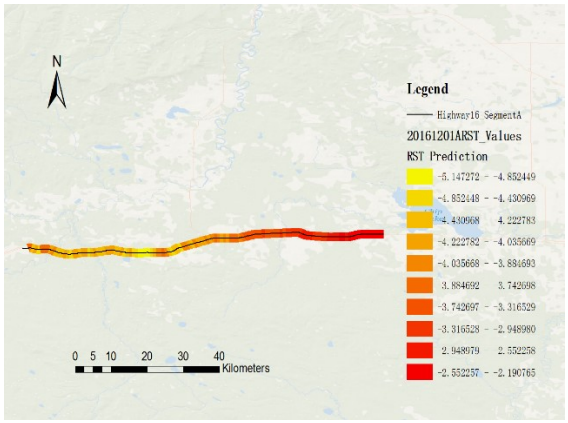
	RMSE: 0.347, Range: 5.24 km	**RMSE: 0.292, Range: 2.55 km**
B	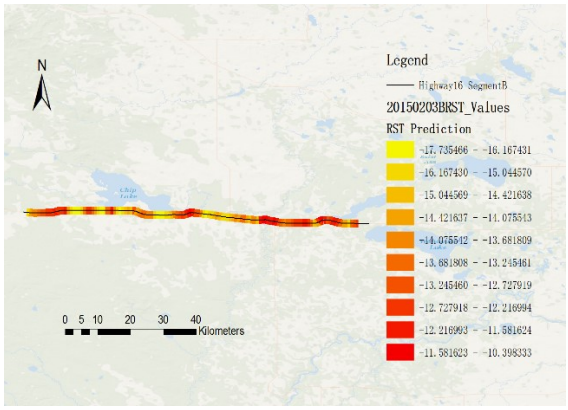	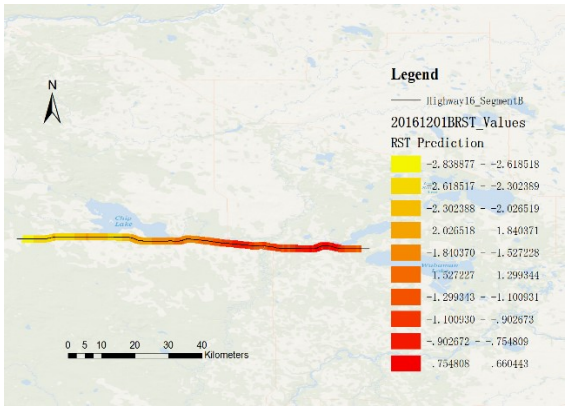
	RMSE: 0.372, Range: 2.51 km	**RMSE: 0.111, Range: 19.04 km**
C	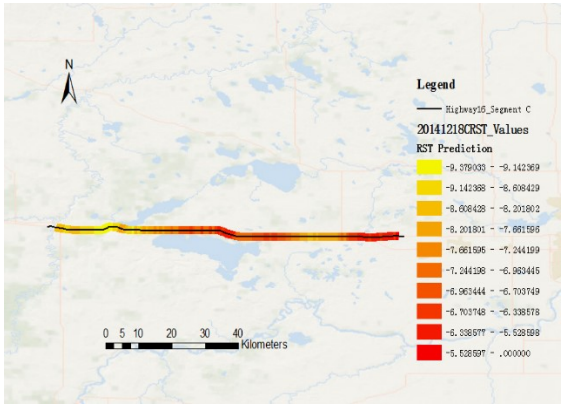	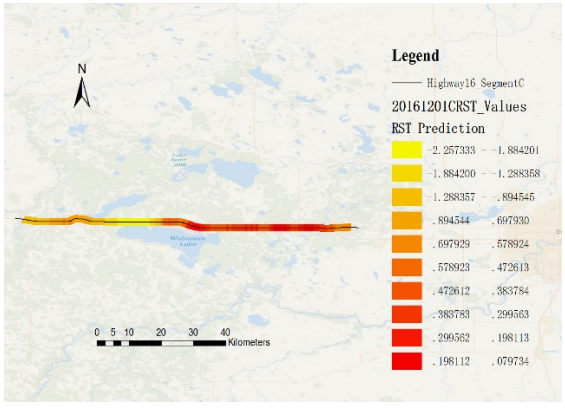
	RMSE: 0.292, Range: 19.71 km	**RMSE: 0.120, Range: 10.29 km**

Table 24. Crossvalidation for Highway 16 RST estimation

	(1) 2014/12/18	(2) 2015/02/09
A	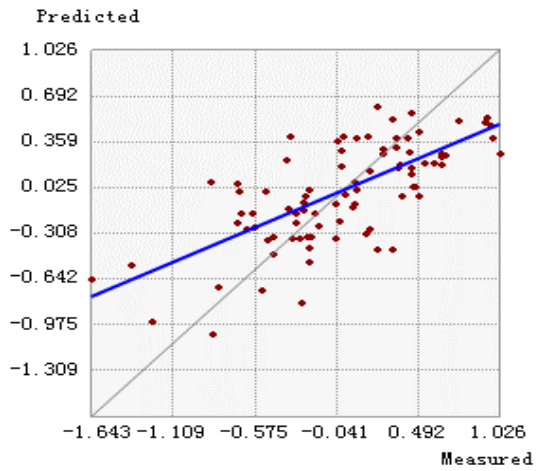	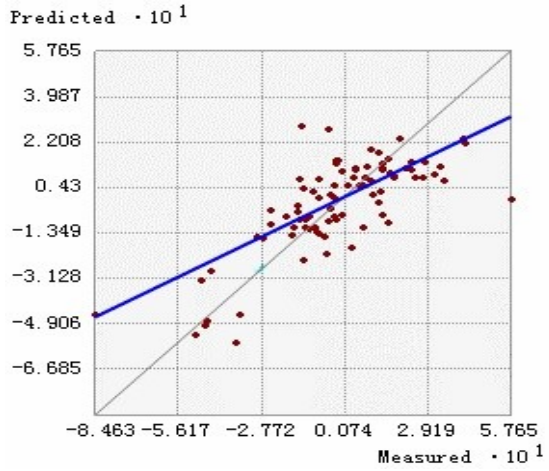
B	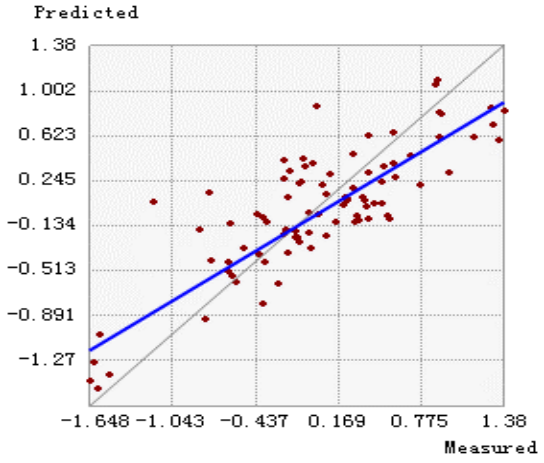	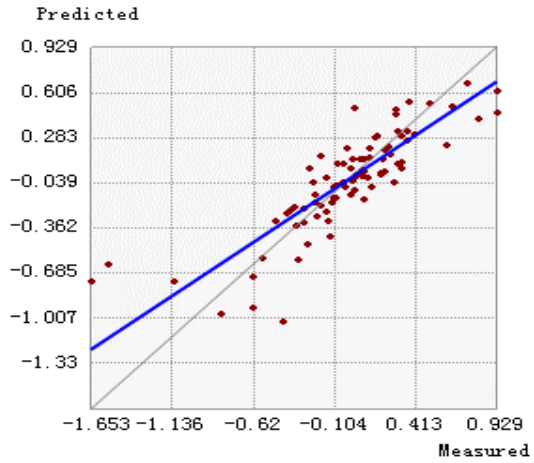
C	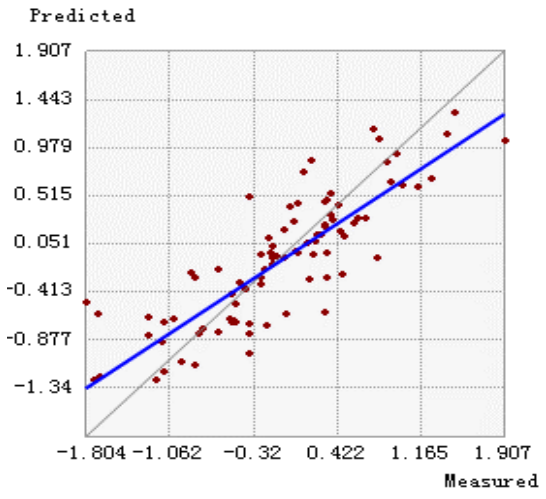	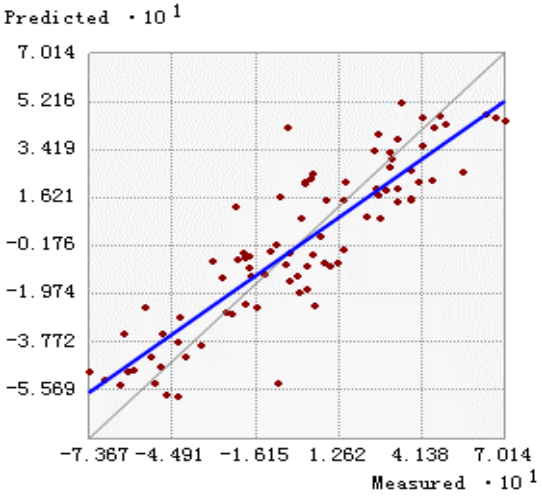

	(3) 2015/02/03	(4) 2016/12/01
A	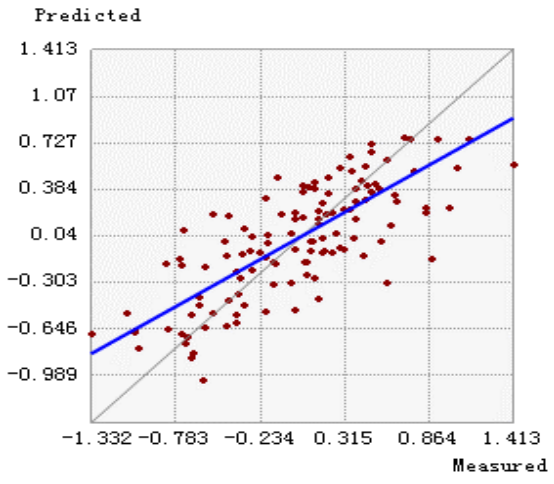	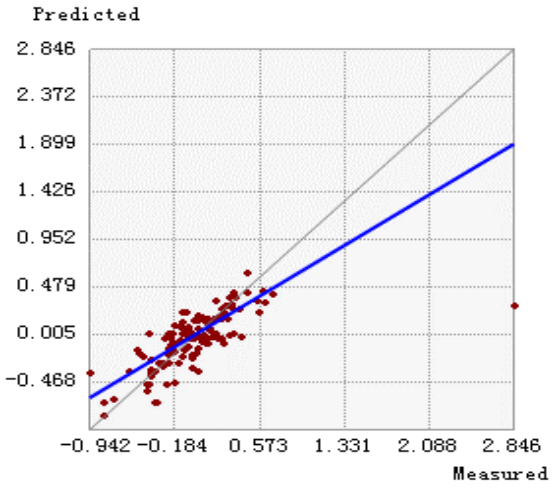
B	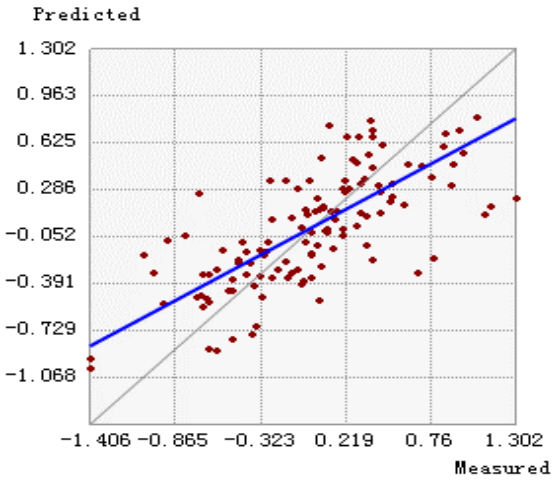	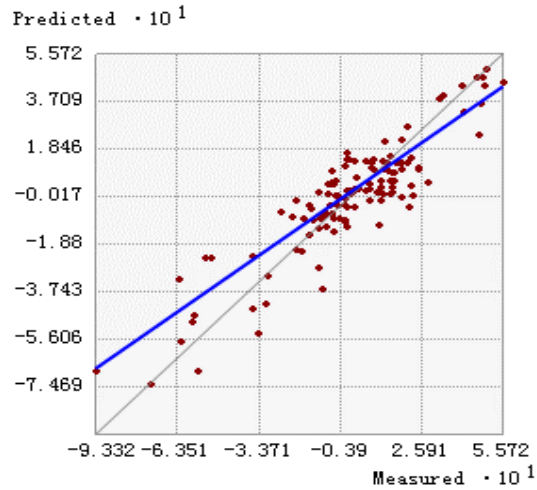
C	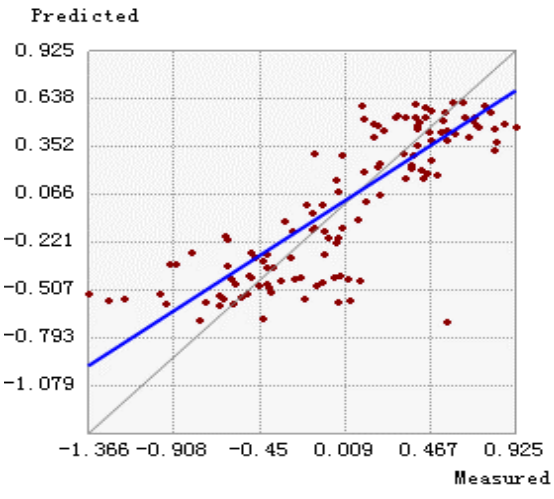	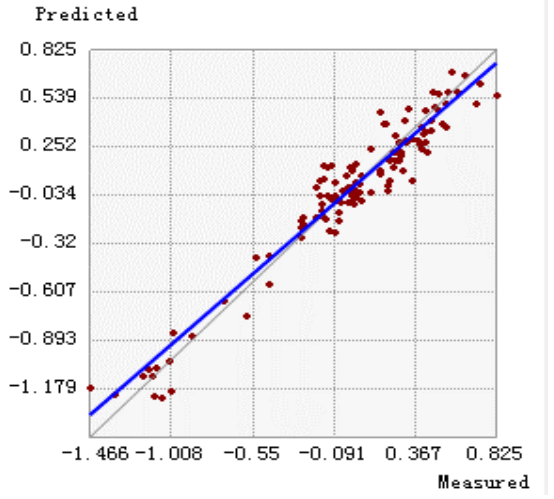

Table 25. Final estimation RSI maps for Highway 16

	(1) 2014/12/18	(2) 2015/02/09
A	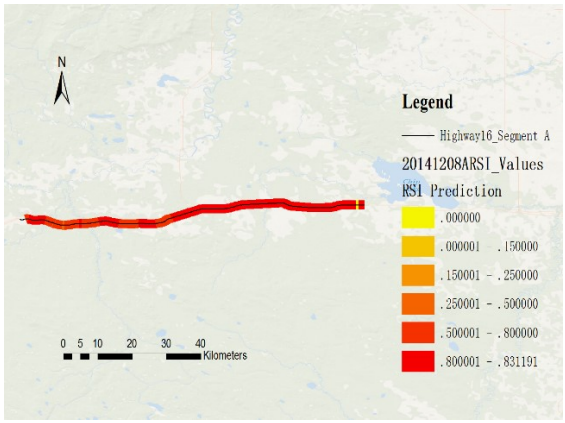	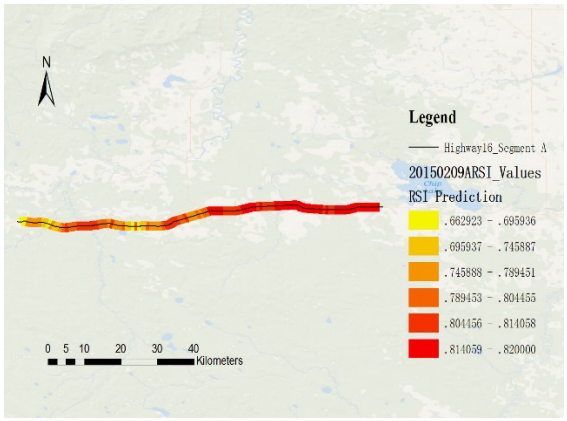
	RMSE: 0.047, Range: 2.35 km	**RMSE: 0.169, Range: 1.79 km**
B	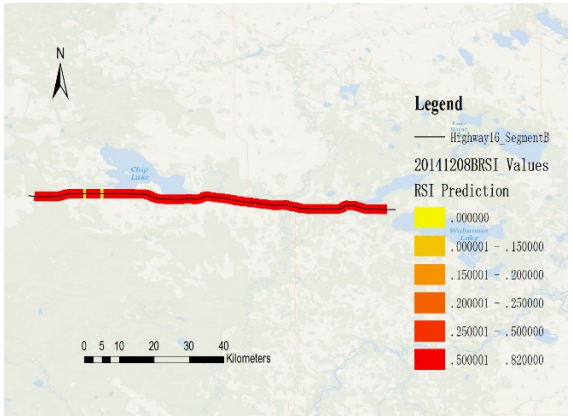	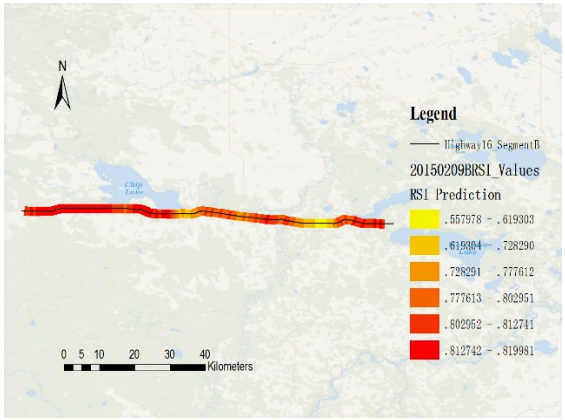
	RMSE: 0.011, Range: 3.84 km	**RMSE: 0.041, Range: 6.81 km**
C	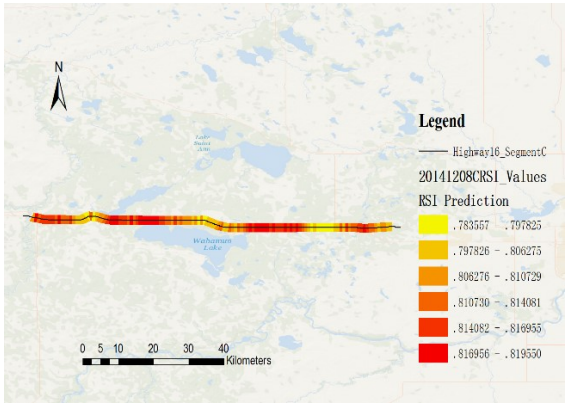	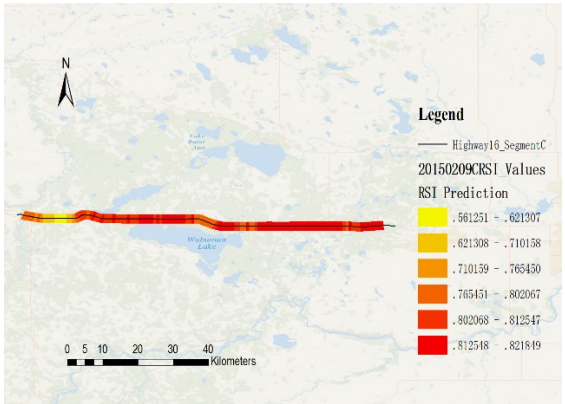
	RMSE: 0.018, Range: 7.57 km	**RMSE: 0.036, Range: 4.38 km**

	(3) 2015/02/03	(4) 2016/12/01
A	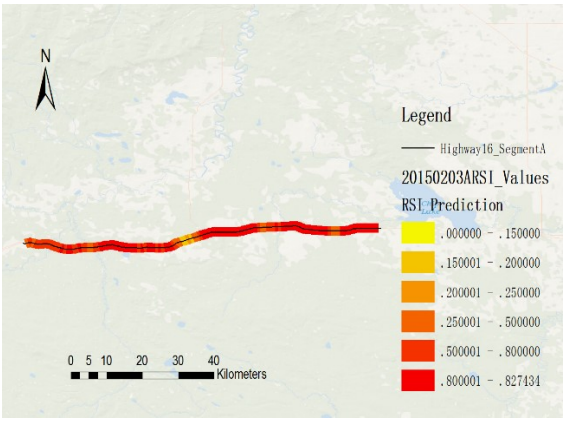	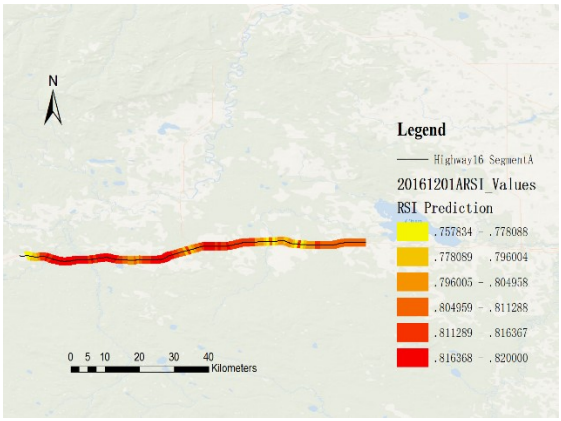
	RMSE: 0.085, Range: 5.18 km	**RMSE: 0.036, Range: 19.92 km**
B	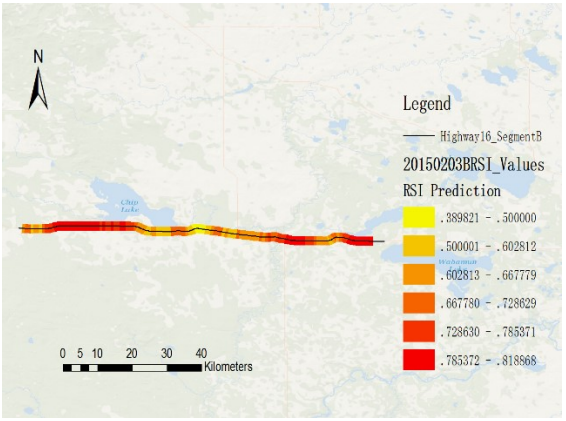	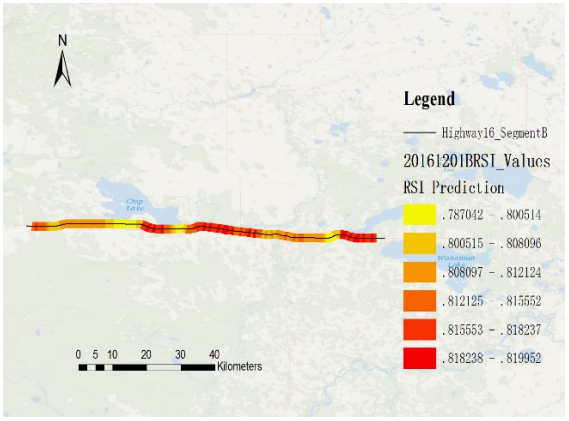
	RMSE: 0.157, Range: 22.11 km	**RMSE: 0.005, Range: 4.98 km**
C	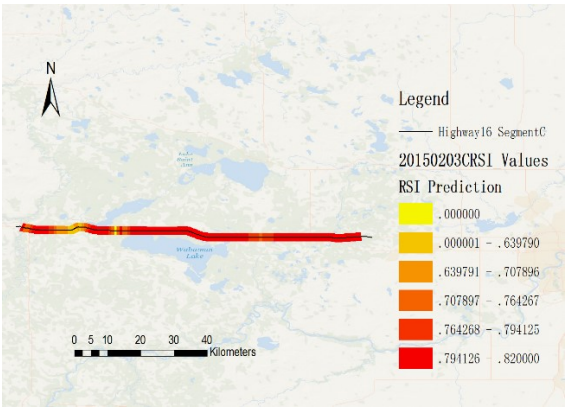	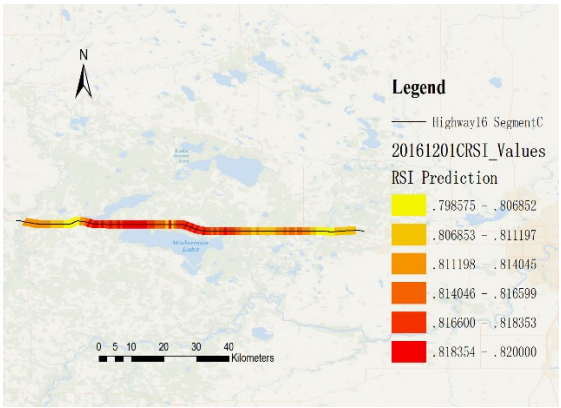
	RMSE: 0.075, Range: 4.44 km	**RMSE: 0.006, Range: 33.93 km**

Table 26. Crossvalidation for Highway 16 RSI estimation

	(1) 2014/12/18	(2) 2015/02/09
A	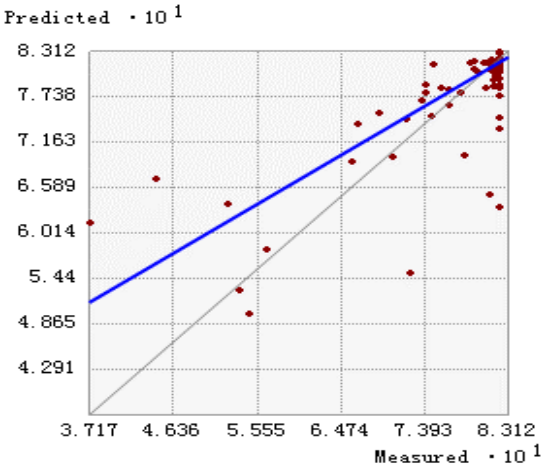	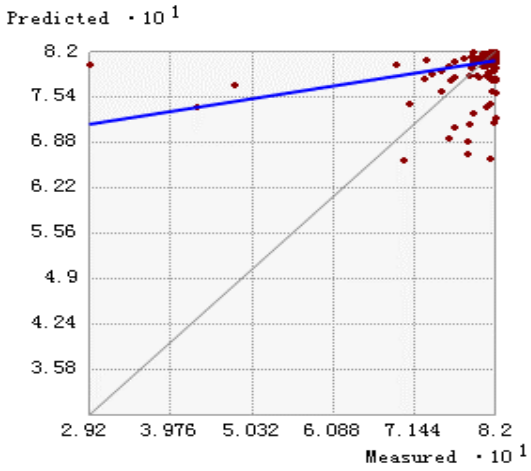
B	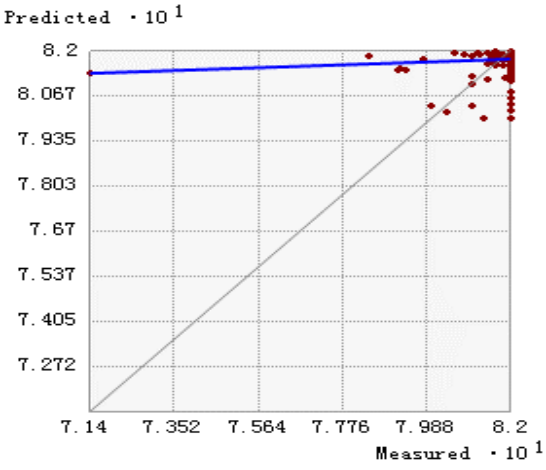	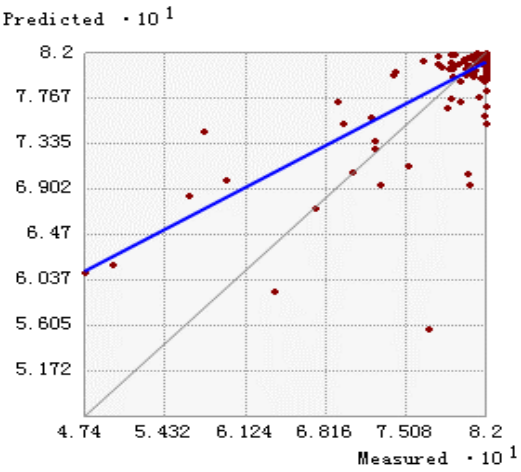
C	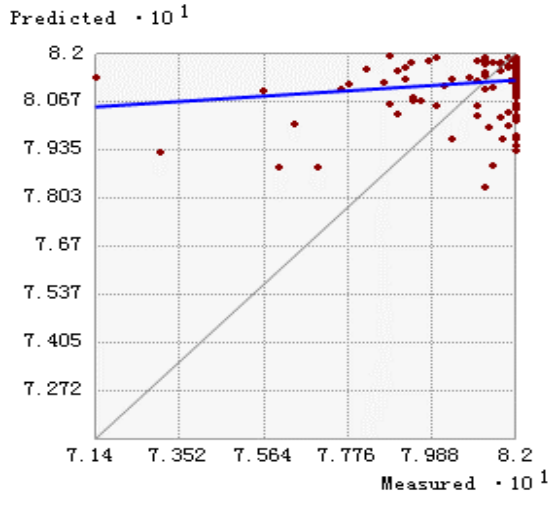	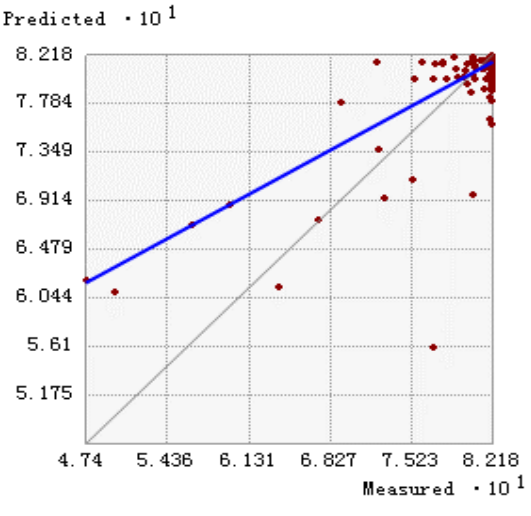

	(3) 2015/02/03	(4) 2016/12/01
A	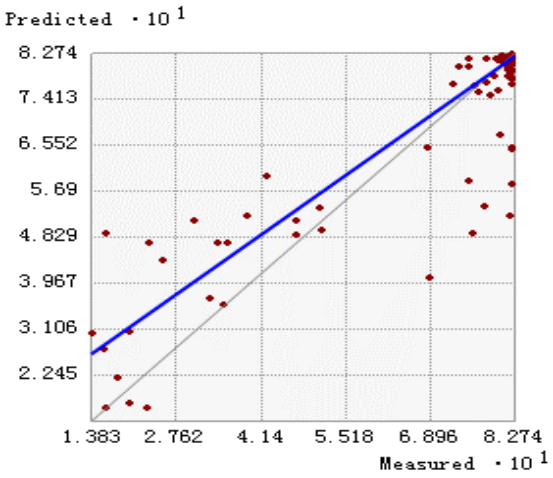	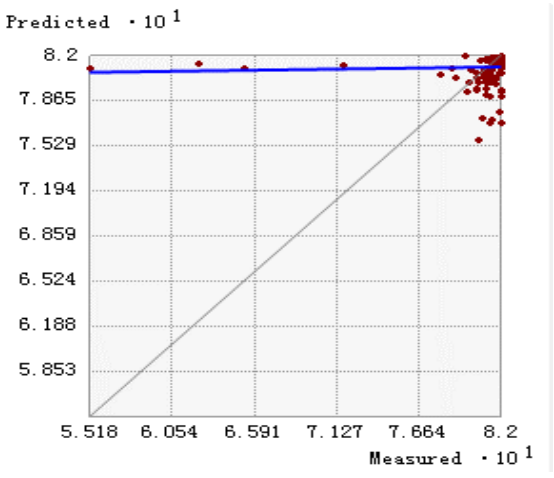
B	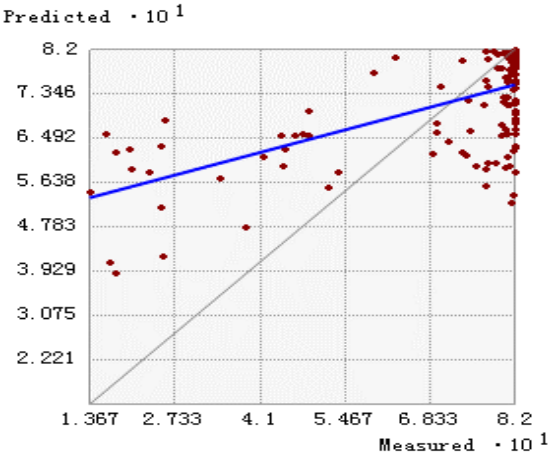	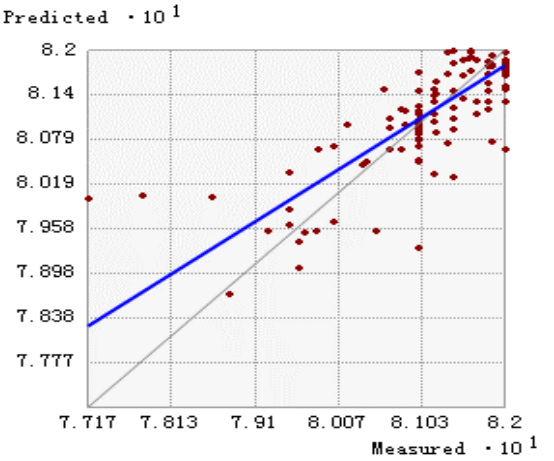
C	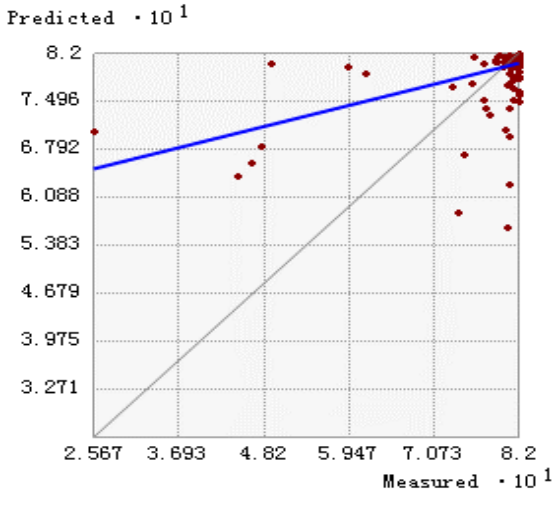	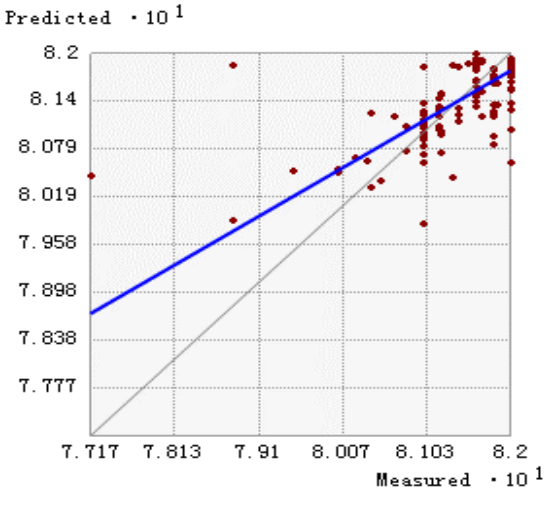

Table 27. Final estimation RST maps for Highway 2

	(1) 2015/02/09	(2) 2015/01/13
A	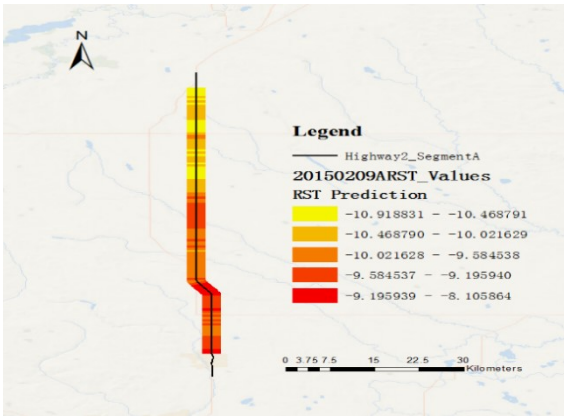	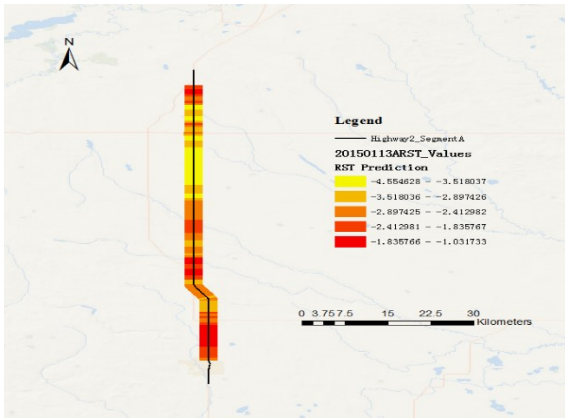
	RMSE: 0.162, Range: 5.13 km	**RMSE: 0.290, Range: 0.94 km**
B	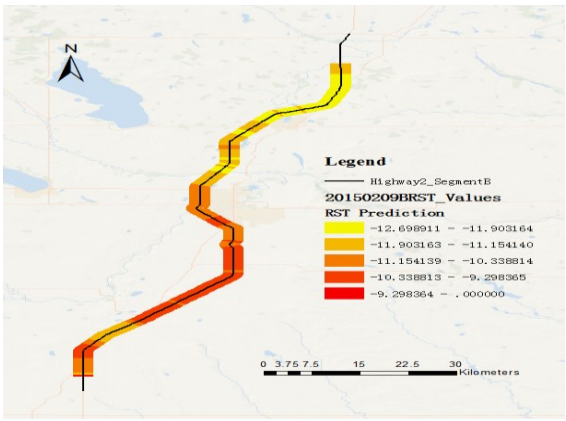	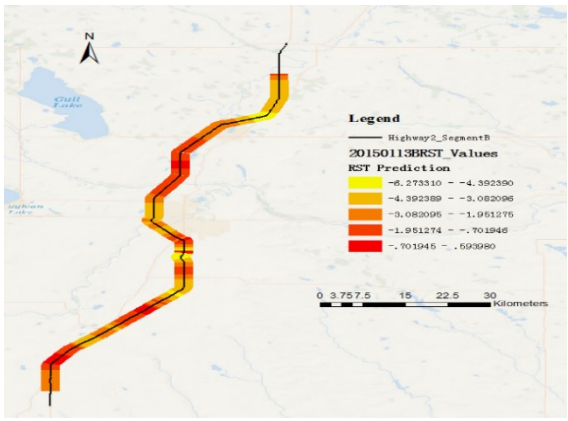
	RMSE: 0.146, Range: 32.34 km	**RMSE: 0.225, Range: 5.77 km**
C	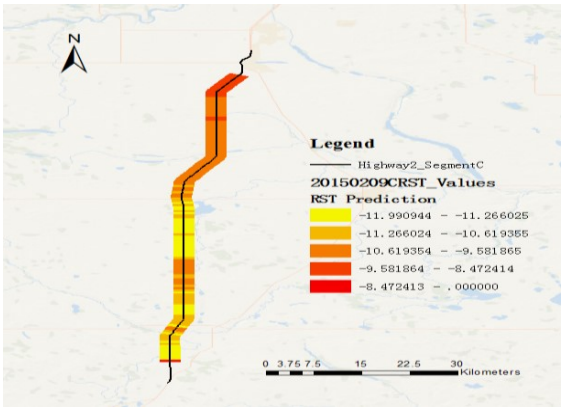	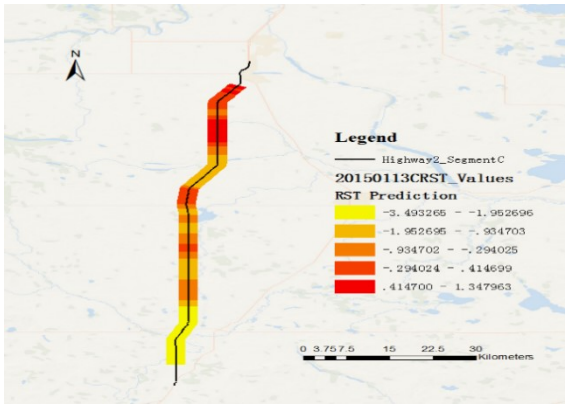
	RMSE: 0.187, Range: 12.79 km	**RMSE: 0.174 , Range: 6.48 km**

Table 28. Crossvalidation for Highway 2 RST estimation

	(1) 2015/02/09	(2) 2015/01/13
A	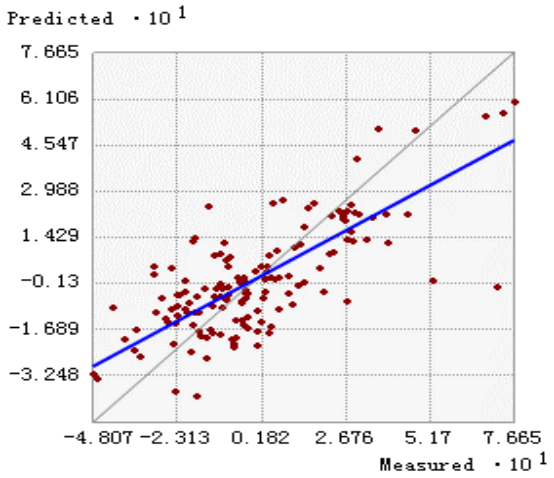	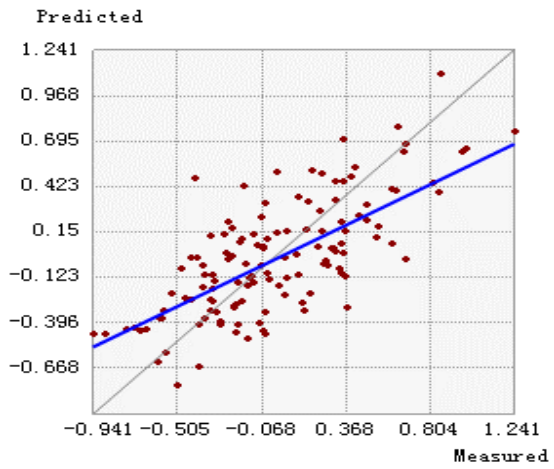
B	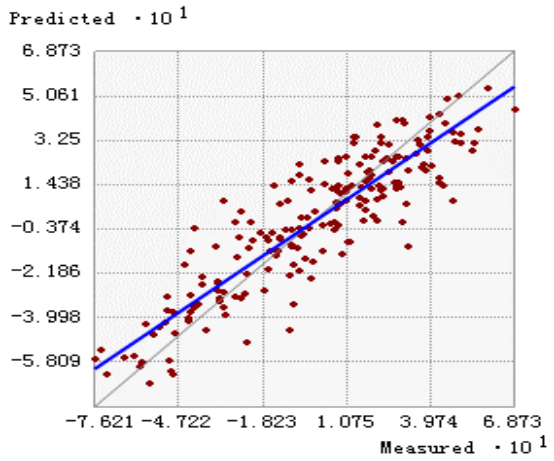	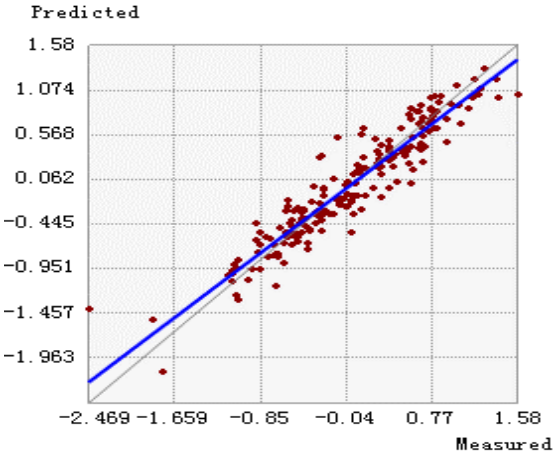
C	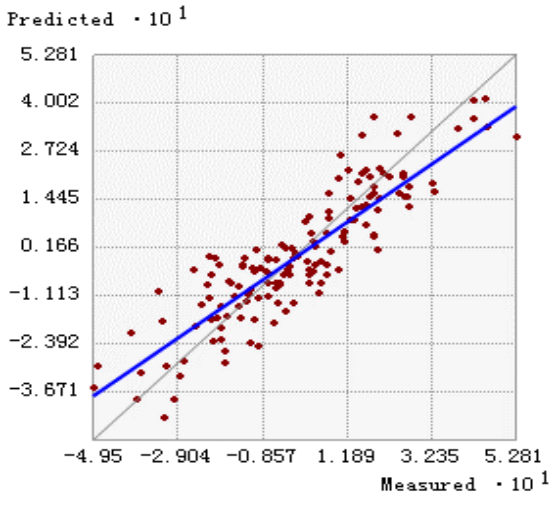	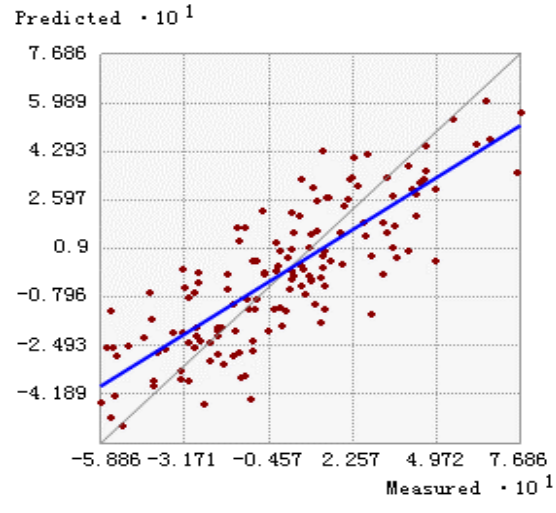

Table 29. Final estimation RSI maps for Highway 2

	(1) 2015/02/09	(2) 2015/01/13
A	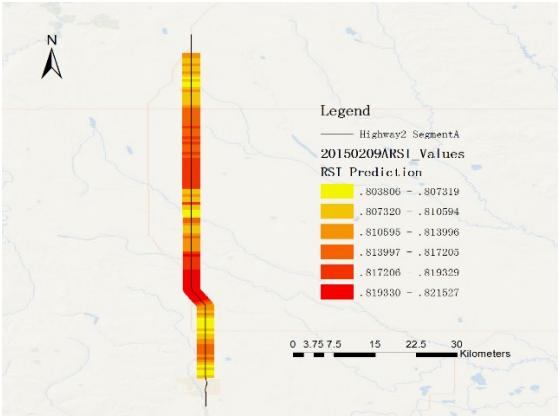	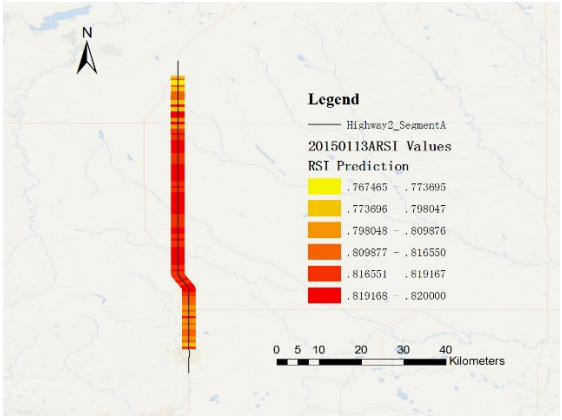
	RMSE: 0.018, Range: 34.73 km	**RMSE: 0.020, Range: 1.43 km**
B	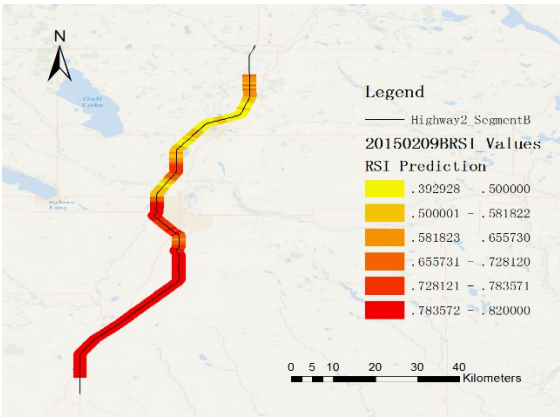	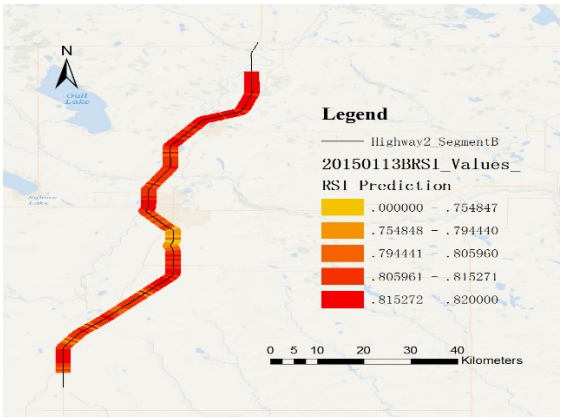
	RMSE: 0.068, Range: 2.17 km	**RMSE: 0.029, Range: 11.80 km**
C	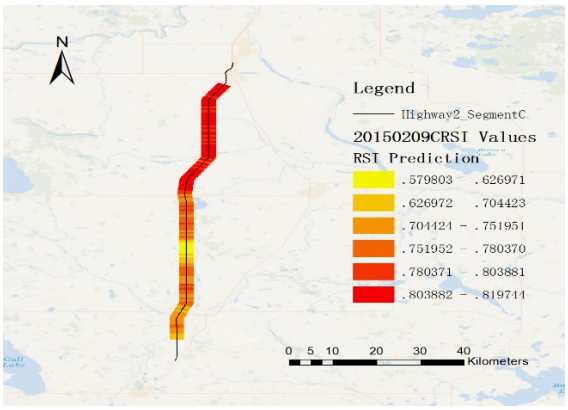	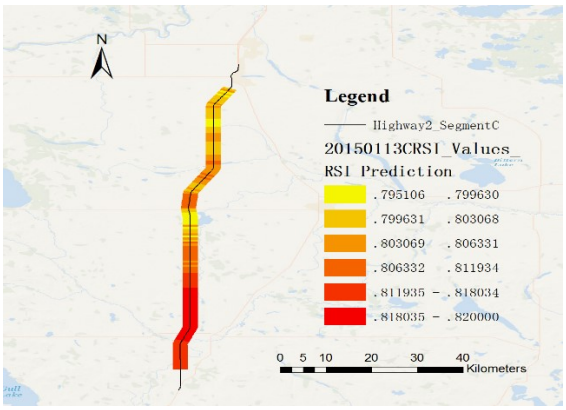
	RMSE: 0.040, Range: 2.63 km	**RMSE: 0.004, Range: 6.02 km**

Table 30. Crossvalidation for Highway 2 RSI estimation

	(1) 2015/02/09	(2) 2015/01/13
A	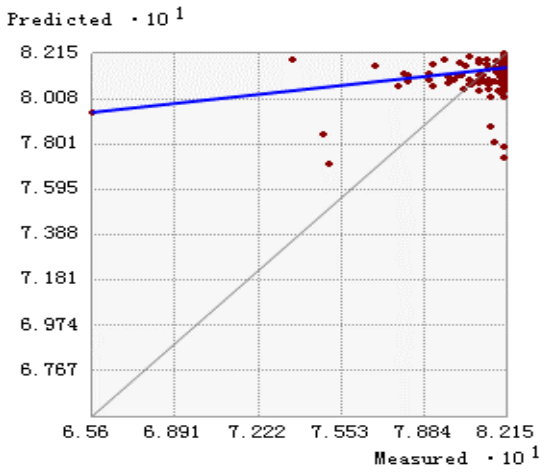	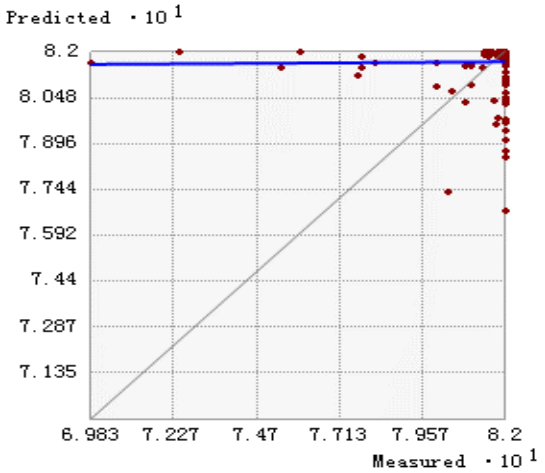
B	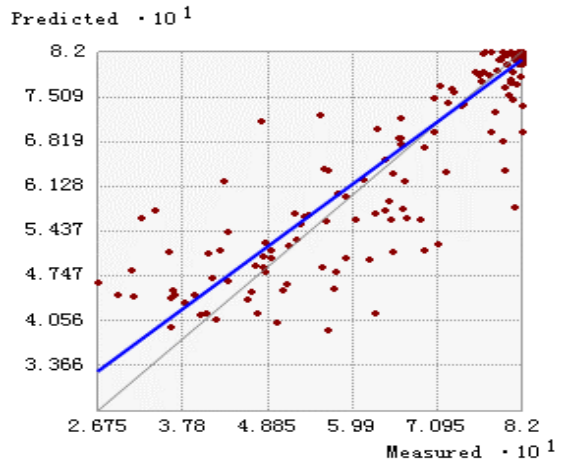	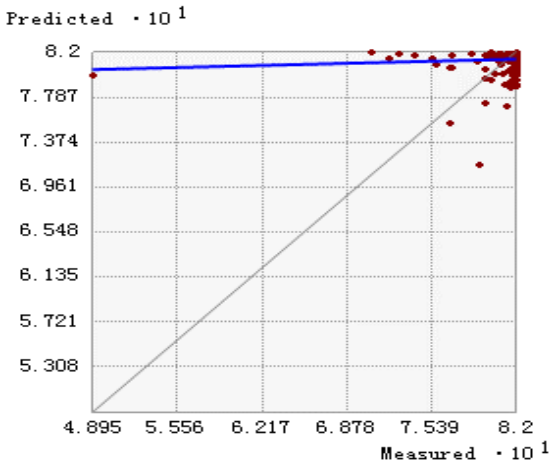
C	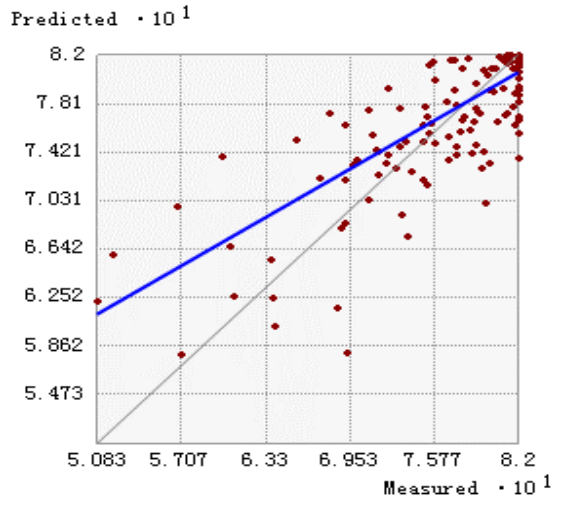	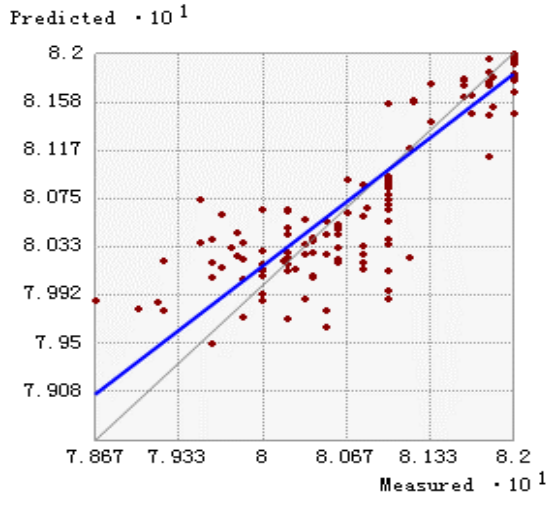

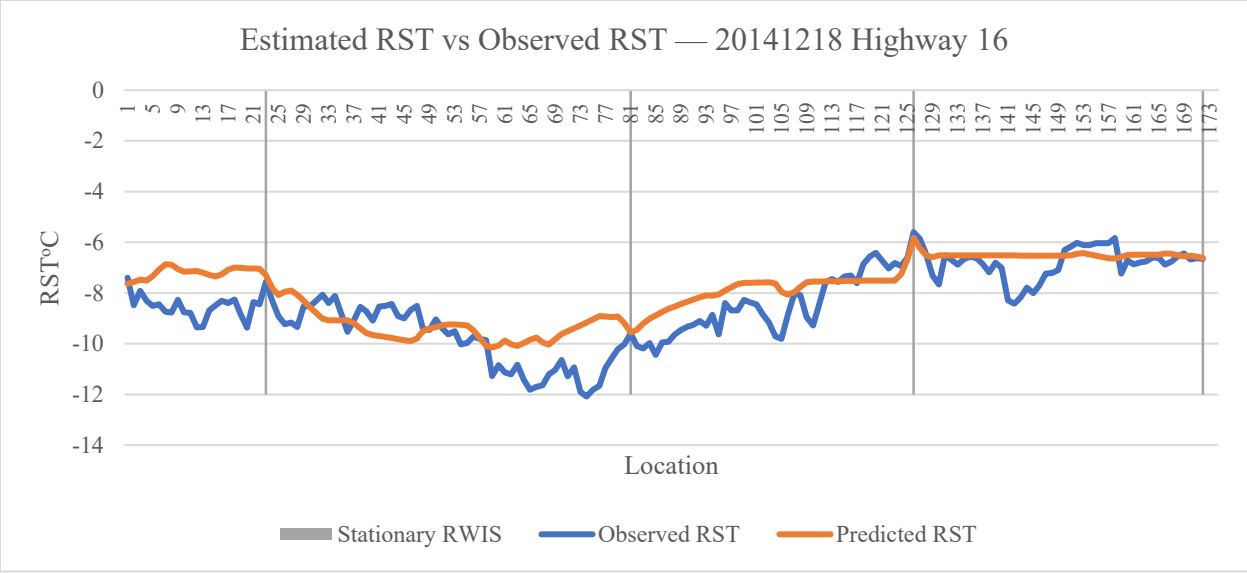

Figure 23. Estimated RST vs Observed RST on 20141218 for Highway 16

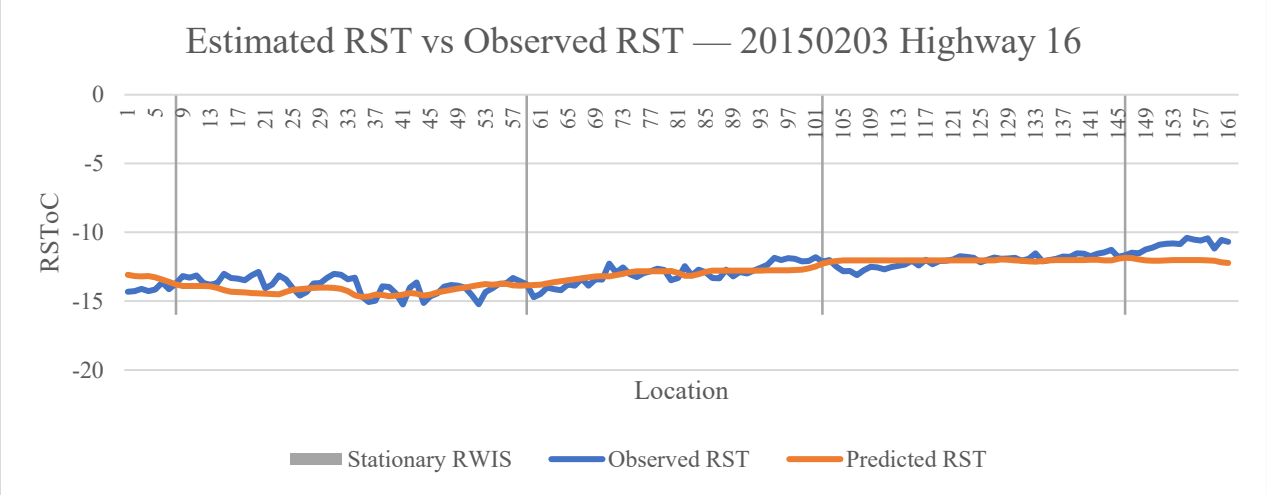

Figure 24. Estimated RST vs Observed RST on 20150203 for Highway 16

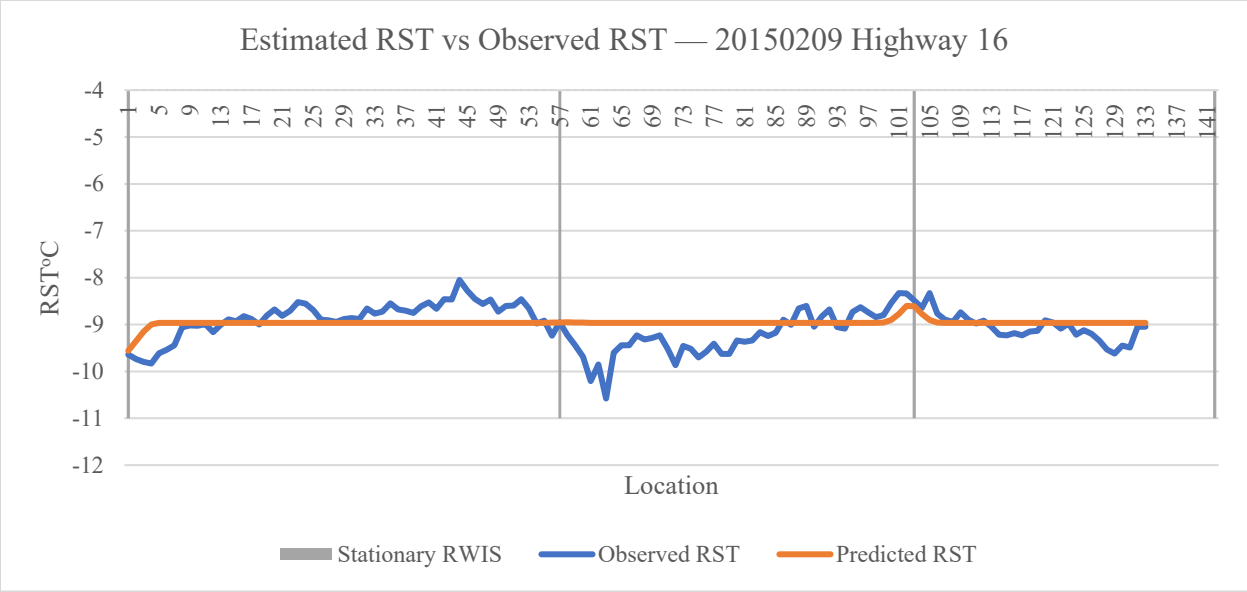

Figure 25. Estimated RST vs Observed RST on 20150209 for Highway 16

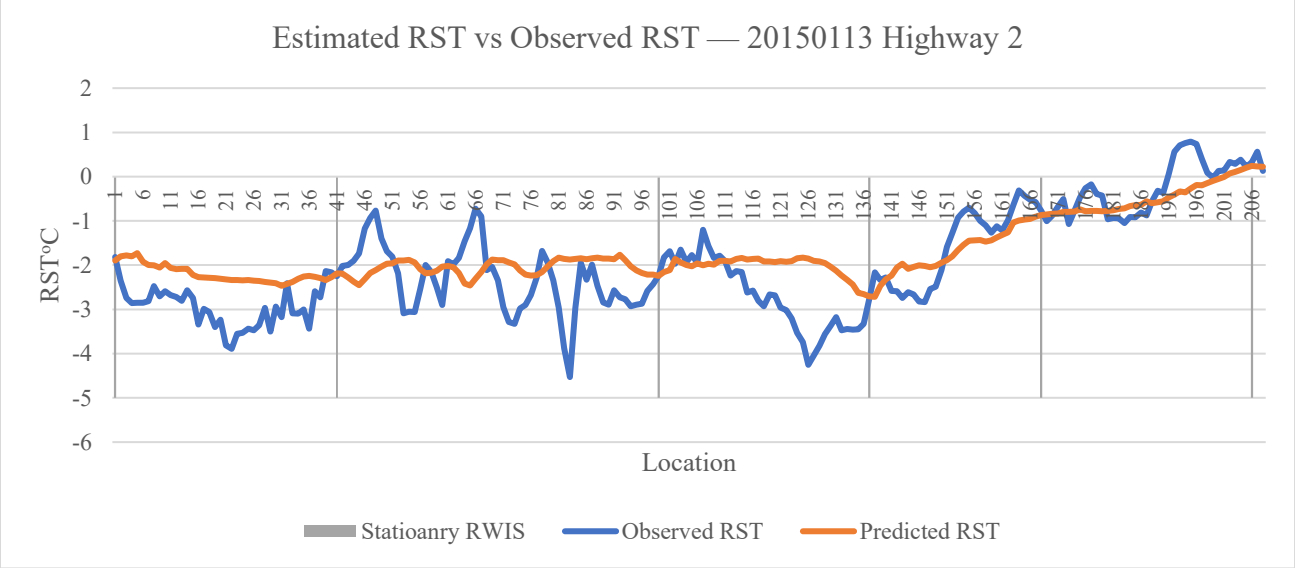

Figure 26. Estimated RST vs Observed RST on 20150113 Highway 2